

Earth's Magnetosphere (Solar wind-Magnetosphere Coupling)

John C. Dorelli

NASA/GSFC, Geospace Physics Lab (Code 673)

Outline

- I. The Chapman-Ferraro problem
- II. Gas dynamics modeling of the magnetosheath
- III. The breakdown of gas dynamics in the sheath
- IV. Magnetopause reconnection
- V. The Sweet-Parker time scale problem
- VI. Collisionless reconnection and the MMS mission

The basic building blocks of the terrestrial magnetosphere

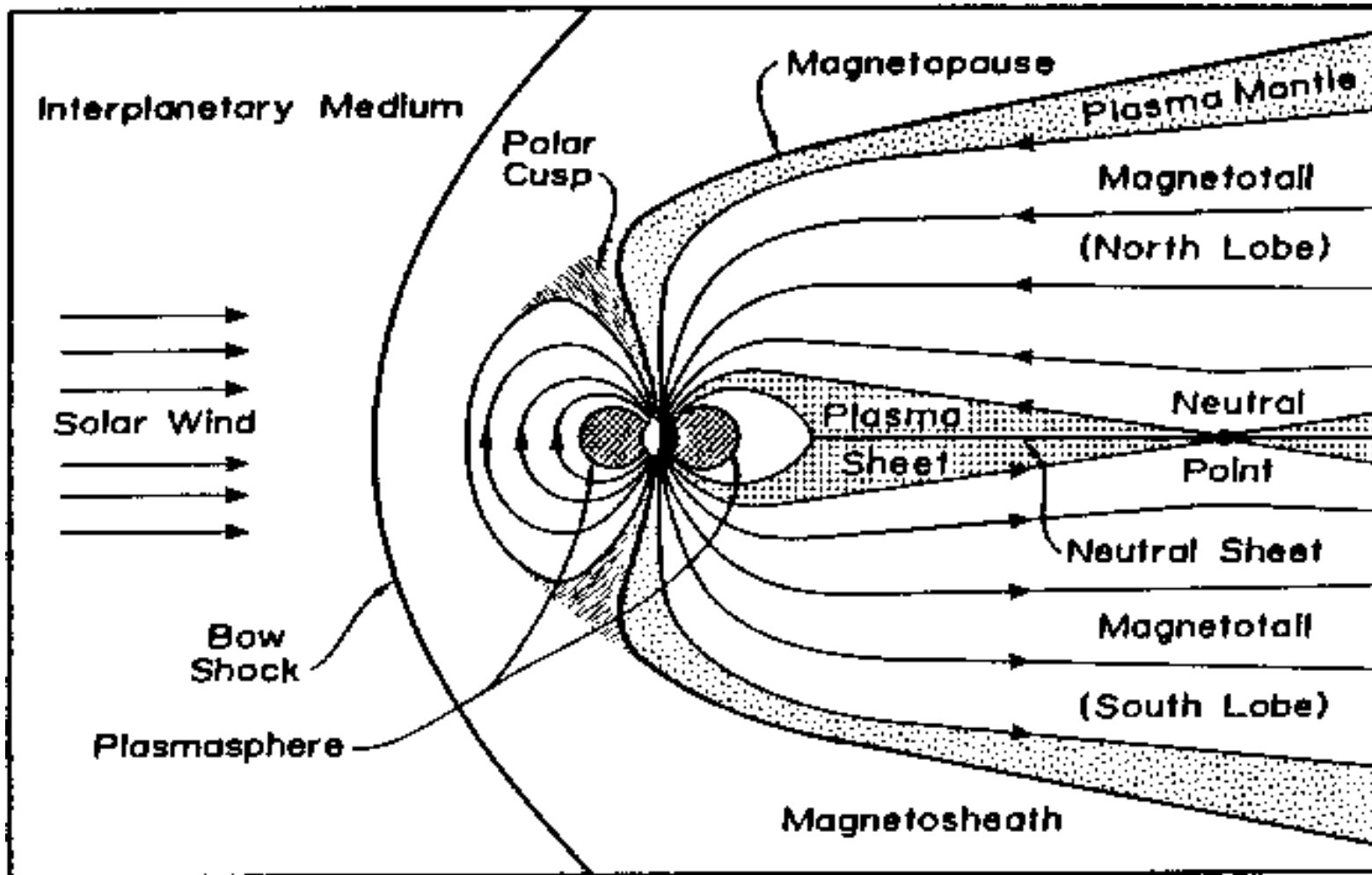
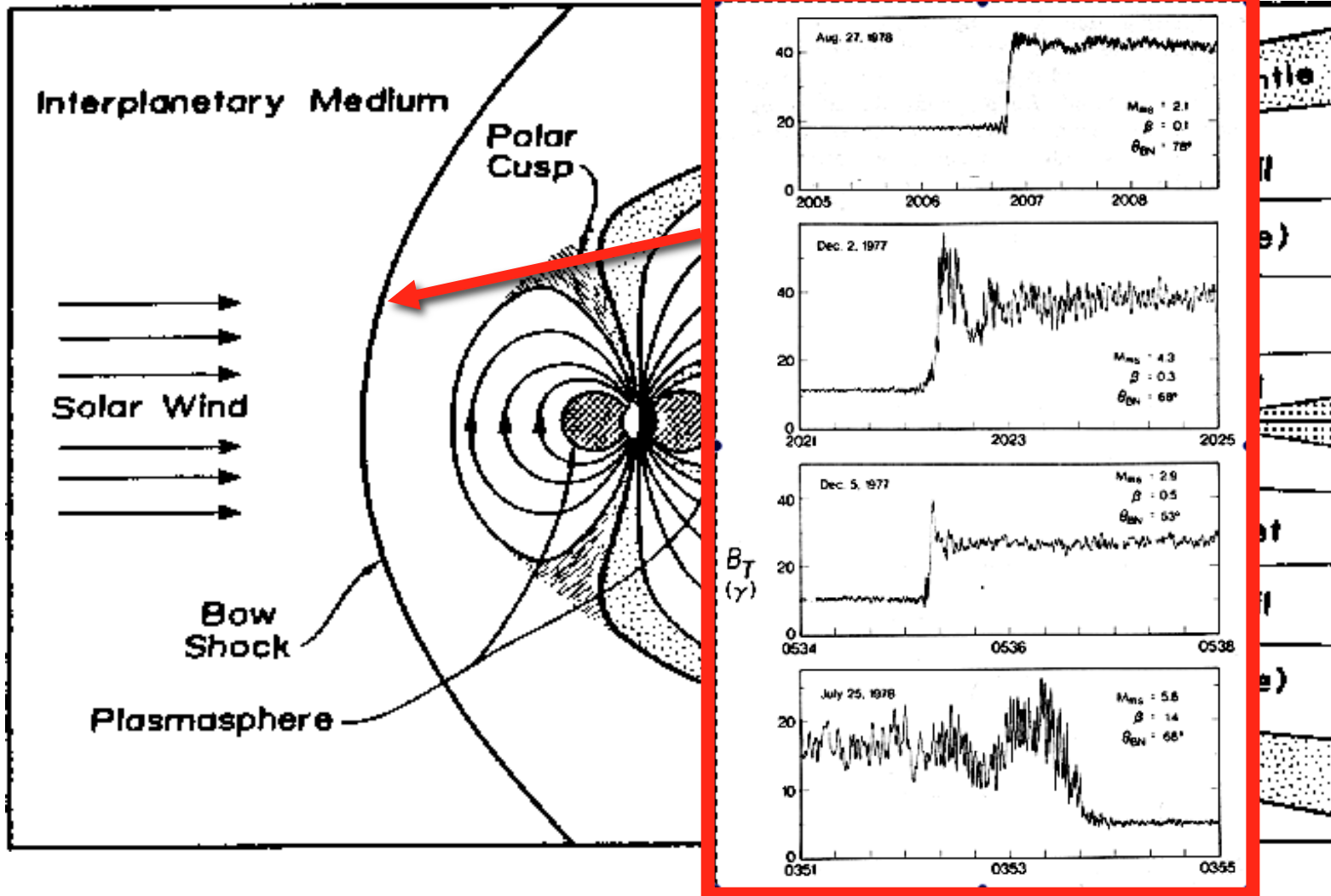


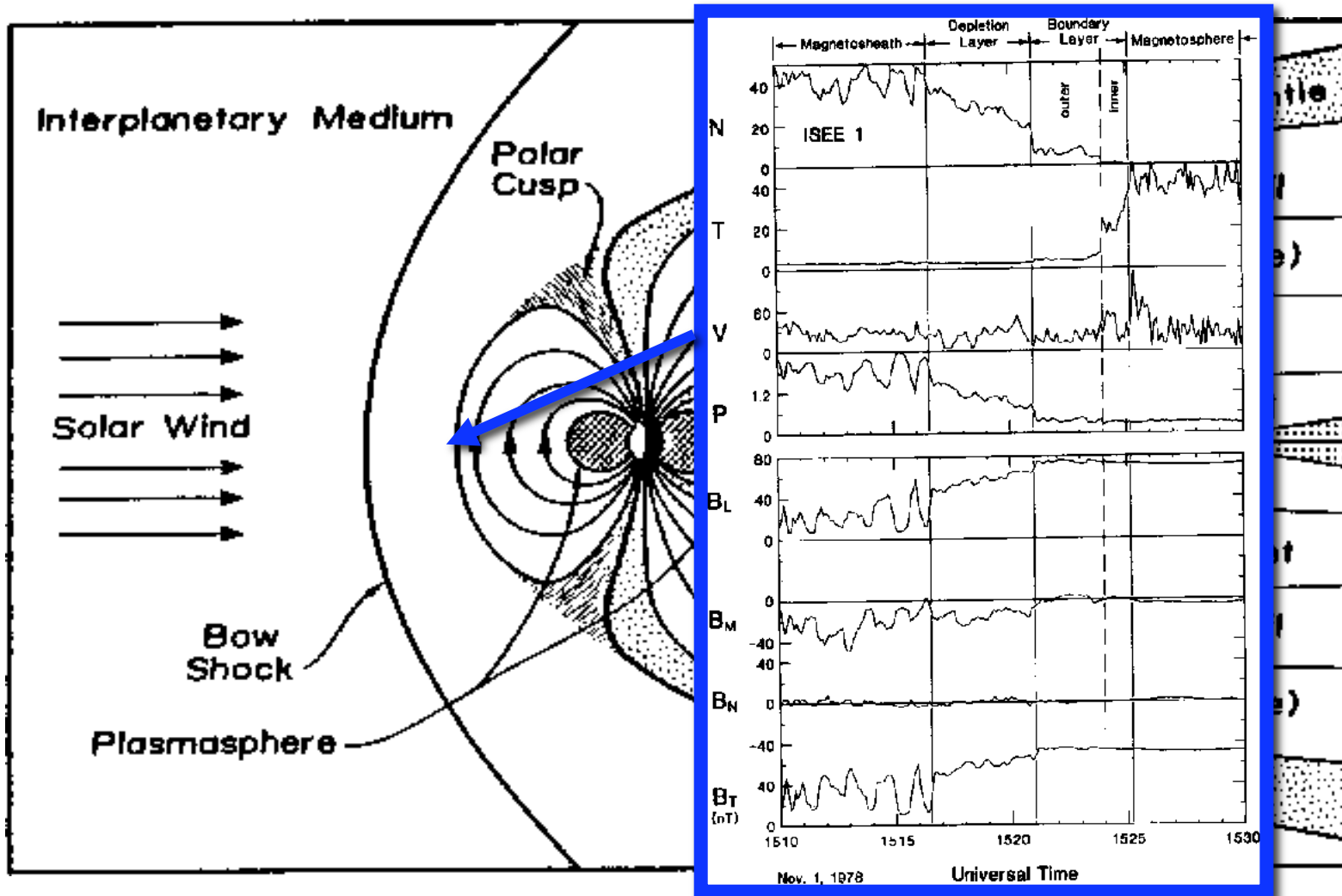
(figure from Russell, C., "The Magnetosphere," in *The Solar Wind and the Earth*, eds. S. -I. Akasofu and Y. Kamide, pp. 73-100, Terra Scientific Publishing Company, Tokyo, 1987.)

Boundaries are not infinitely thin (kinetic scale structure)



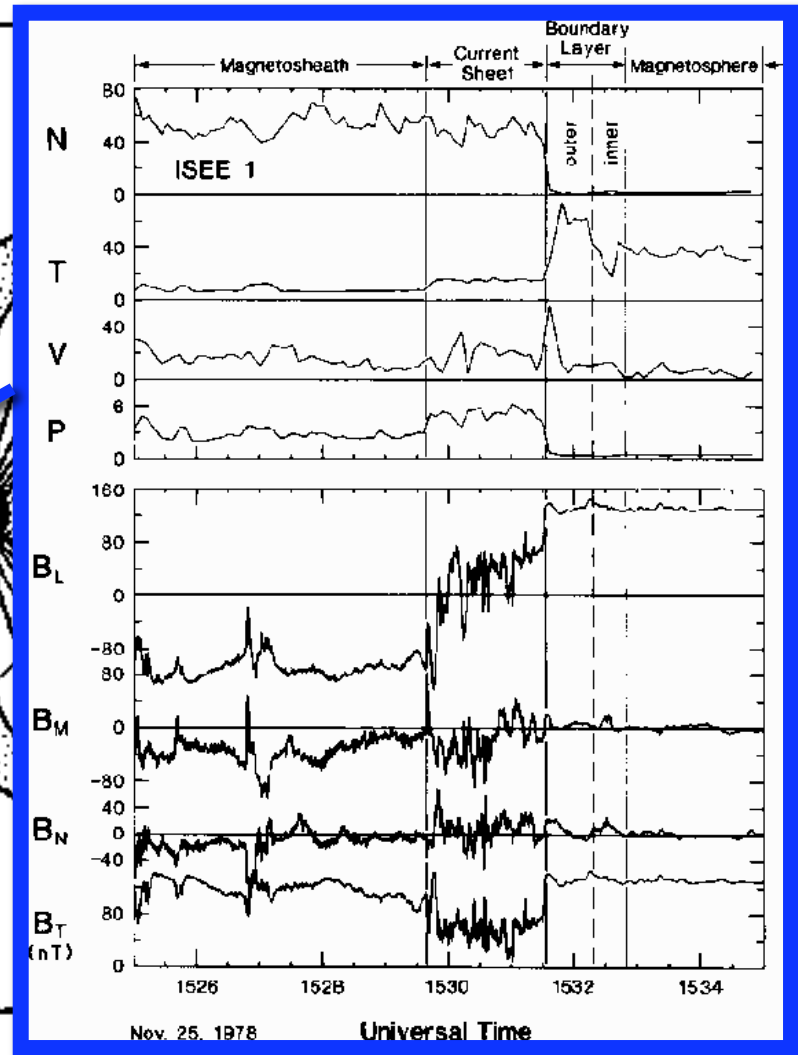
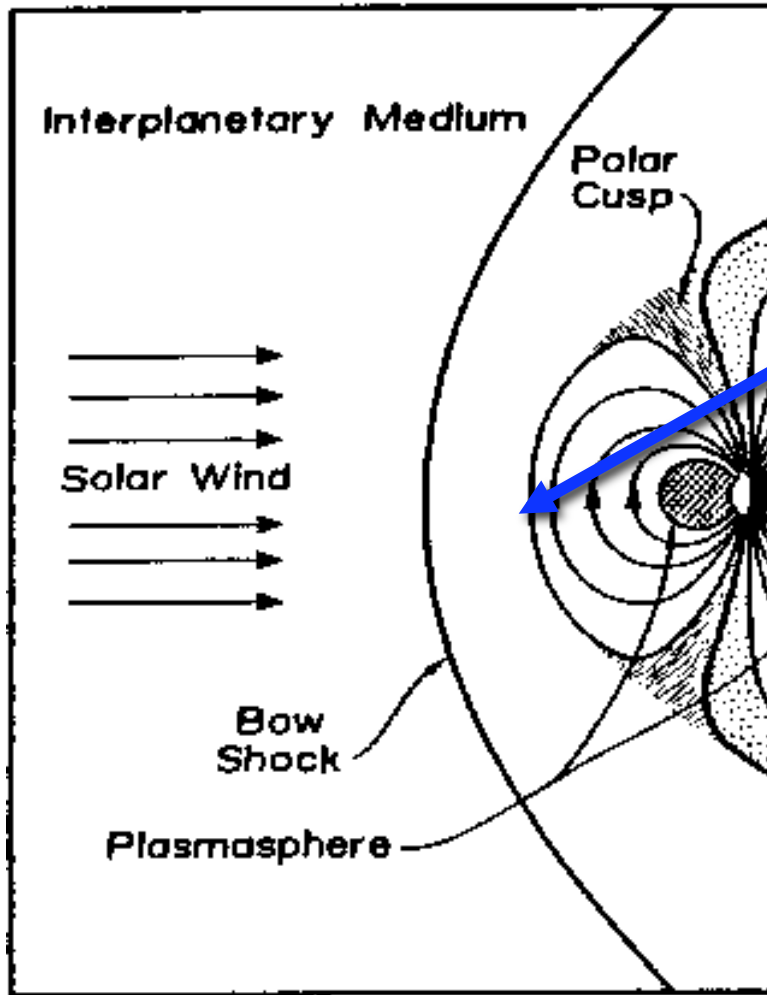
ISEE (International Sun Earth Explorer) made possible the study of the internal structure of the bow shock and magnetopause.

Boundaries are not infinitely thin (kinetic scale structure)



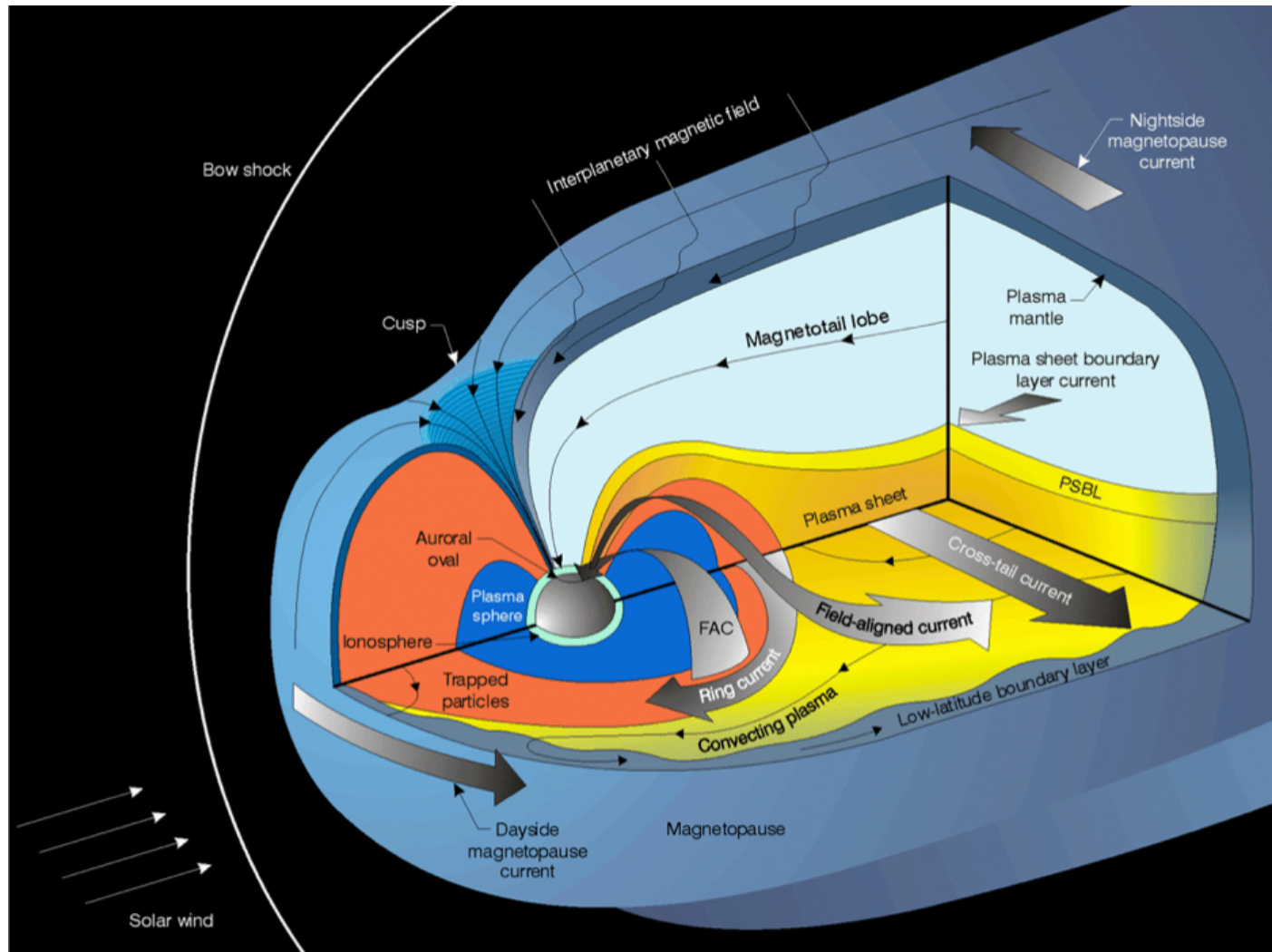
ISEE (International Sun Earth Explorer) made possible the study of the internal structure of the bow shock and magnetopause.

Boundaries are not infinitely thin (kinetic scale structure)



ISEE (International Sun Earth Explorer) made possible the study of the internal structure of the bow shock and magnetopause.

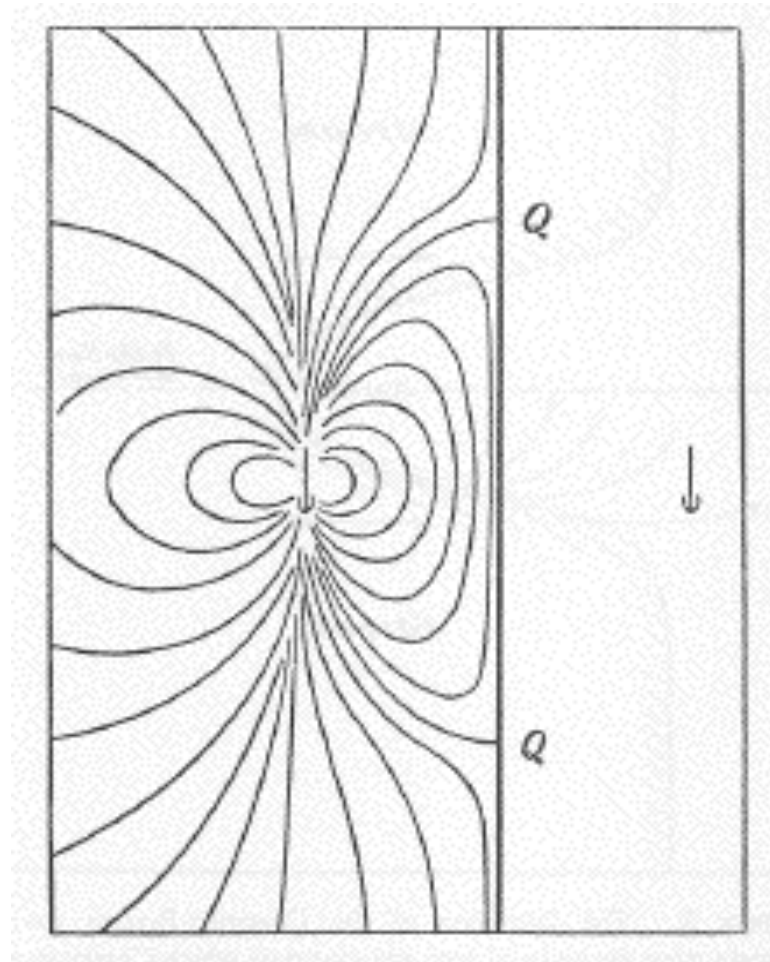
Magnetospheric current systems



The Chapman-Ferraro Magnetosphere



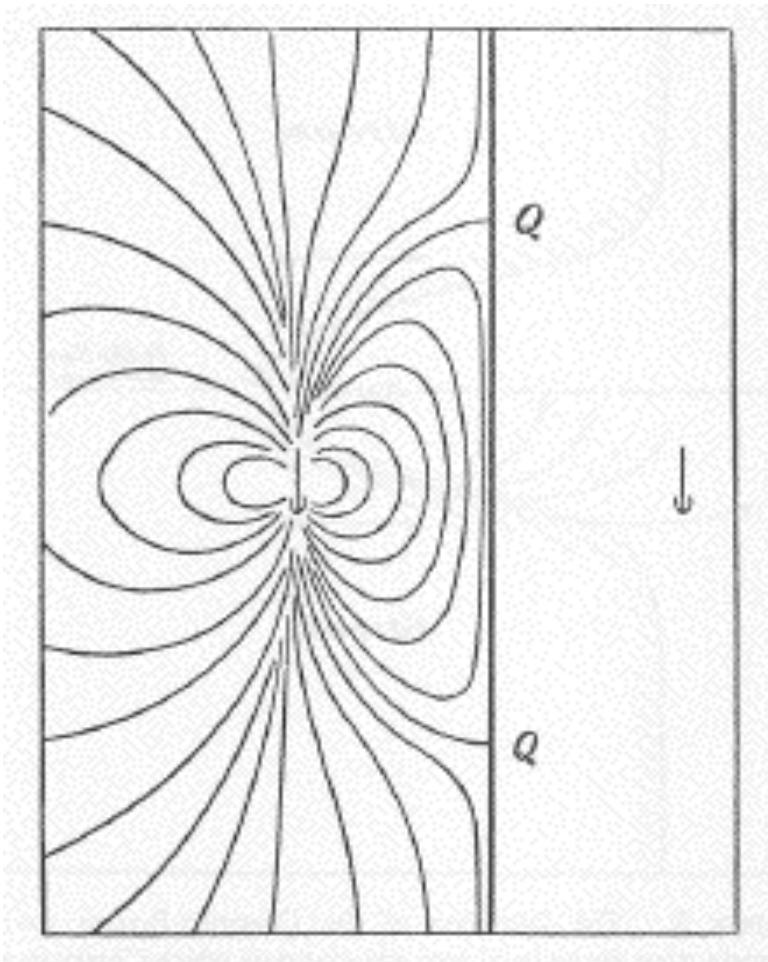
S. Chapman



V. C. A. Ferraro

Chapman, S., and V. C. A. Ferraro, A new theory of magnetic storms, *Terrest. Magnetism and Atmospheric Elec.*, 36, 171-186, 1931.

The Chapman-Ferraro Problem



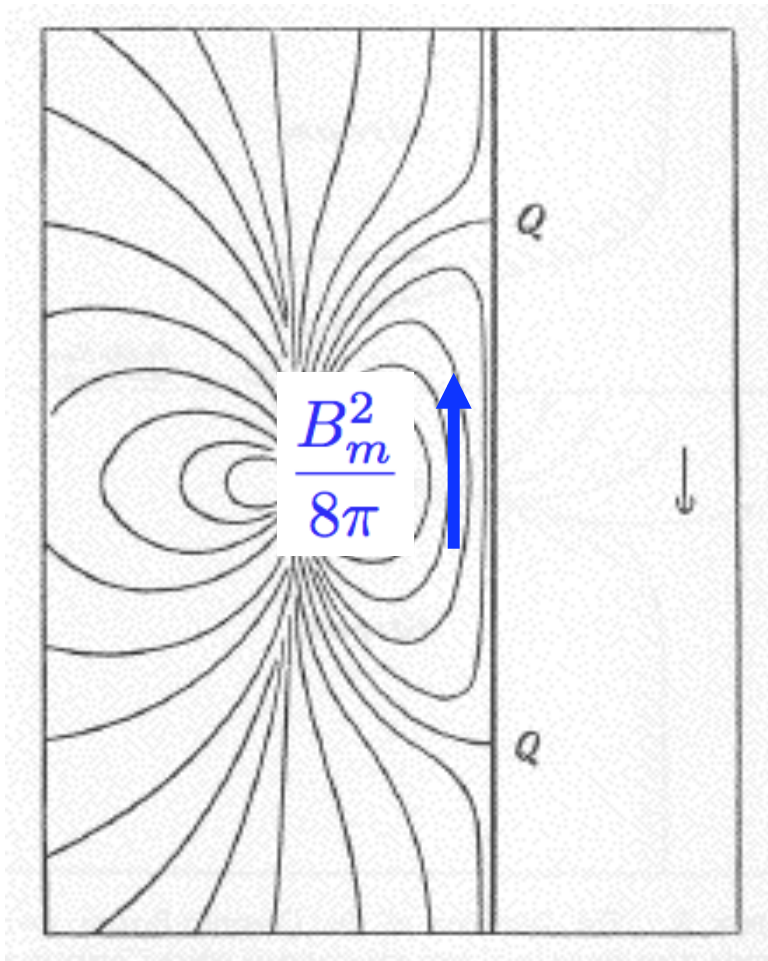
Find the surface that confines Earth's field and excludes the solar wind field.

If current density is confined to a set of pre-defined surfaces, one solves Laplace's equation for the magnetic potential:

$$B = -\nabla\Phi_M$$
$$\nabla^2\Phi_M = 0$$

We impose the boundary condition that the component of B normal to the pre-defined surfaces vanishes.

The Chapman-Ferraro Problem



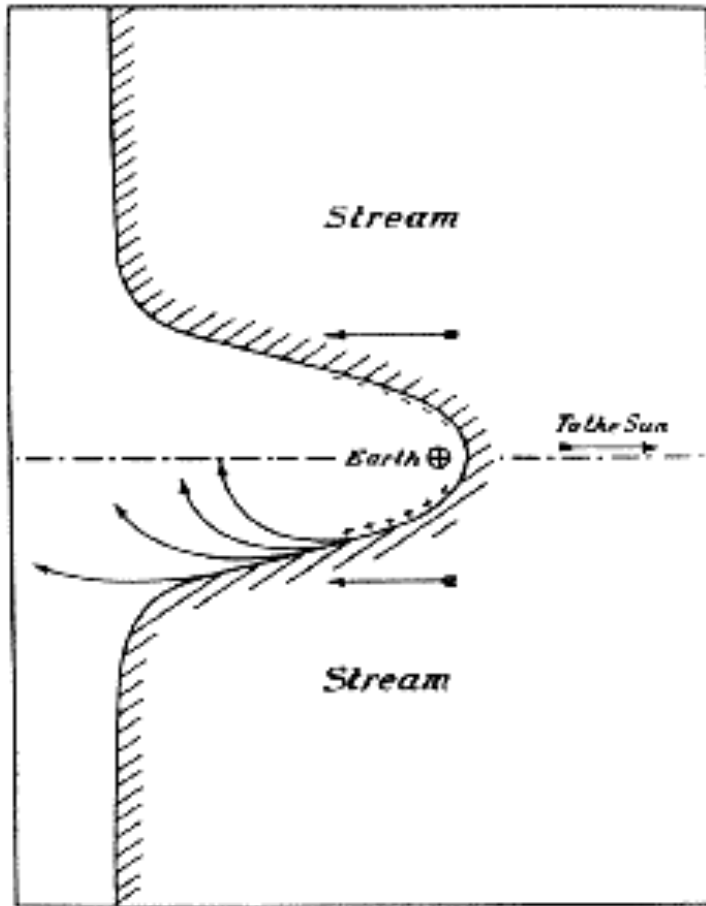
What about force balance?

$$\nabla \cdot \left[\rho \mathbf{V} \mathbf{V} + \left(p + \frac{B^2}{8\pi} \right) \mathbf{I} - \frac{\mathbf{B} \mathbf{B}}{4\pi} \right] = 0$$

← $\rho_{sw} V_{sw}^2$

Magnetic pressure in the magnetosphere
balances solar wind dynamic pressure

The Chapman-Ferraro Magnetosphere



The magnetosphere carves out a cavity in the solar wind.

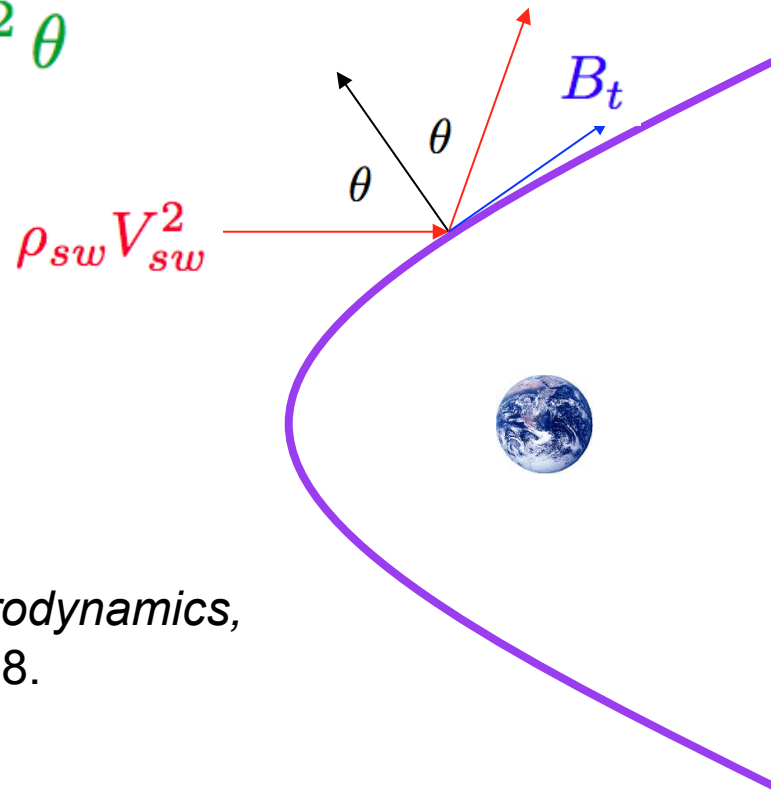
Neither solar wind plasma nor solar wind magnetic flux has access to the cavity.

Chapman, S., and V. C. A. Ferraro, A new theory of magnetic storms, *Terrest. Magnetism and Atmospheric Elec.*, 36, 171-186, 1931.

Computing the shape of the magnetopause I:
“Specular Reflection” off of a highly conducting boundary

$$\frac{B_t^2}{8\pi} = 2\rho_{sw} V_{sw}^2 \cos^2 \theta$$

$$B_n = 0$$



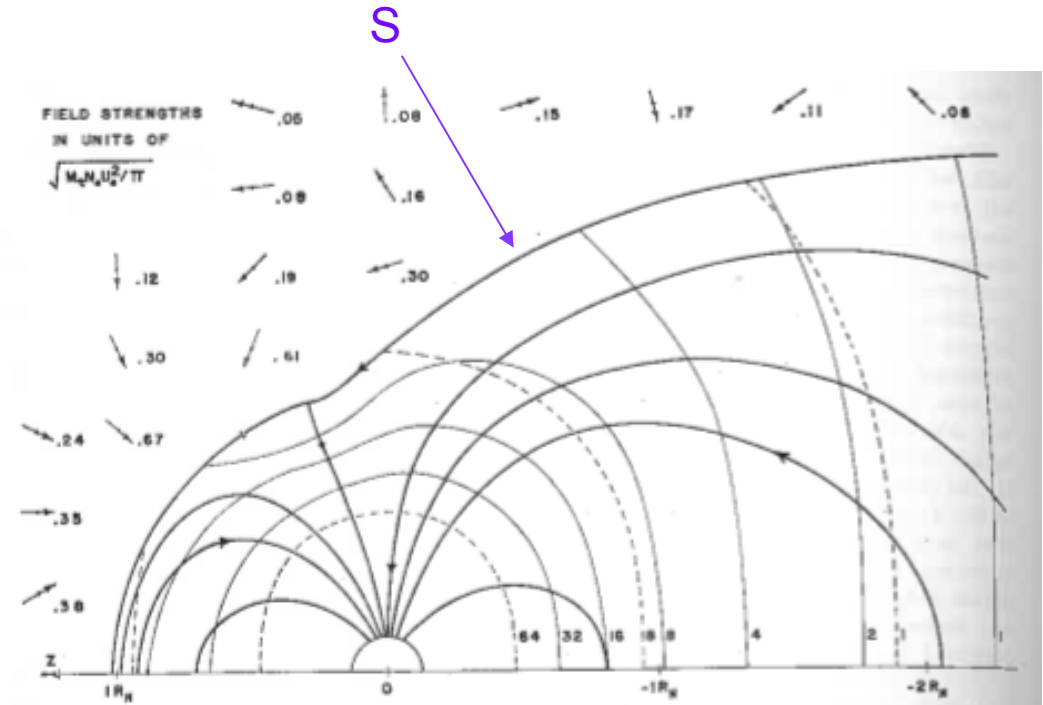
J. W. Dungey, *Cosmic Electrodynamics*,
Cambridge U. Press, 1958.

A brute force solution....

$$\frac{B_t^2}{8\pi} = 2\rho_{sw} V_{sw}^2 \cos^2 \theta$$

$$B_n = 0$$

1. Specify that magnetic field vanishes outside boundary surface S.
2. Parameterize the surface S (37 independent parameters in Midgley and Davis!).
3. Pressure balance relates surface current to the shape of the surface.
4. Spherical-harmonics expansion of surface current with coefficients chosen (by searching 37-dimensional parameter space) to cancel dipole outside surface.



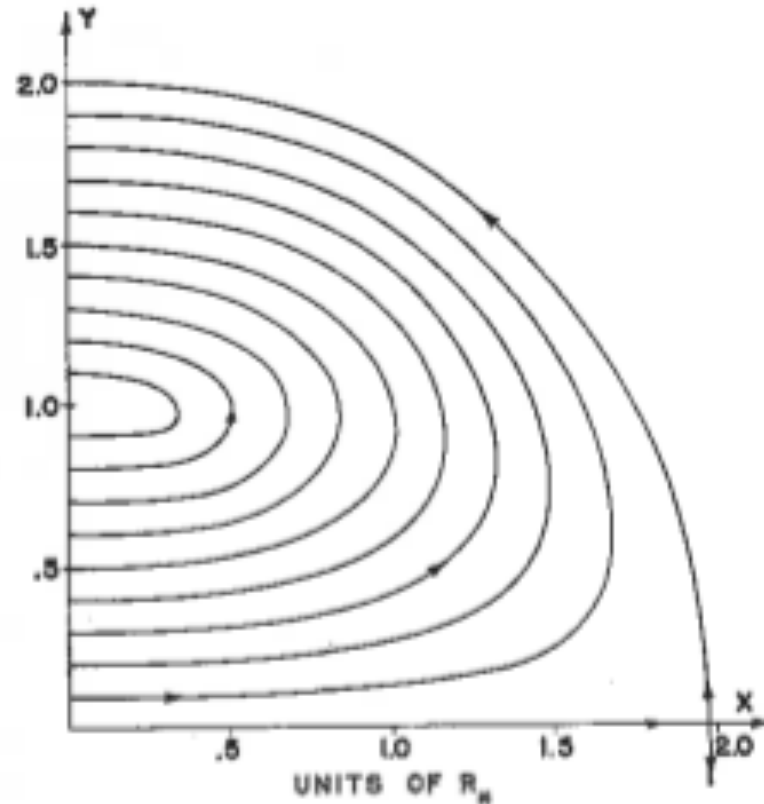
J. E. Midgley and L. Davis, *J. Geophys. Res.*, 68, 1963.

The Chapman-Ferraro current system

$$\frac{B_t^2}{8\pi} = 2\rho_{sw} V_{sw}^2 \cos^2 \theta$$

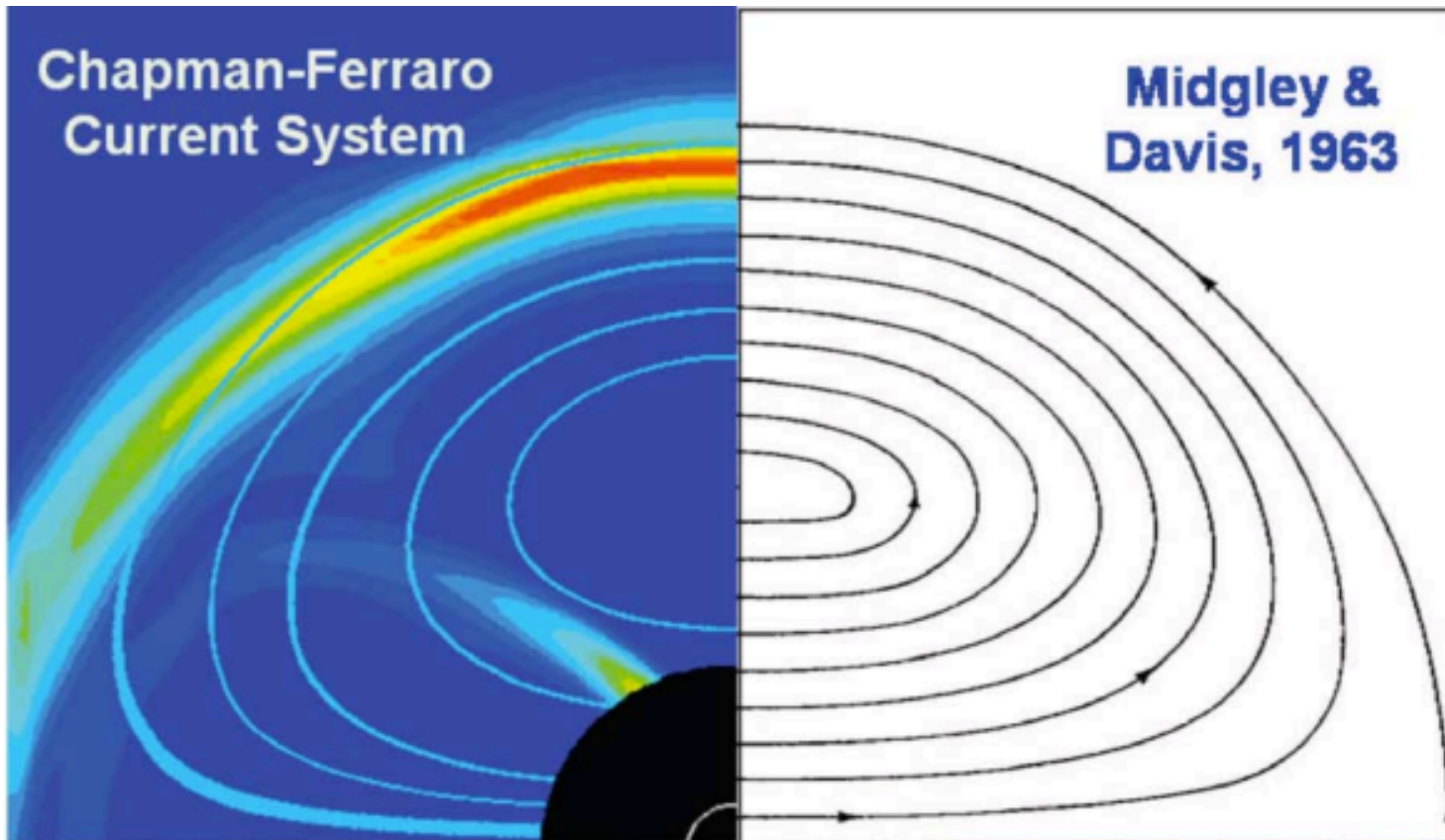
$$B_n = 0$$

1. Specify that magnetic field vanishes outside boundary surface S.
2. Parameterize the surface S (37 independent parameters in Midgley and Davis!).
3. Pressure balance relates surface current to the shape of the surface.
4. Spherical-harmonics expansion of surface current with coefficients chosen (by searching 37-dimensional parameter space) to cancel dipole outside surface.



J. E. Midgley and L. Davis, *J. Geophys. Res.*, 68, 1963.

The Chapman-Ferraro current system



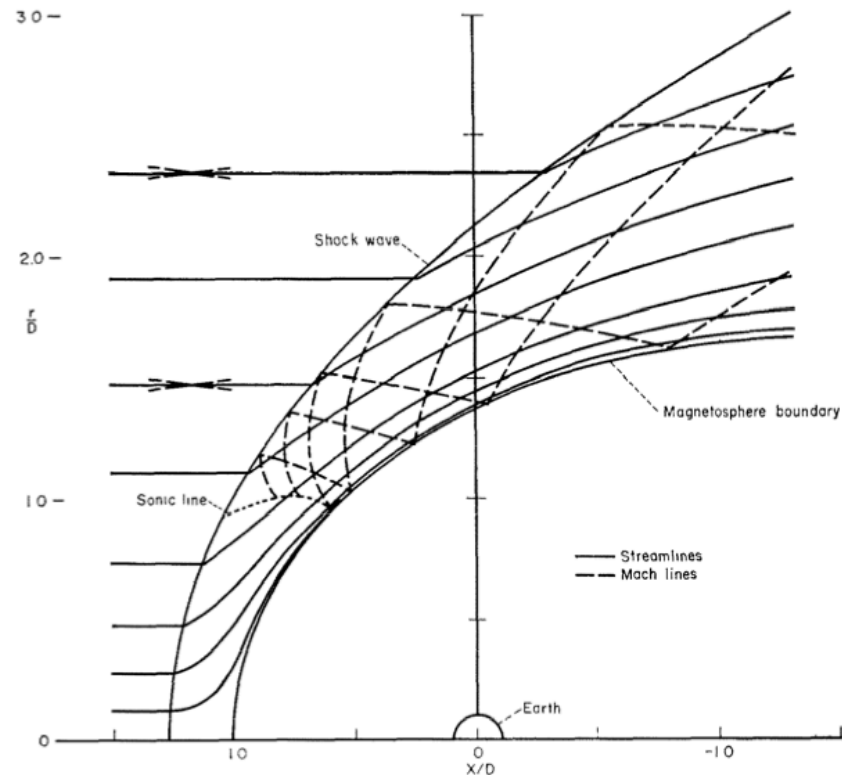
Global MHD simulations do a pretty good job of modeling the Chapman-Ferraro current system under “typical” (i.e., not strongly driven) solar wind conditions.

The structure of the magnetosheath

$$\frac{B_t^2}{8\pi} = K \rho_{sw} V_{sw}^2 \cos^2 \theta$$
$$B_n = 0 \quad K \approx 0.881$$

The “specular reflection” idea is not a very realistic model of the deflection of the solar wind around the magnetopause.

It turns out that gas dynamics (in which the magnetic field is neglected) does a pretty good job of describing the plasma flow in the magnetosheath.



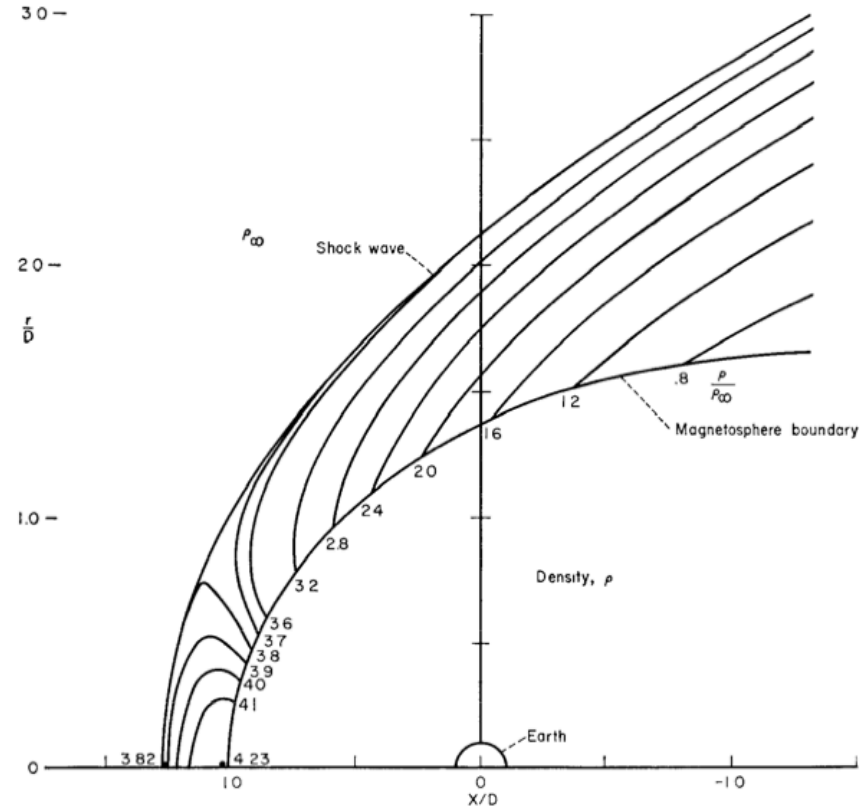
J. R. Spreiter, A. L. Summers and A. Y. Alksne, *Planet. Space Sci.*, 14, 1966.

Density pileup at the subsolar magnetosheath

$$\frac{B_t^2}{8\pi} = K \rho_{sw} V_{sw}^2 \cos^2 \theta$$

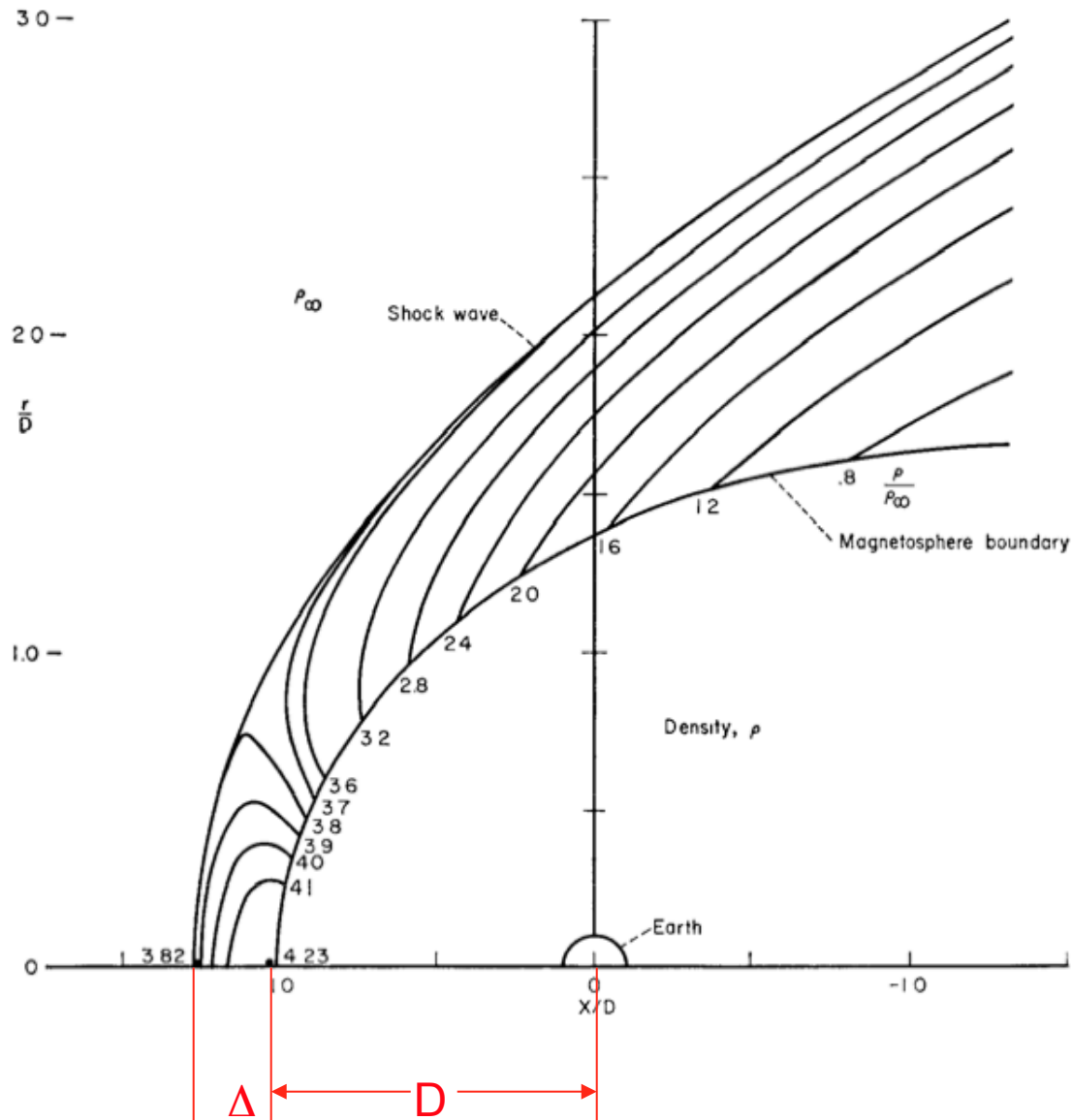
$$B_n = 0 \quad K \approx 0.881$$

Gas dynamics predicts that the plasma density in the magnetosheath should increase as one approaches the subsolar point along the Sun-Earth line.



J. R. Spreiter, A. L. Summers and A. Y. Alksne, *Planet. Space Sci.*, 14, 1966.

Bow shock stand-off distance

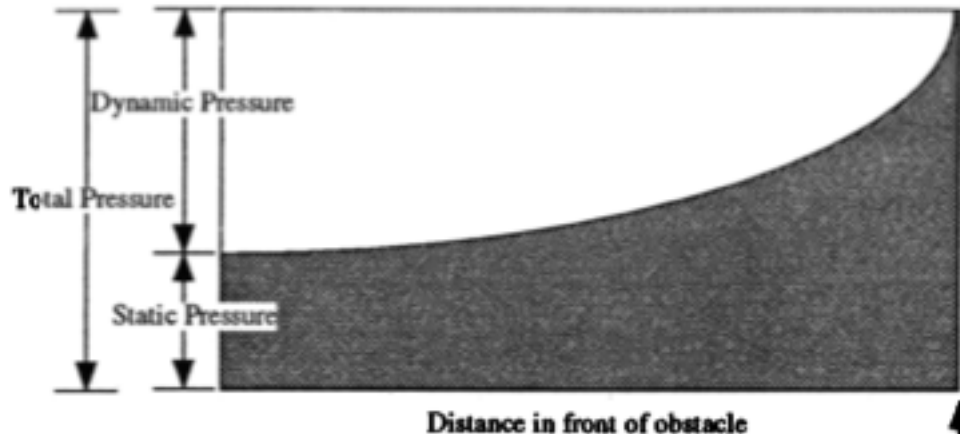


$$\frac{\rho_1}{\rho_\infty} = \frac{(\gamma + 1)M_\infty^2}{(\gamma - 1)M_\infty^2 + 2}$$

$$\frac{\Delta}{D} = 1.1 \frac{\rho_\infty}{\rho_1}$$

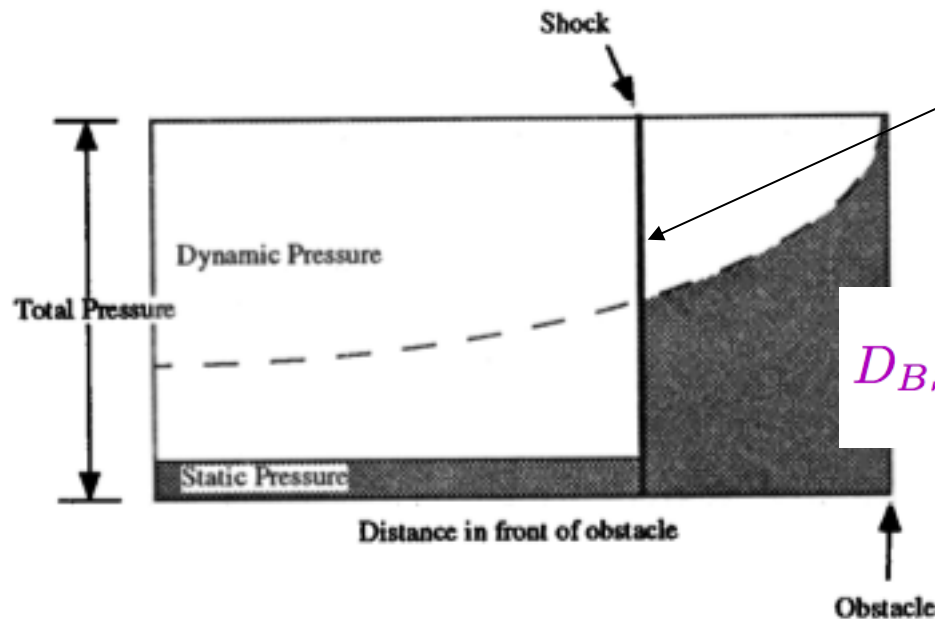
This relationship breaks down when the upstream mach number approaches 1.

Bow shock stand-off distance



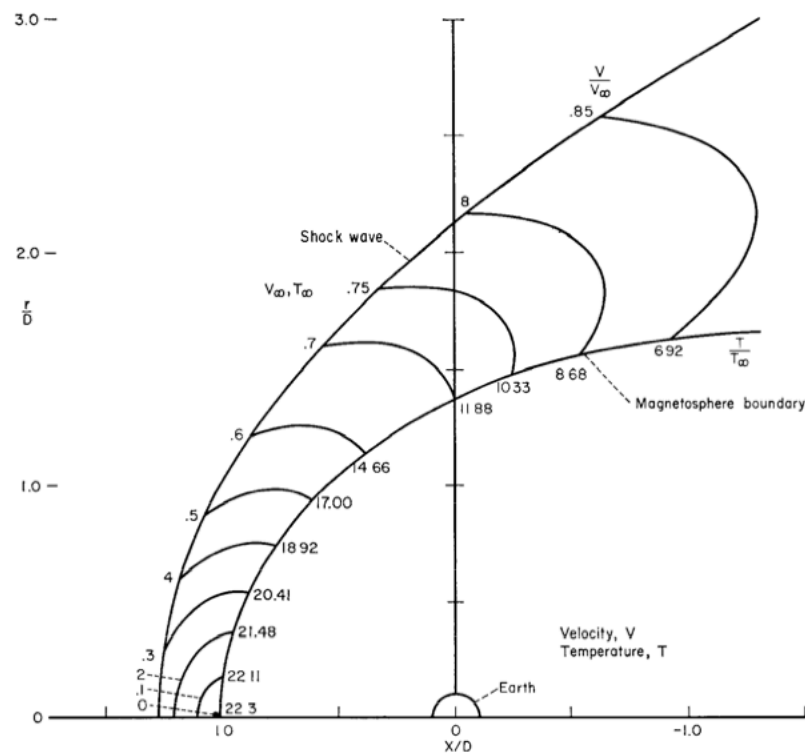
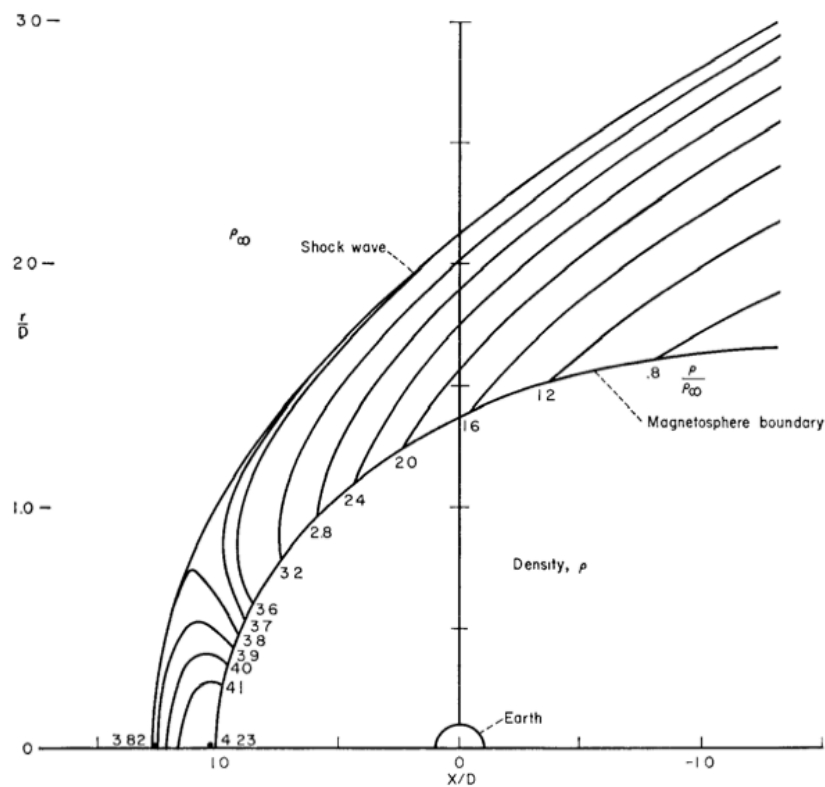
$$\frac{\rho_1}{\rho_\infty} = \frac{(\gamma + 1)M_\infty^2}{(\gamma - 1)M_\infty^2 + 2}$$

Fast mode shock is set up at that location where the Rankine-Hugoniot relations yield just the right increase in static pressure to deflect the subsonic downstream flow....



$$D_{BS} = D_{OB} \left[1 + 1.1 \frac{(\gamma - 1)M_\infty^2 + 2}{(\gamma + 1)(M_\infty^2 - 1)} \right]$$

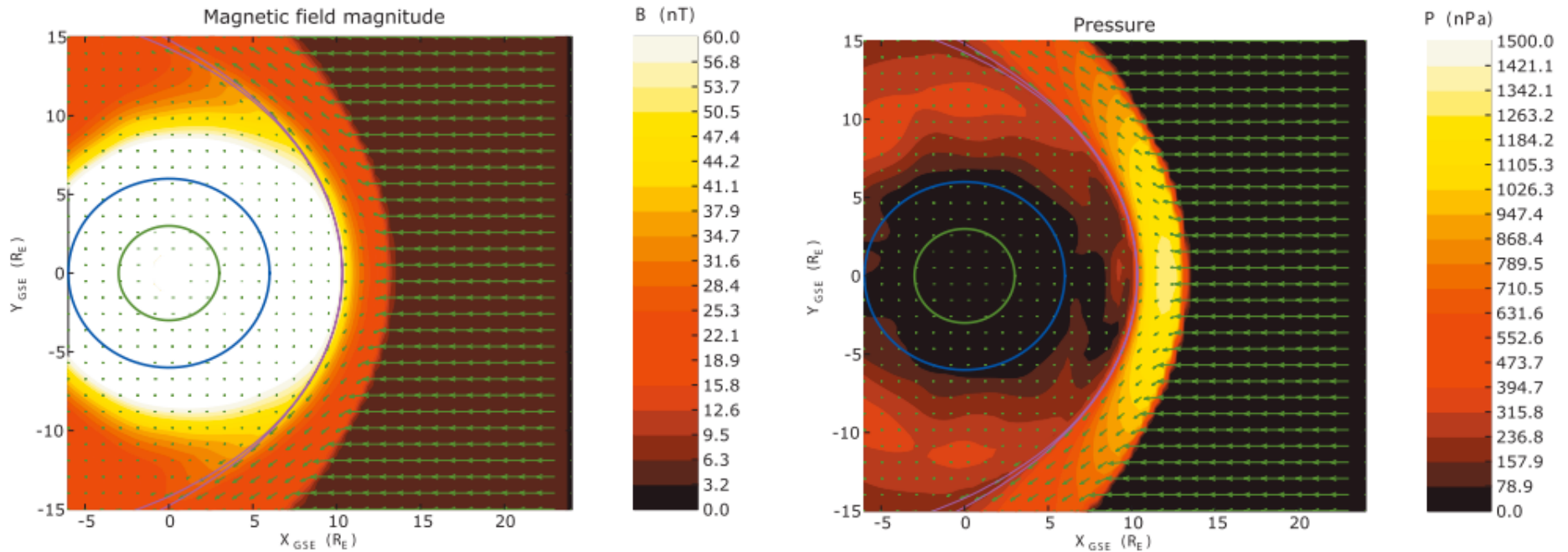
Pressure pileup at subsolar magnetopause



Pressure must increase as we approach the subsolar magnetopause (to divert the solar wind around the magnetopause).

What happens when we include the magnetic field?

What about the solar wind magnetic field?



e.g., J. Dorelli and A. Bhattacharjee, *J. Geophys. Res.*, 114, 2009

Pressure (and density) decrease, while magnetic energy increases, as one approaches the subsolar magnetopause.

The “weak field” approximation breaks down when the solar wind magnetic field is included!

How do we calculate the sheath magnetic field?

$$\frac{\partial \mathbf{B}}{\partial t} = -c \nabla \times \mathbf{E}$$

Solve Faraday's law with a prescribed velocity field (e.g., from gas dynamics solution).

How do we calculate the sheath magnetic field?

$$\frac{\partial \mathbf{B}}{\partial t} = -c \nabla \times \mathbf{E}$$

0

Look for steady state solutions....

Solve Faraday's law with a prescribed velocity field (e.g., from gas dynamics solution).

How do we calculate the sheath magnetic field?

$$\nabla \times \mathbf{E} = 0$$

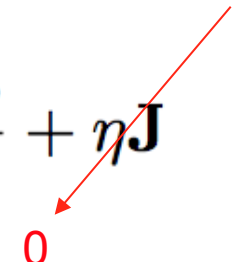
$$\mathbf{E} = -\frac{\mathbf{V} \times \mathbf{B}}{c} + \eta \mathbf{J}$$

Resistive MHD Ohm's law....

Solve Faraday's law with a prescribed velocity field (e.g., from gas dynamics solution).

How do we calculate the sheath magnetic field?

$$\nabla \times \mathbf{E} = 0$$

$$\mathbf{E} = -\frac{\mathbf{V} \times \mathbf{B}}{c} + \eta \mathbf{J}$$


Neglect resistive diffusion term (i.e., no magnetic reconnection!)

Solve Faraday's law with a prescribed velocity field (e.g., from gas dynamics solution).

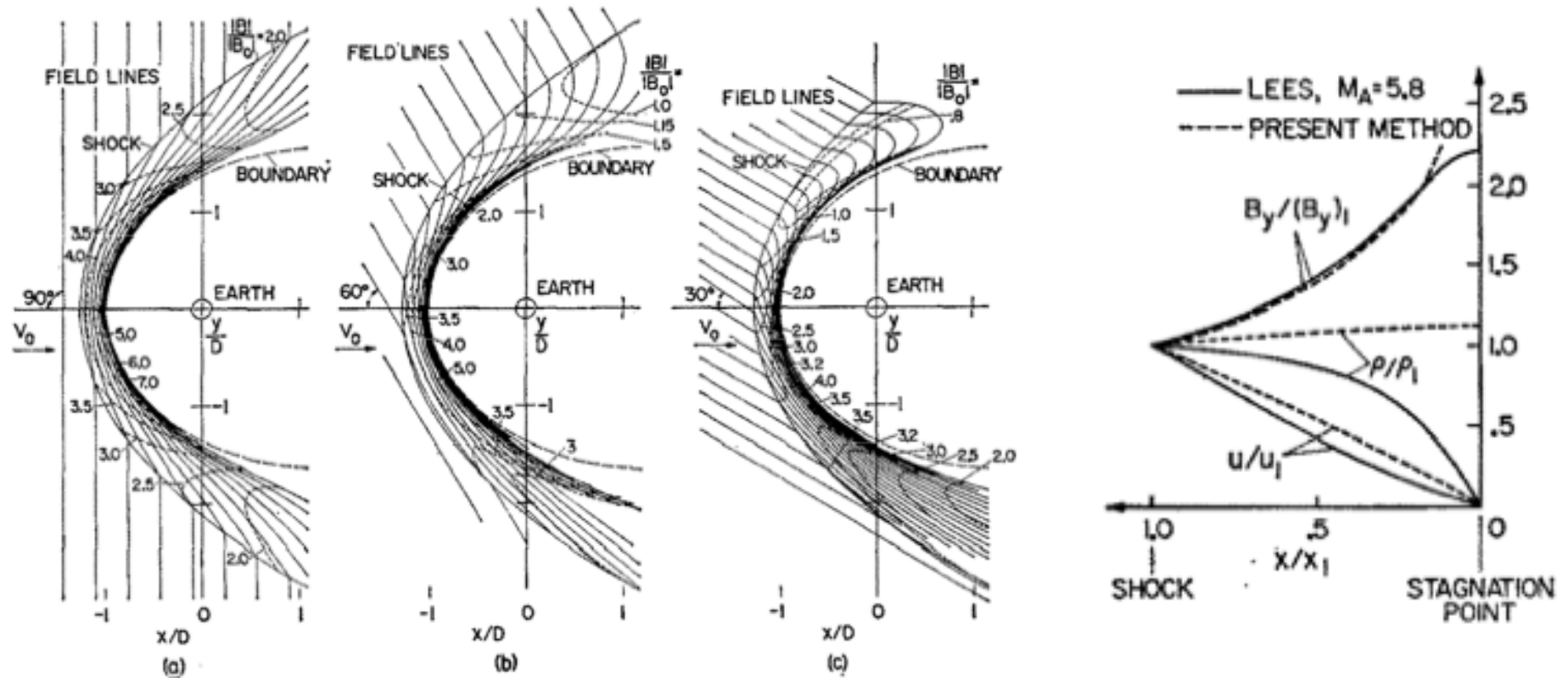
How do we calculate the sheath magnetic field?

$$\nabla \times (\mathbf{V} \times \mathbf{B}) = 0$$

We have a system of first order PDEs for the three components of the magnetic field.

Solve Faraday's law with a prescribed velocity field (e.g., from gas dynamics solution).

How do we calculate the sheath magnetic field?

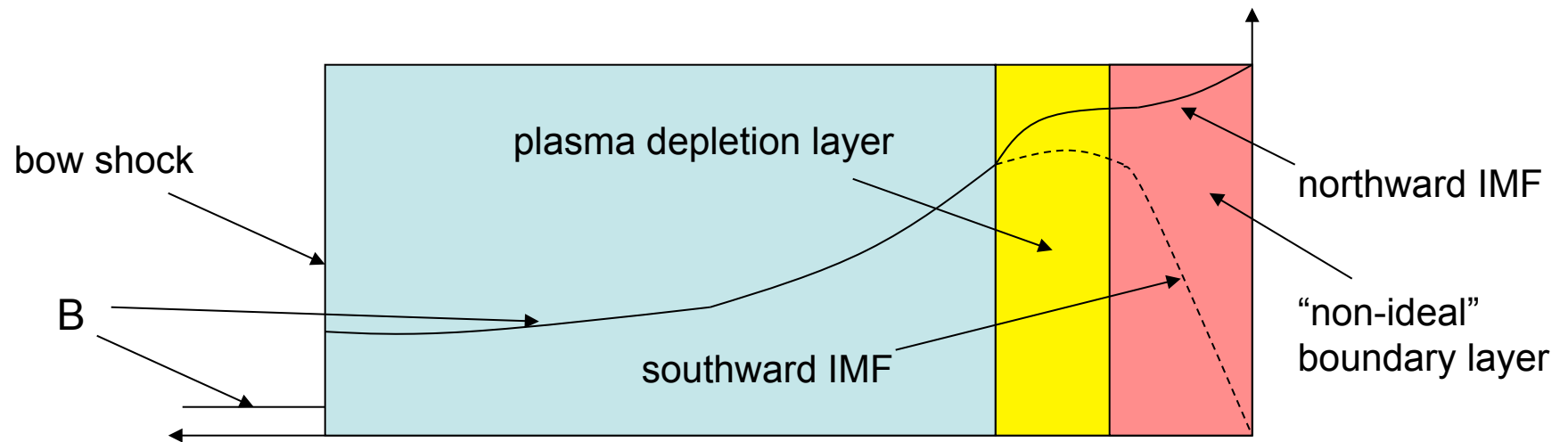


Alksne, A., *Planet. Space Sci.*, 15, 1967.

PROBLEM: With Spreiter *et al.* gas dynamics solution, the magnetic field blows up at the subsolar magnetopause! Obviously, Spreiter *et al.* needs to be modified to incorporate some missing physics.

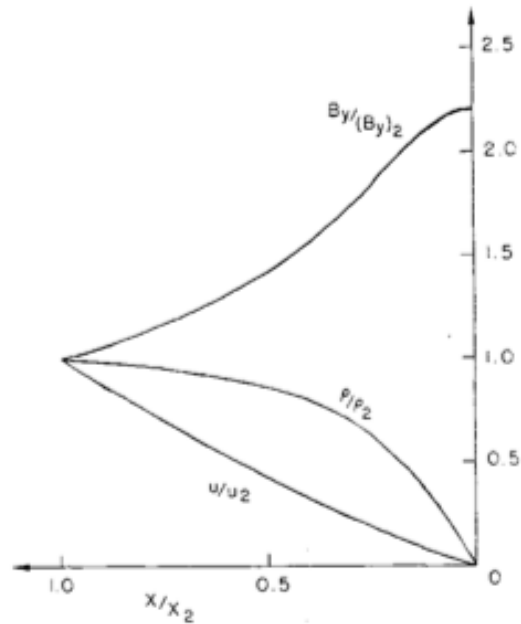
What went wrong (what physics did we leave out)?

1. The magnetosheath is rather compressible; magnetic pileup near the magnetopause should result in a sharp density drop there (so-called “plasma depletion layer.”)
2. Ideal MHD should break down in a thin layer around the magnetopause (i.e., the magnetopause thickness is not zero; it is a thin boundary layer within which the frozen-flux theorem is violated!)



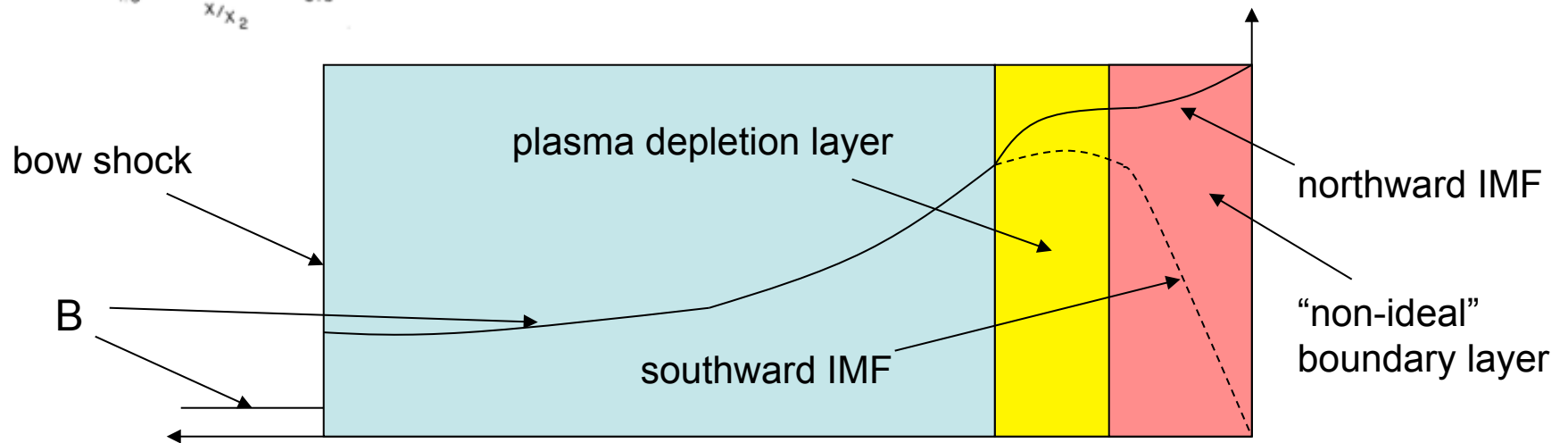
Plasma depletion layer

Lees, L., AIAA Journal, 2, 1964.

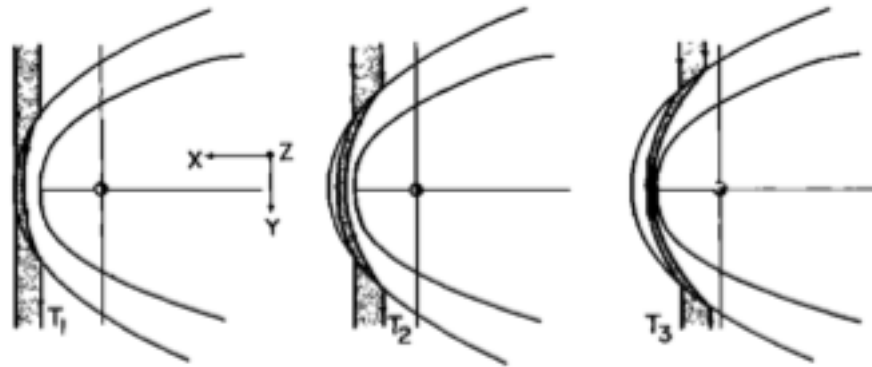


Better: magnetic field remains finite; however....

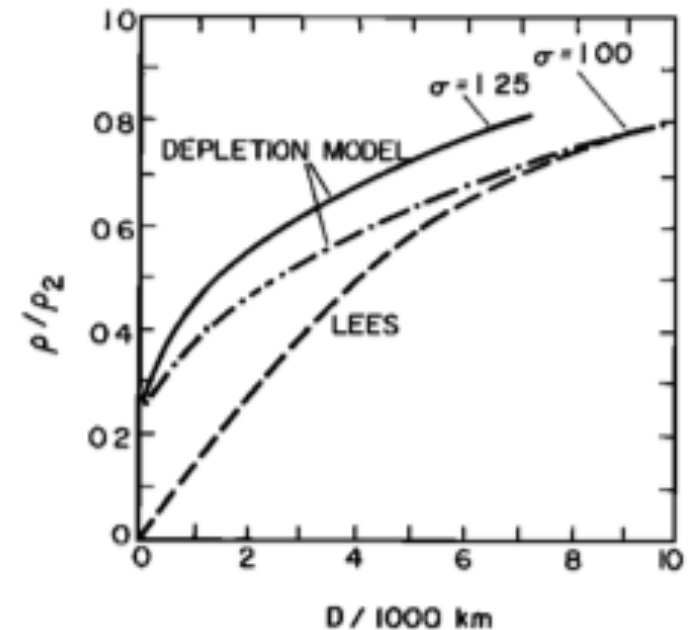
plasma density drops to zero at the magnetopause boundary (**not observed!**).



Breakdown of cylindrical symmetry of flow field near the magnetopause?



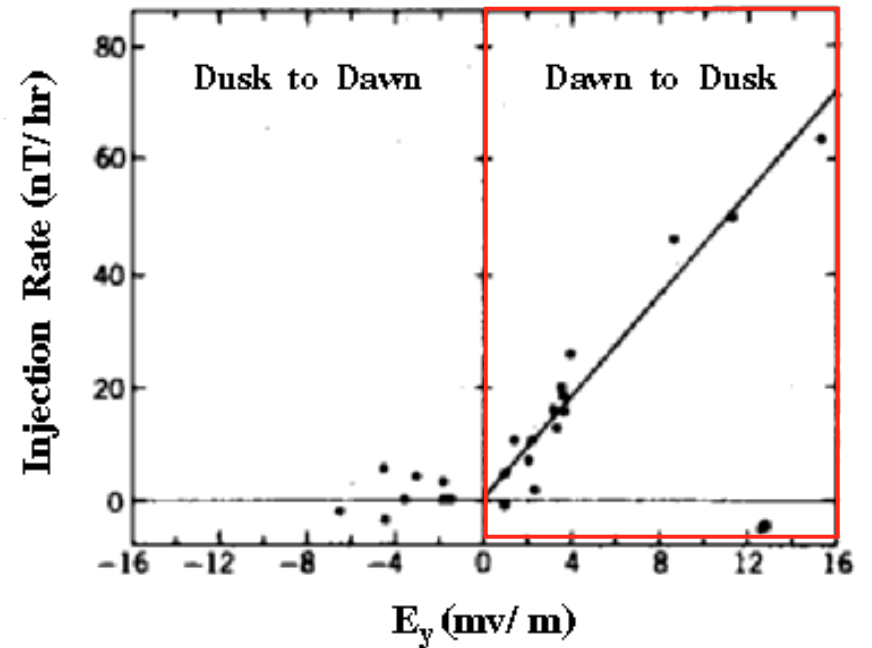
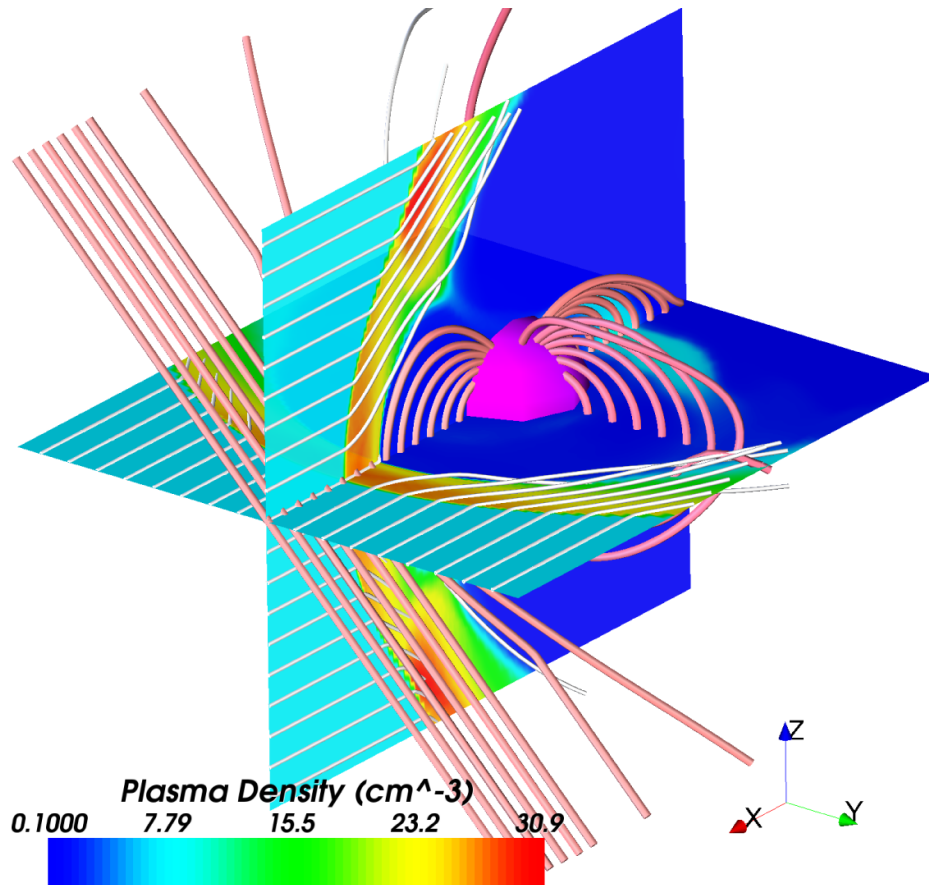
Zwan, B. J. and R. A. Wolf, *J. Geophys. Res.*,
81, 1976.



Asymmetry of plasma acceleration parallel and perpendicular to flux tube (with less acceleration parallel to flux tube) results in less depletion as a function of distance from the magnetopause.

Where does magnetic reconnection fit into all of this?

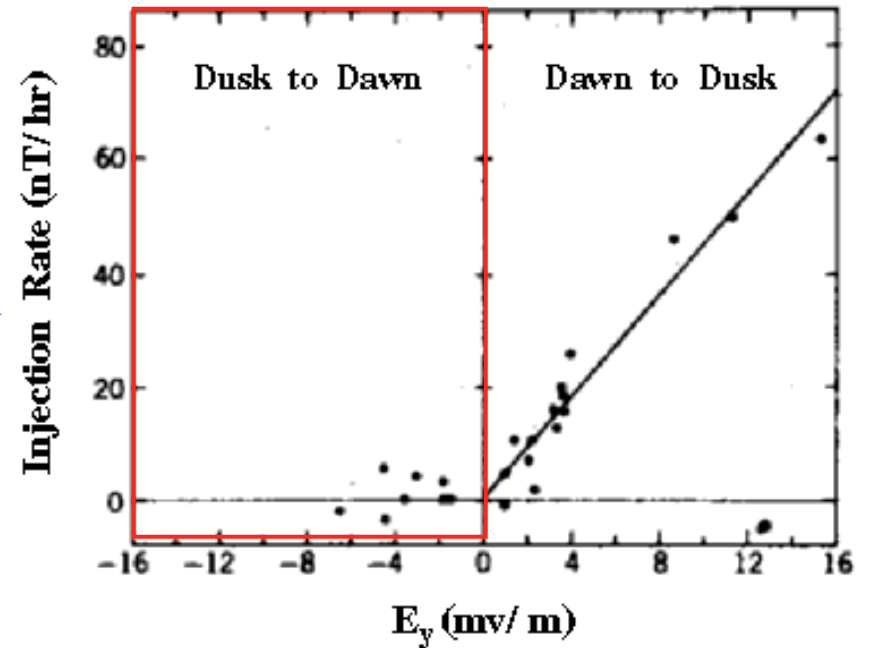
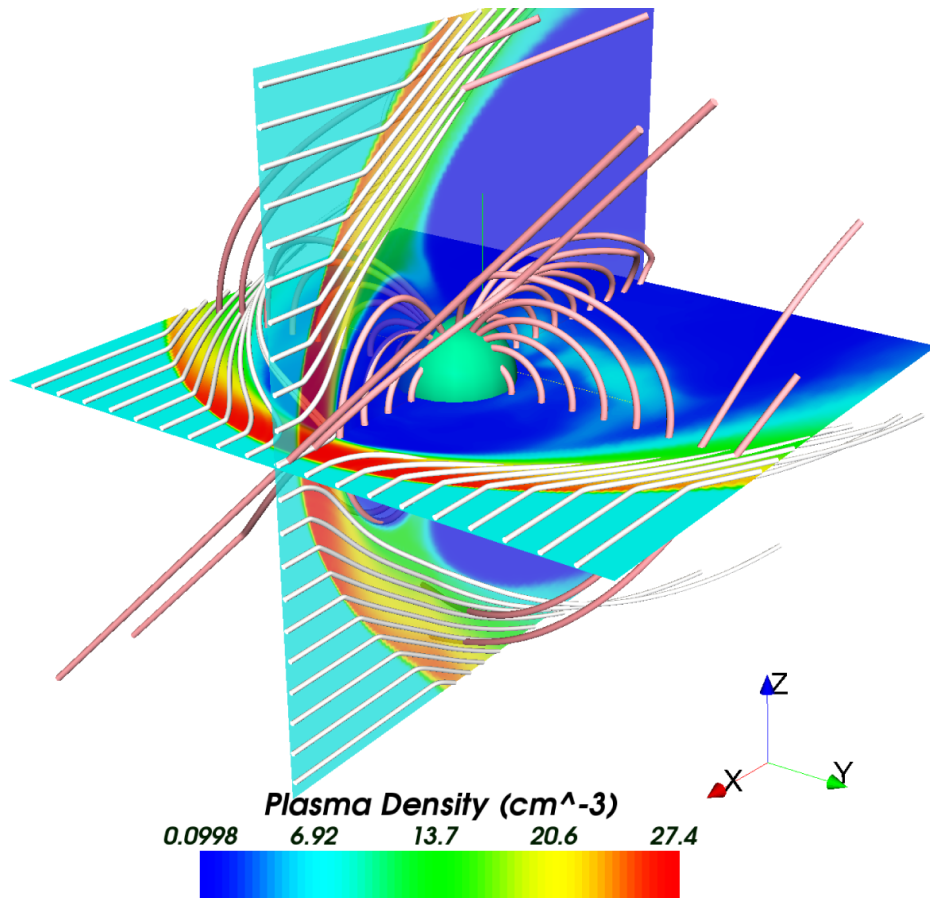
“Half-wave rectifier” effect



Burton et al., Science, 189, 717, 1975.

Magnetic storms (characterized by an enhancement in the ring current) occur during sustained periods of southward IMF.

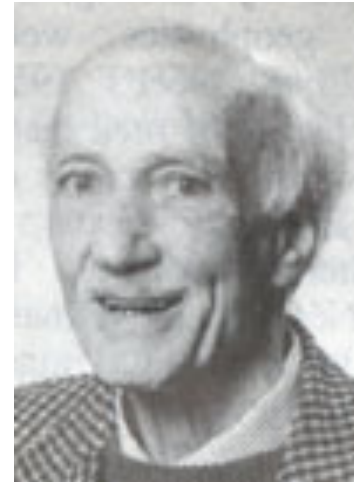
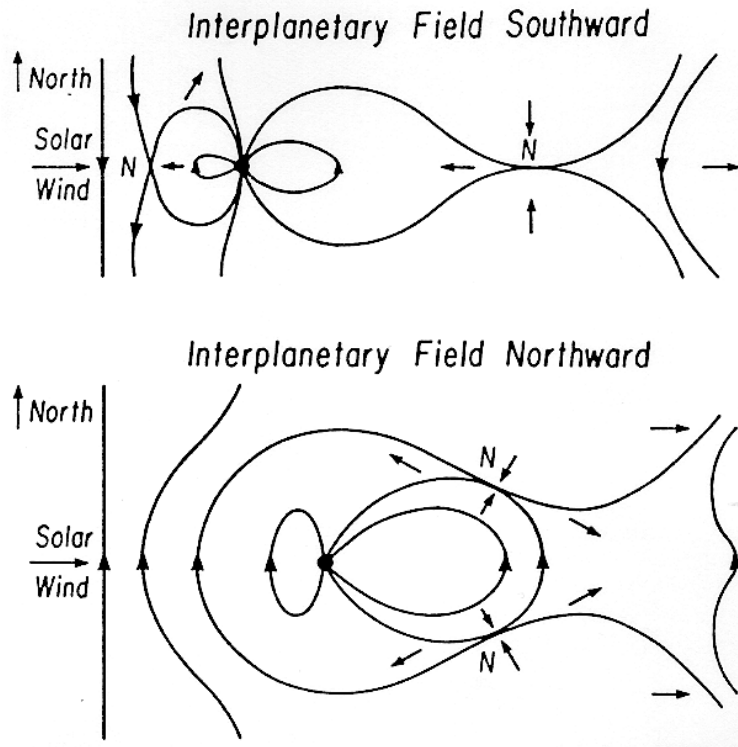
Dependence of geomagnetic activity on IMF orientation



Burton et al., Science, 189, 717, 1975.

Not much ring current enhancement during northward IMF

Magnetopause reconnection

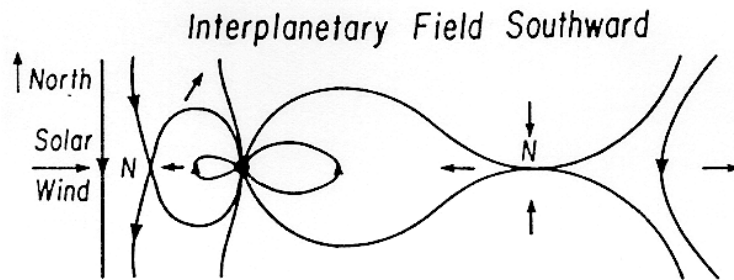


Dungey, J. W., PRL, 6, 47-48, 1961.

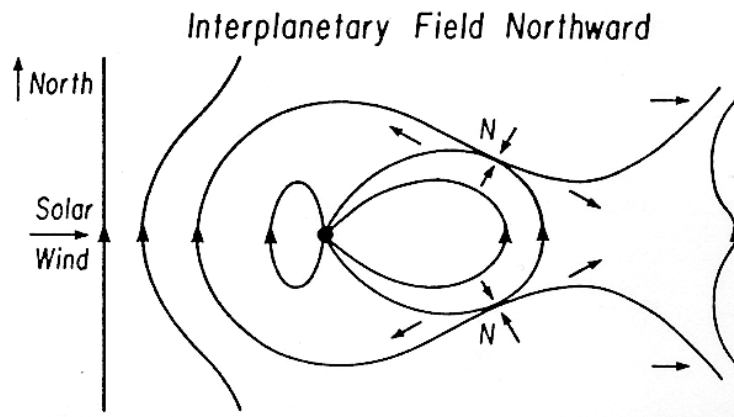
Dungey, J. W., in Geophysics: The Earth's Environment, eds., C. Dewitt *et al.*, 1963.

Breakdown of ideal MHD in a thin layer around the magnetopause implies that the solar wind field and plasma has access to the magnetosphere.

Magnetopause reconnection



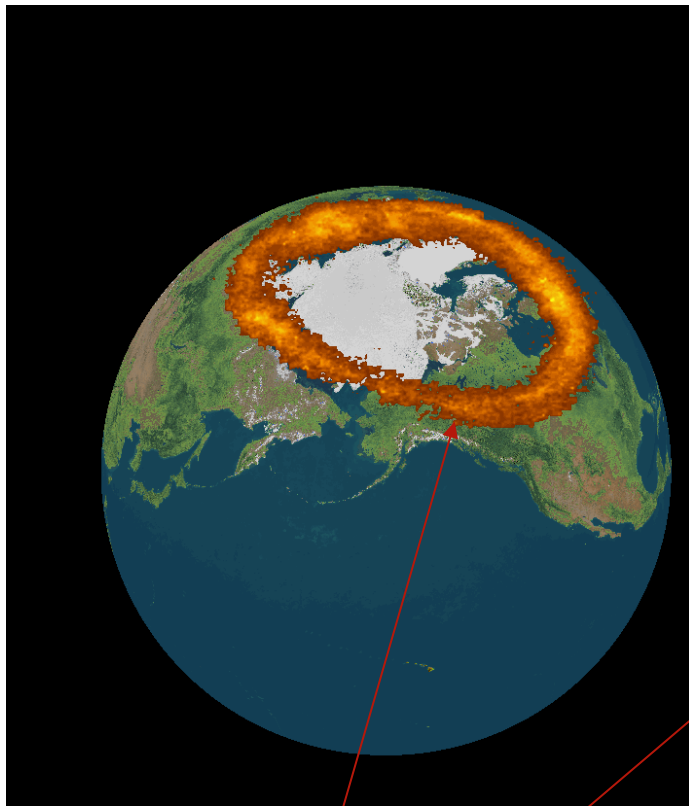
High geomagnetic activity
(magnetospheric storms and substorms)



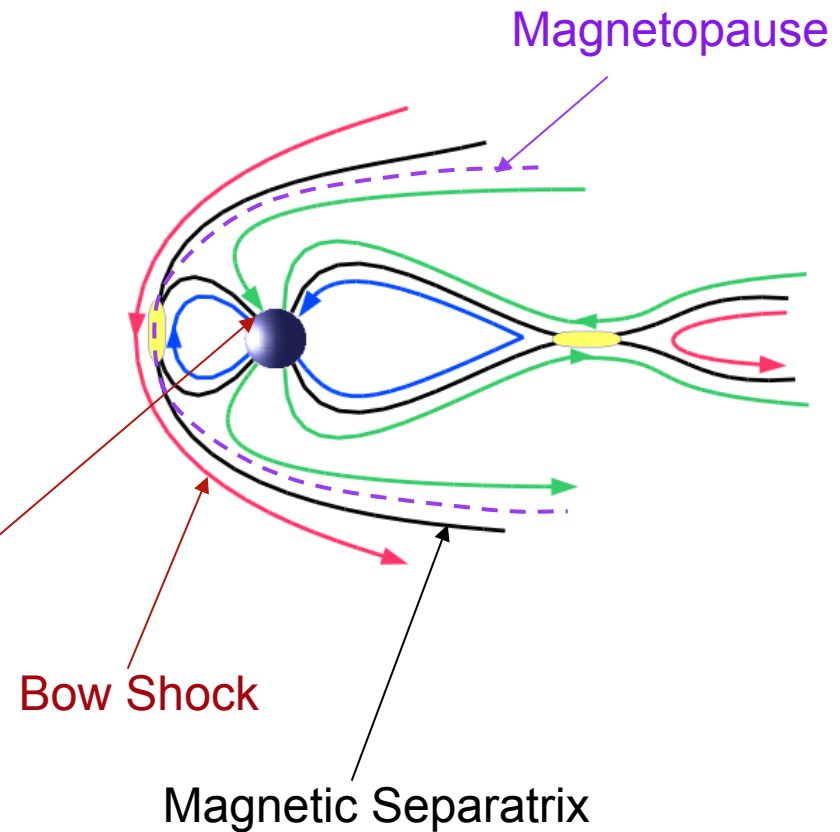
Low geomagnetic activity
(fewer storms and substorms)

“Magnetopause phenomena are more complicated as a result of merging. This is why I no longer work on the magnetopause.” -- J. W. Dungey

The auroral oval

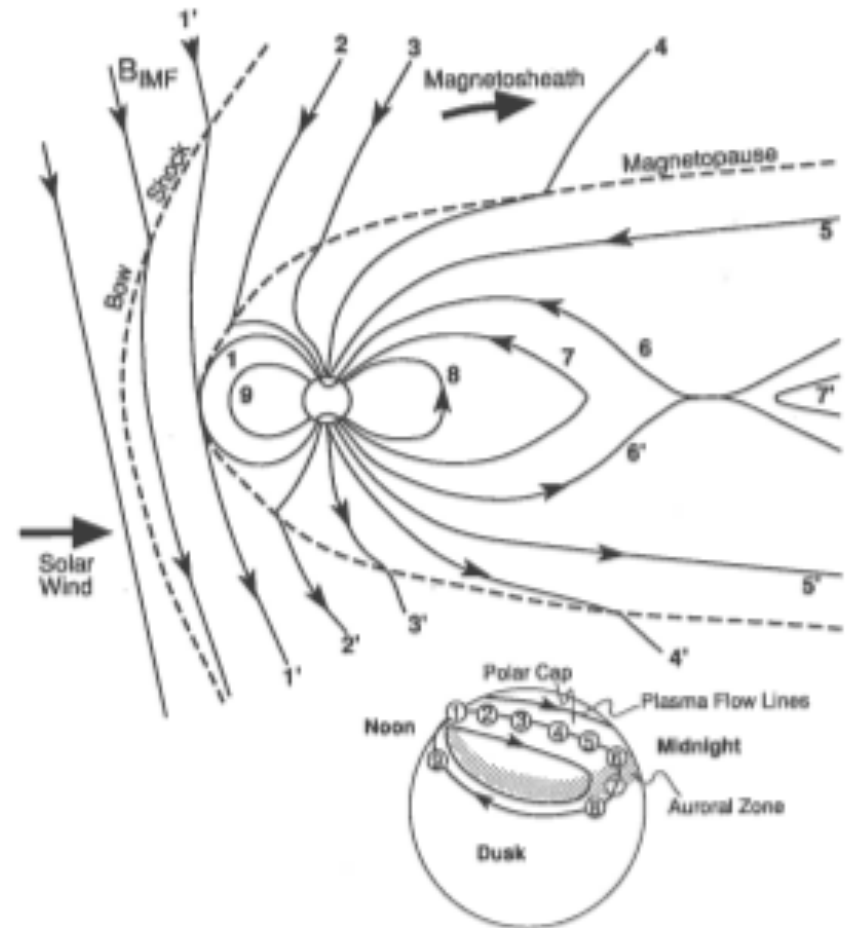
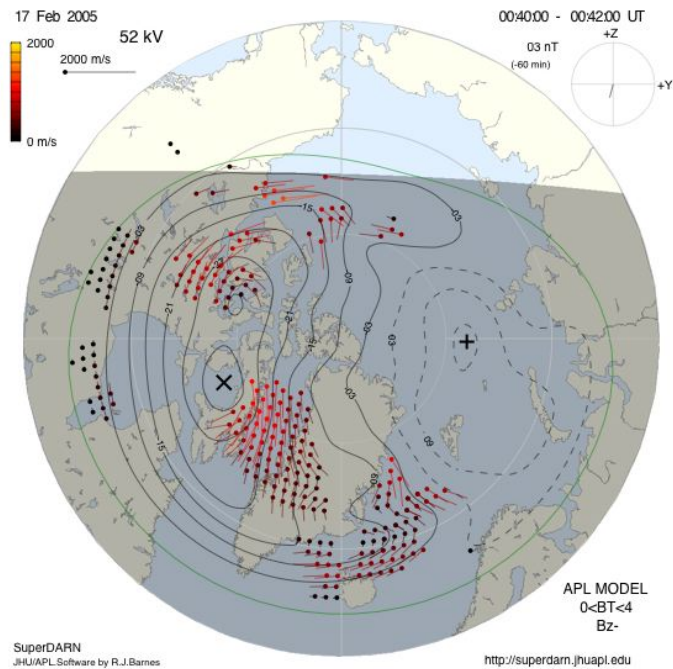


Polar VIS UV image of auroral oval (from <http://eiger.physics.uiowa.edu/~vis/examples>)



Auroral oval marks the boundary between open and closed field lines; the reconnection rate can be determined from radar observations of ionospheric convection (e.g., de la Beaujardiere *et al.*, J. Geophys. Res., 96, 13,907-13,912, 1991.).

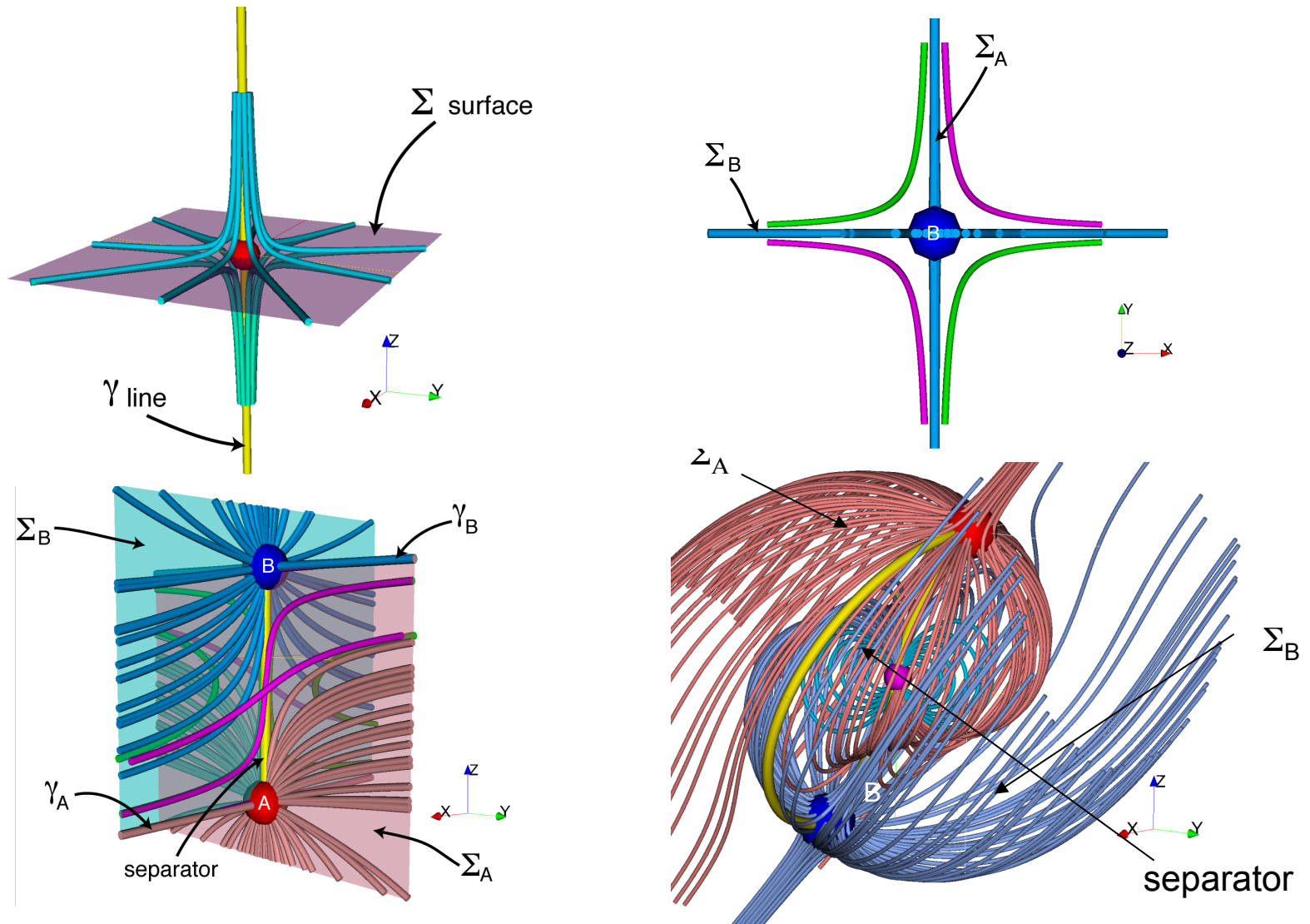
Global magnetospheric convection



SuperDARN Radar Array

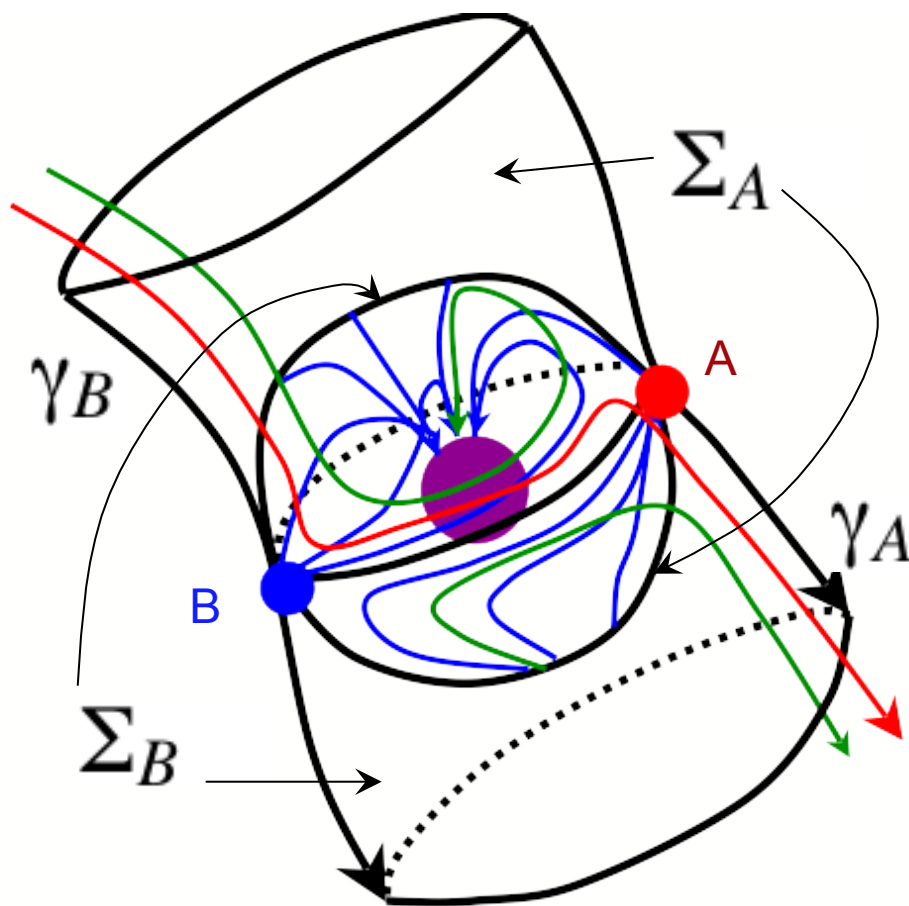
From "Introduction to Space Physics," eds.,
Kivelson, M. G. and C. T. Russell, Cambridge
U. Press, 1995.

3D Reconnection



Lau, Y.-T. and J. M. Finn, Three-dimensional kinematic reconnection in the presence of field nulls and closed field lines, Ap. J., 350, 672, 1990.

How efficient is dayside reconnection?



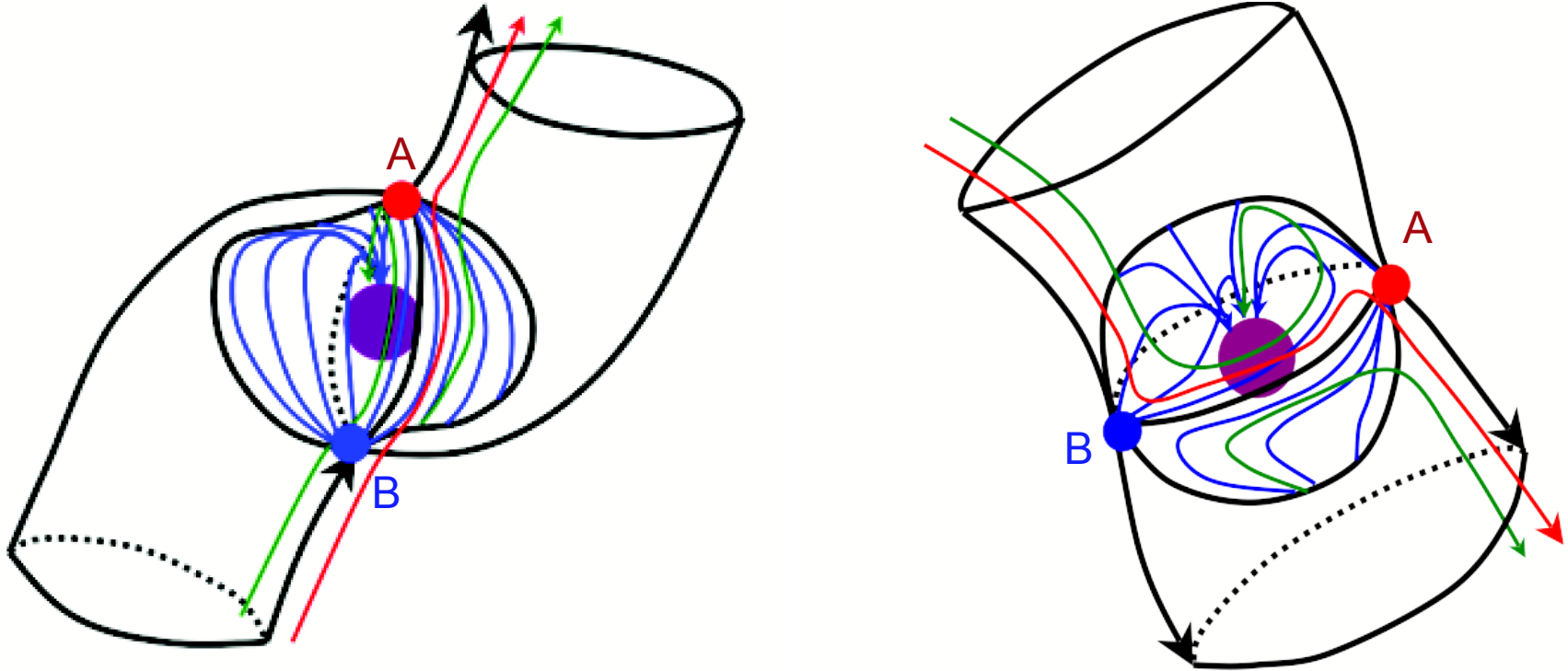
Forbes, T. G. and T. W. Speiser, Mathematical models of the open magnetosphere: applications to dayside auroras, *J. Geophys. Res.*, 76, 7542-7551, 1971.

Stern, D., A study of the electric field in an open magnetospheric model, *J. Geophys. Res.*, 78, 7292-7305, 1973.

Cowley, S. W. H., A qualitative study of the reconnection between the earth's magnetic field and an interplanetary field of arbitrary orientation, *Radio Sci.*, 8, 903, 1973.

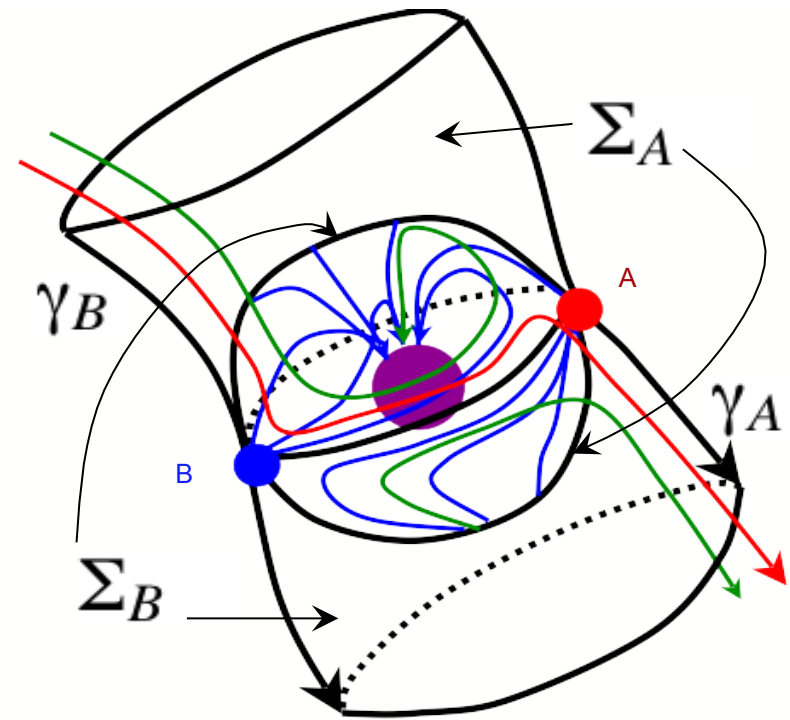
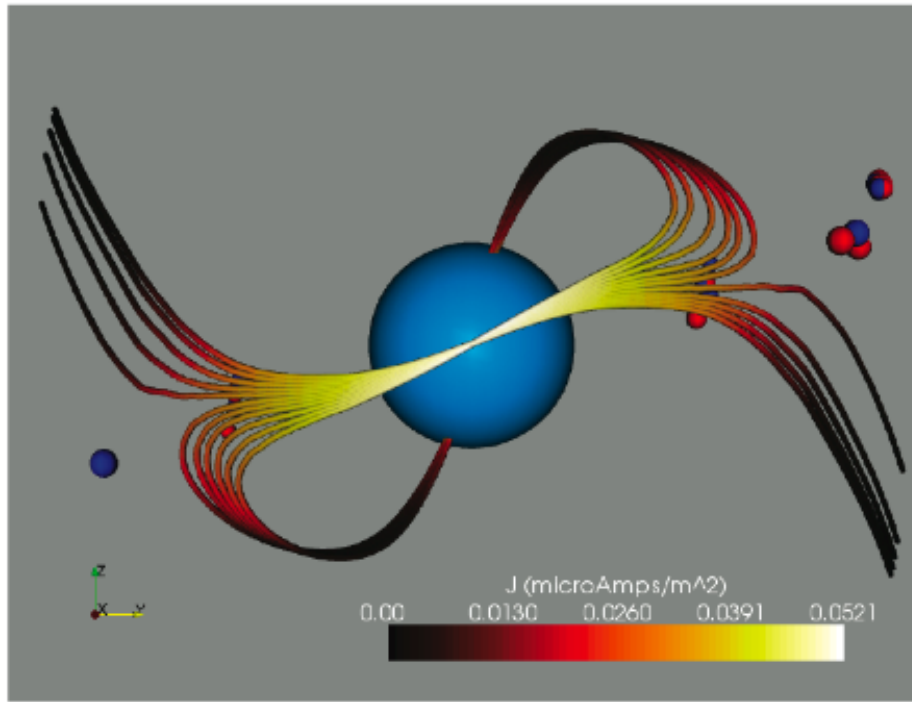
Lau, Y.-T. and John M. Finn, Three-dimensional kinematic reconnection in the presence of field nulls and closed field lines, *Ap. J.*, 350, 672-691, 1990.

Northward vs. Southward IMF



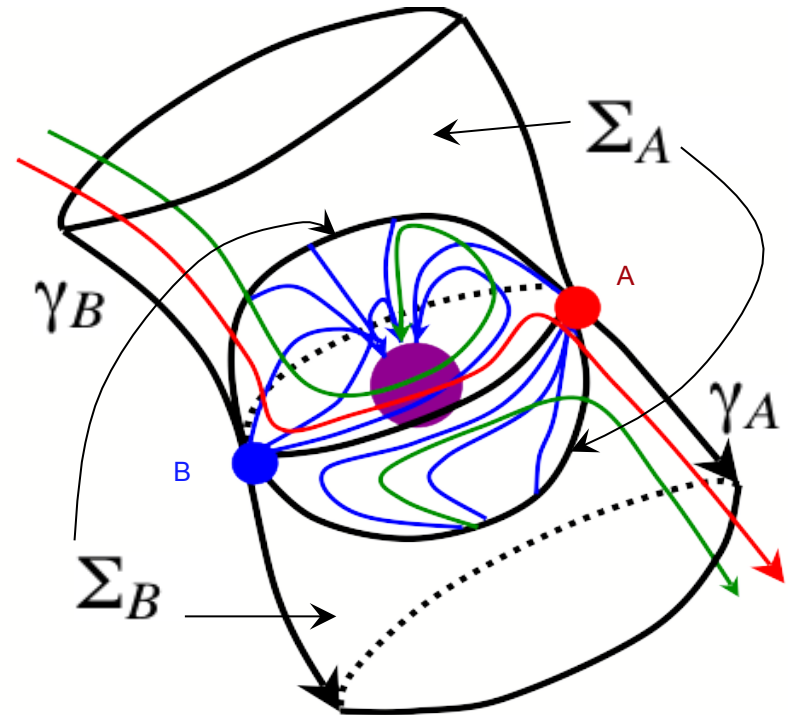
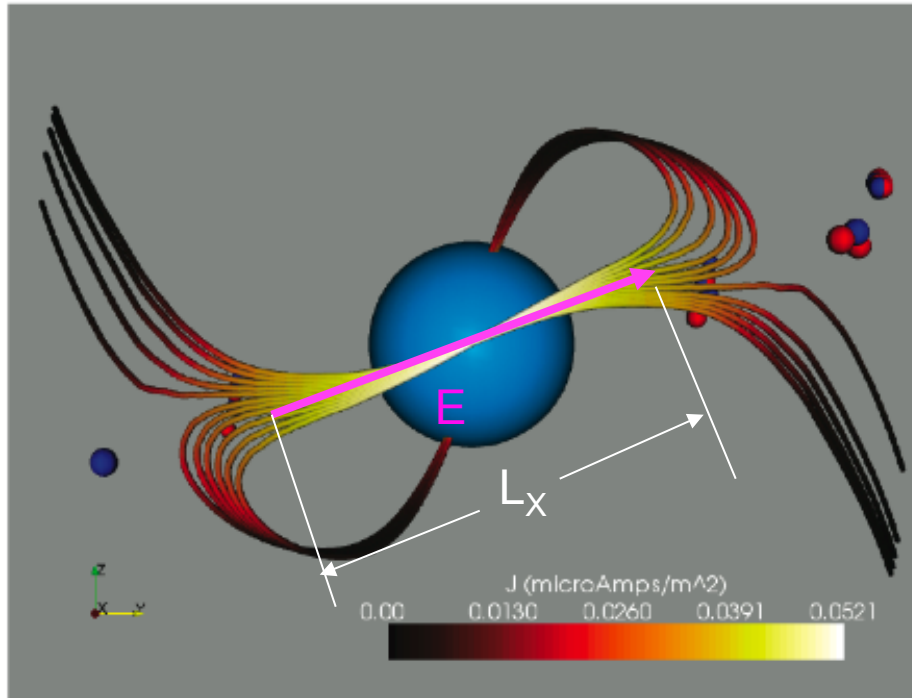
In 3D Dungey's topology is independent of the IMF orientation!

How efficient is dayside reconnection?



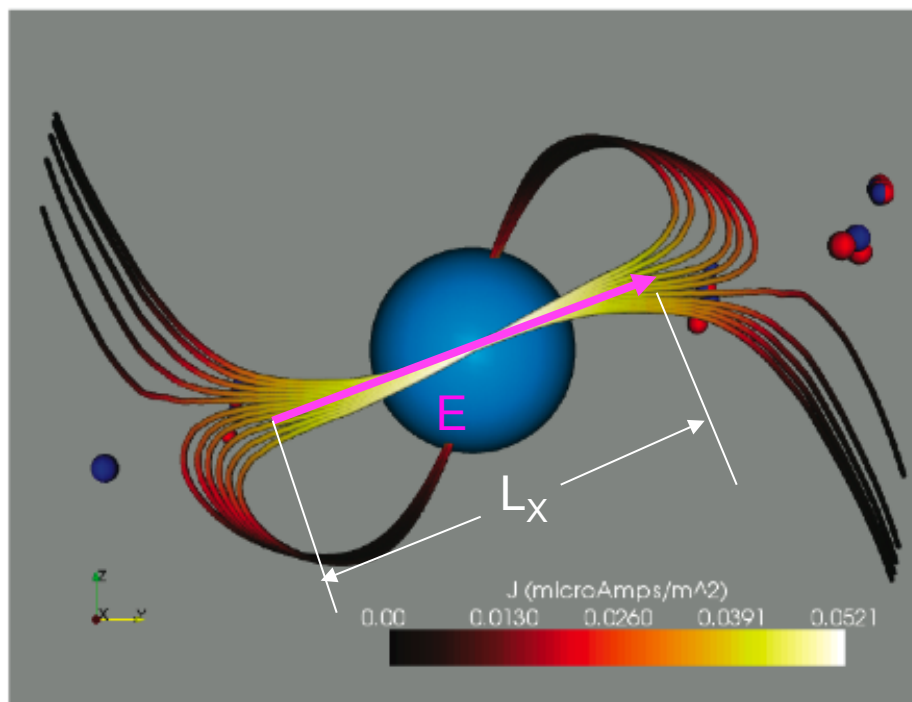
Rate at which open polar cap flux is created is given by the line integral of the electric field along the dayside magnetic separator (**Faraday's Law**).

How efficient is dayside reconnection?



Rate at which open polar cap flux is created is given by the line integral of the electric field along the dayside magnetic separator (**Faraday's Law**).

How efficient is dayside reconnection?

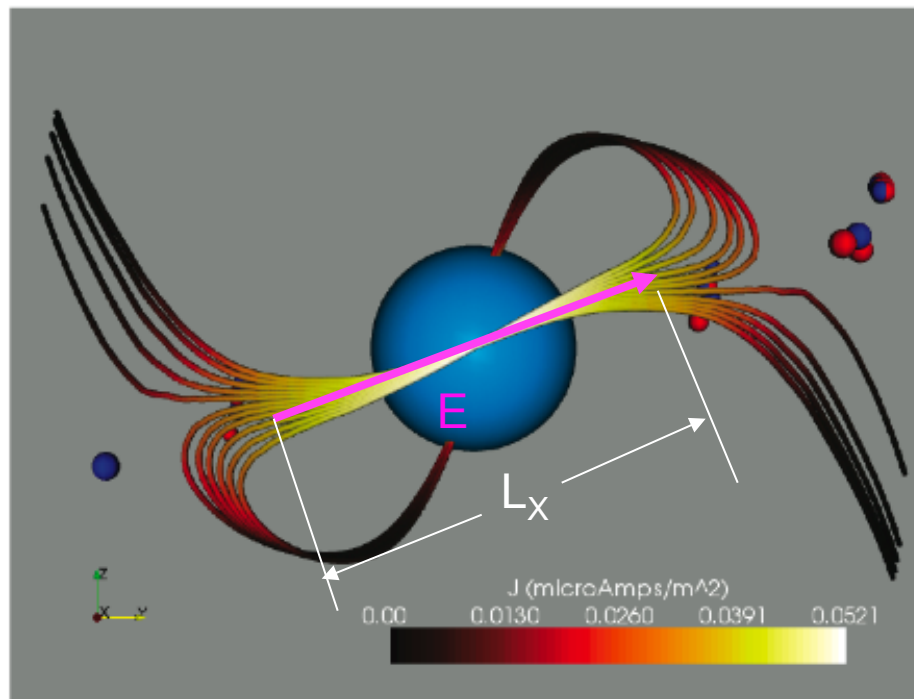


$$E \approx 0.1 \frac{V_A B_{sw}}{c}$$
$$\frac{d\Phi}{dt} \approx c E L_X \approx 0.1 V_A B_{sw} L_X$$

“Fast” reconnection

Rate at which open polar cap flux is created is given by the line integral of the electric field along the dayside magnetic separator (**Faraday's Law**).

How efficient is dayside reconnection?



$$E \approx 0.1 \frac{V_A B_{sw}}{c}$$

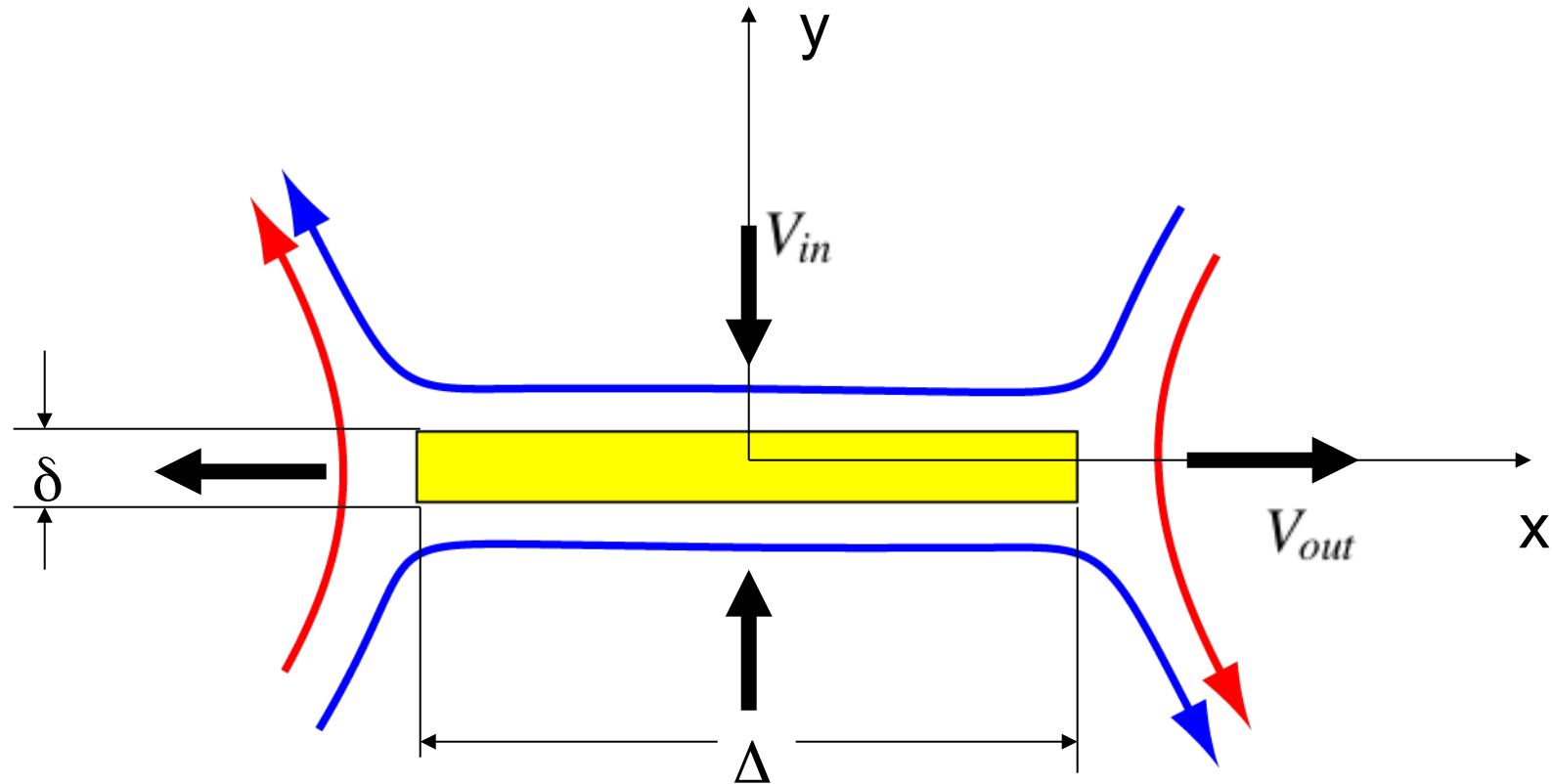
$$\frac{d\Phi}{dt} \approx cEL_X \approx 0.1V_A B_{sw}L_X$$

$$E \approx 0.1 - 0.5 \text{ mV/m}$$

$$V_R \approx 10 - 100 \text{ kV}$$

Rate at which open polar cap flux is created is given by the line integral of the electric field along the dayside magnetic separator (**Faraday's Law**).

Flux Pileup and the Sweet-Parker timescale problem



Momentum equation: $V_{out} \approx V_A \longrightarrow V_{in} \approx \frac{V_A}{S^{1/2}}$

Lundquist number: $S \equiv \frac{4\pi\Delta V_A}{c^2\eta}$

Flux Pileup and the Sweet-Parker timescale problem

Parker, E. N., Comments on the reconnection rate of magnetic fields, *J. Plasma Phys.*, 9, 49-63, 1973.

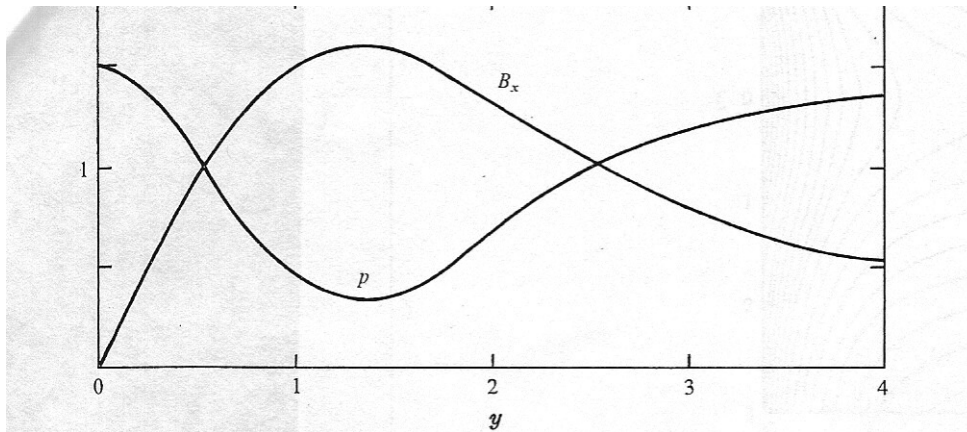


FIGURE 3. A plot of the magnetic field B_x and fluid pressure p as a function of distance y from the neutral plane, based on (47). The diffusion coefficient has the uniform value η and the velocity potential is again $\psi = \alpha xy$. Distance y is in units of the diffusion length $(\eta/\alpha)^{1/2}$.

2D incompressible MHD equations. Bulk velocity has the following form:

$$V_x = V_0 x$$

$$V_y = -V_0 y$$

$$V_{in} B_{in} = \frac{\delta}{\Delta} V_A B_{in}$$

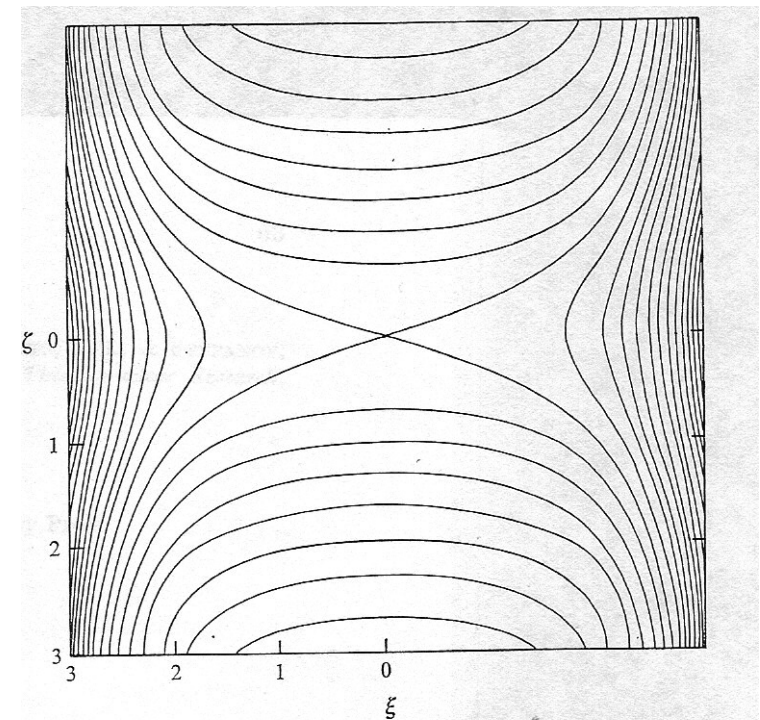
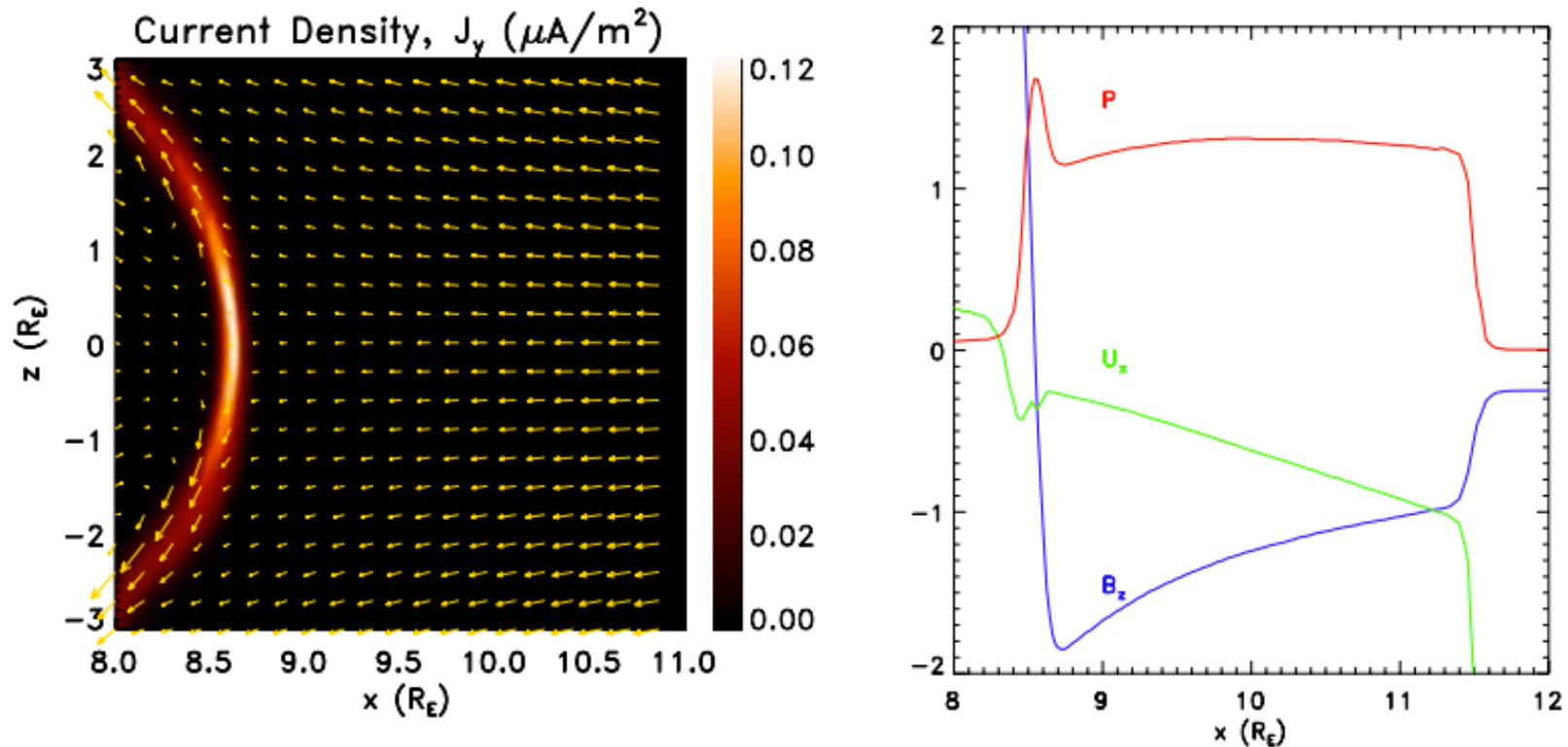


FIGURE 4. The magnetic lines of force for uniform η , $\psi = \alpha xy$ and $\nu = 0.1$, based on (44).

The upstream magnetic field increases to compensate for the reduction in resistivity (and consequent reduction of inflow speed).

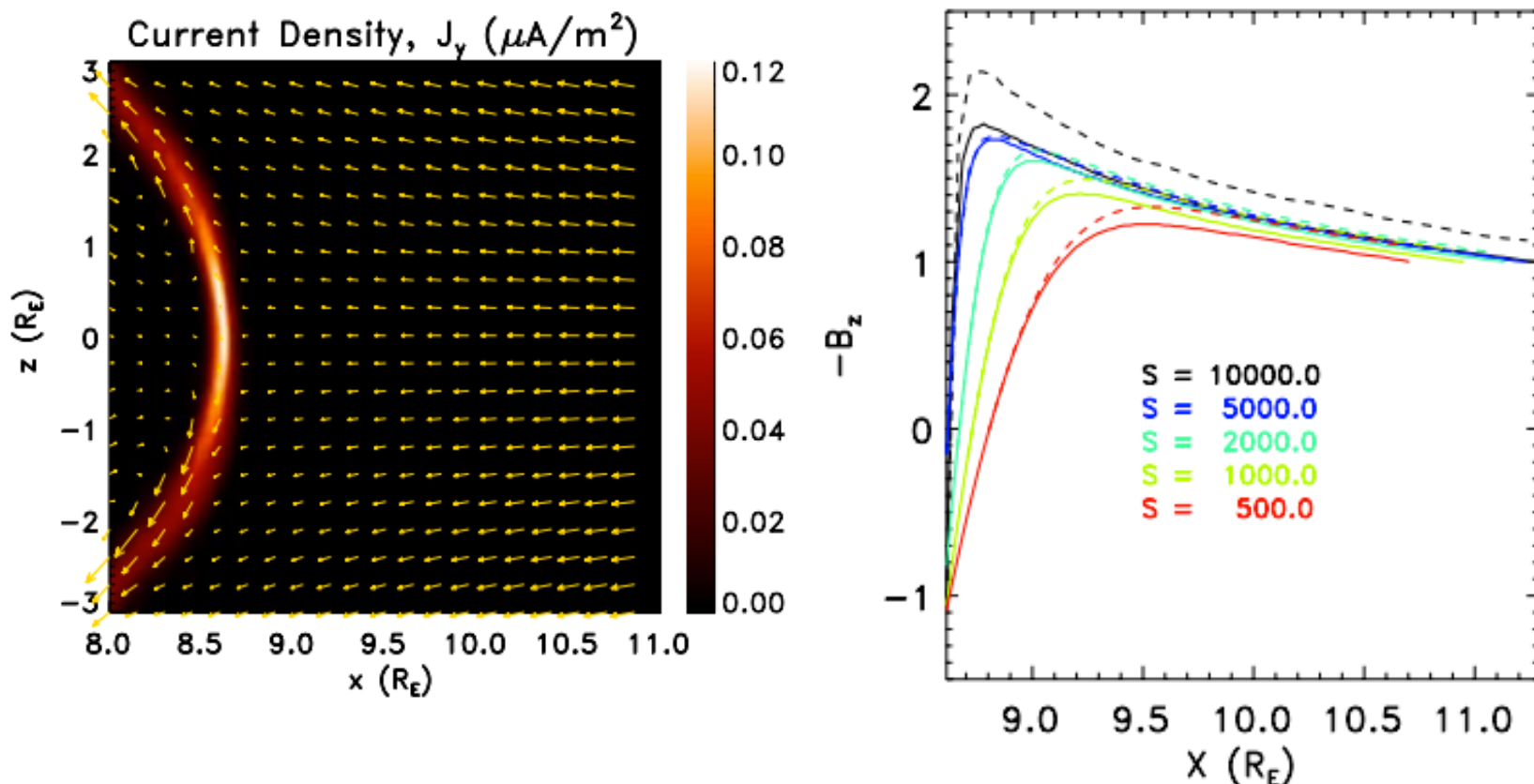
Flux pileup reconnection in global MHD simulations



J. C. Dorelli *et al.*, *J. Geophys. Res.*, 109, 2004.

In high Lundquist number resistive MHD simulations, flux pileup occurs under both northward and southward IMF conditions!

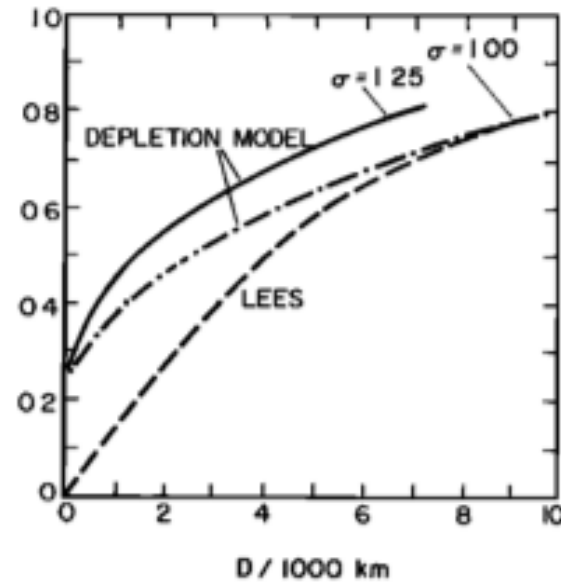
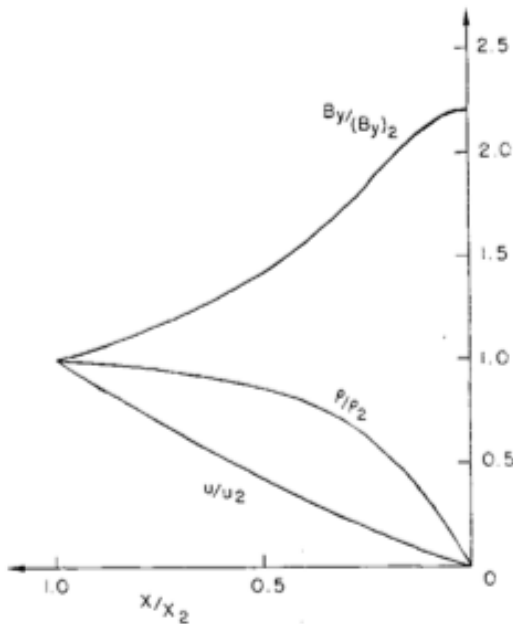
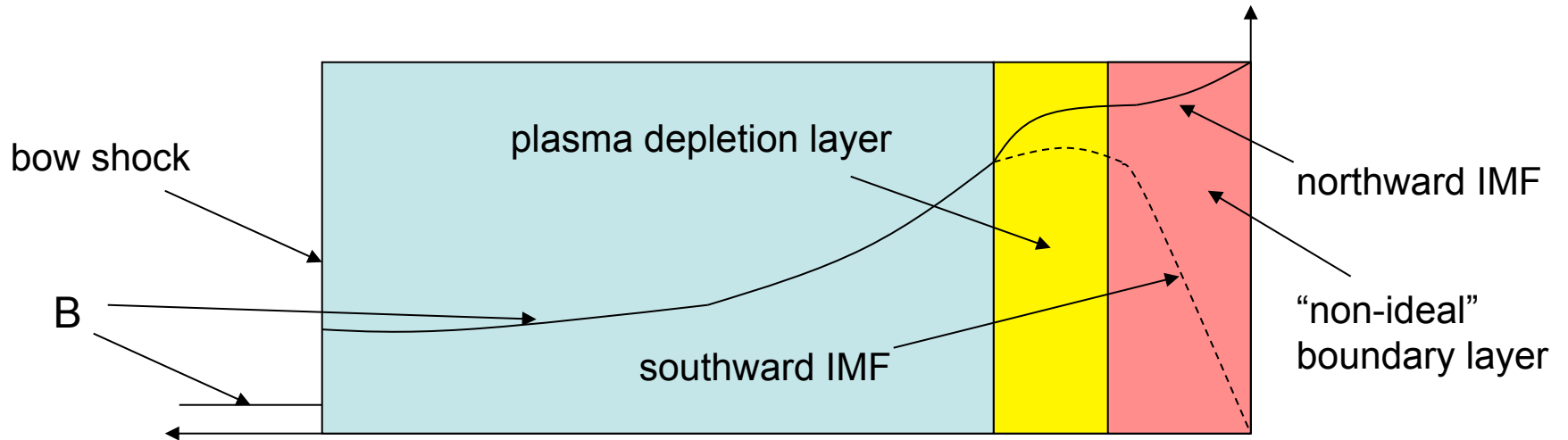
Flux pileup reconnection in global MHD simulations



J. C. Dorelli *et al.*, *J. Geophys. Res.*, 109, 2004.

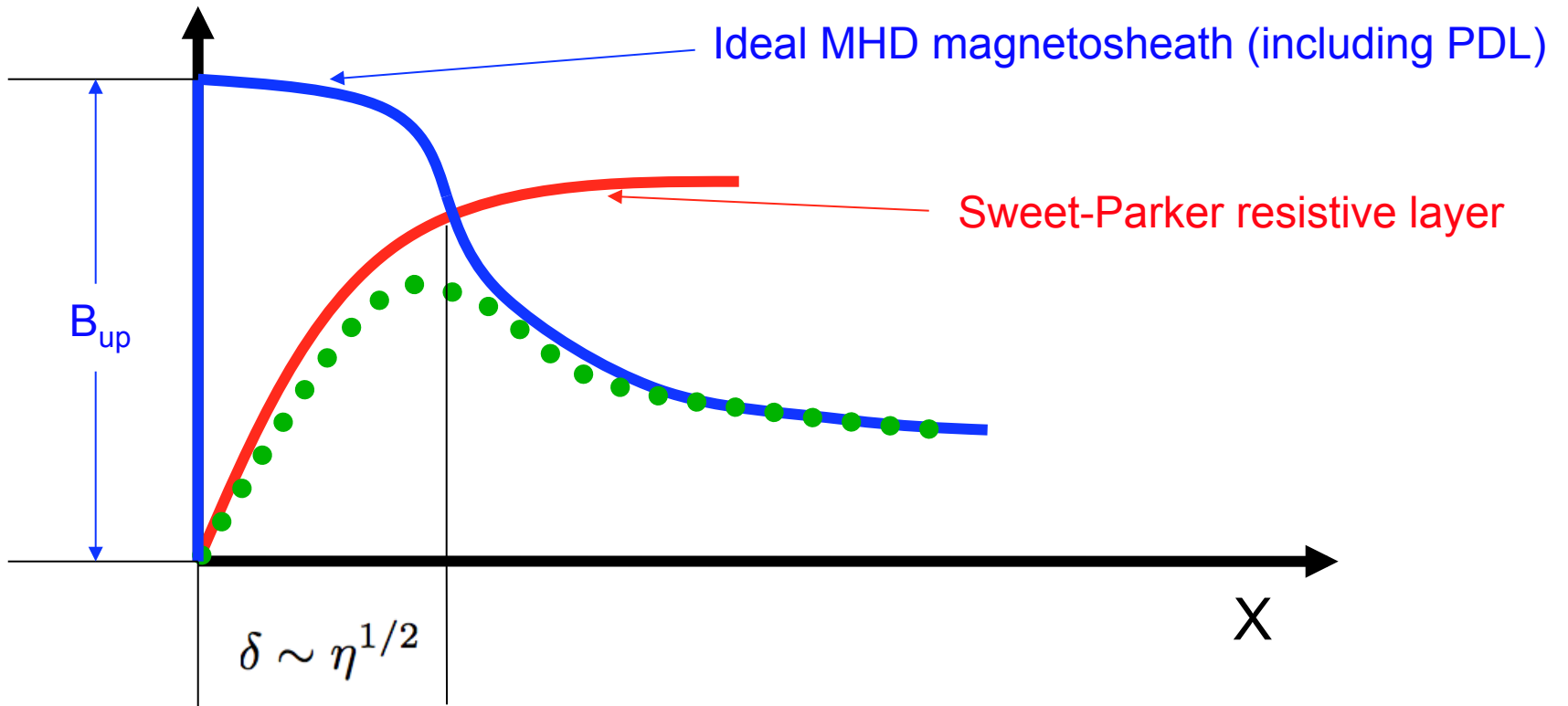
The amount of pileup increases with decreasing resistivity since the resistive boundary layer thickness decreases (i.e., the classical magnetosheath pileup region extends closer to the magnetopause).

Recall the physics of the plasma depletion layer....



Even in the ideal MHD limit, the magnetic field at the subsolar magnetopause cannot be larger than that corresponding to the maximum possible plasma depletion.

What impact does the PDL have on the reconnection rate?

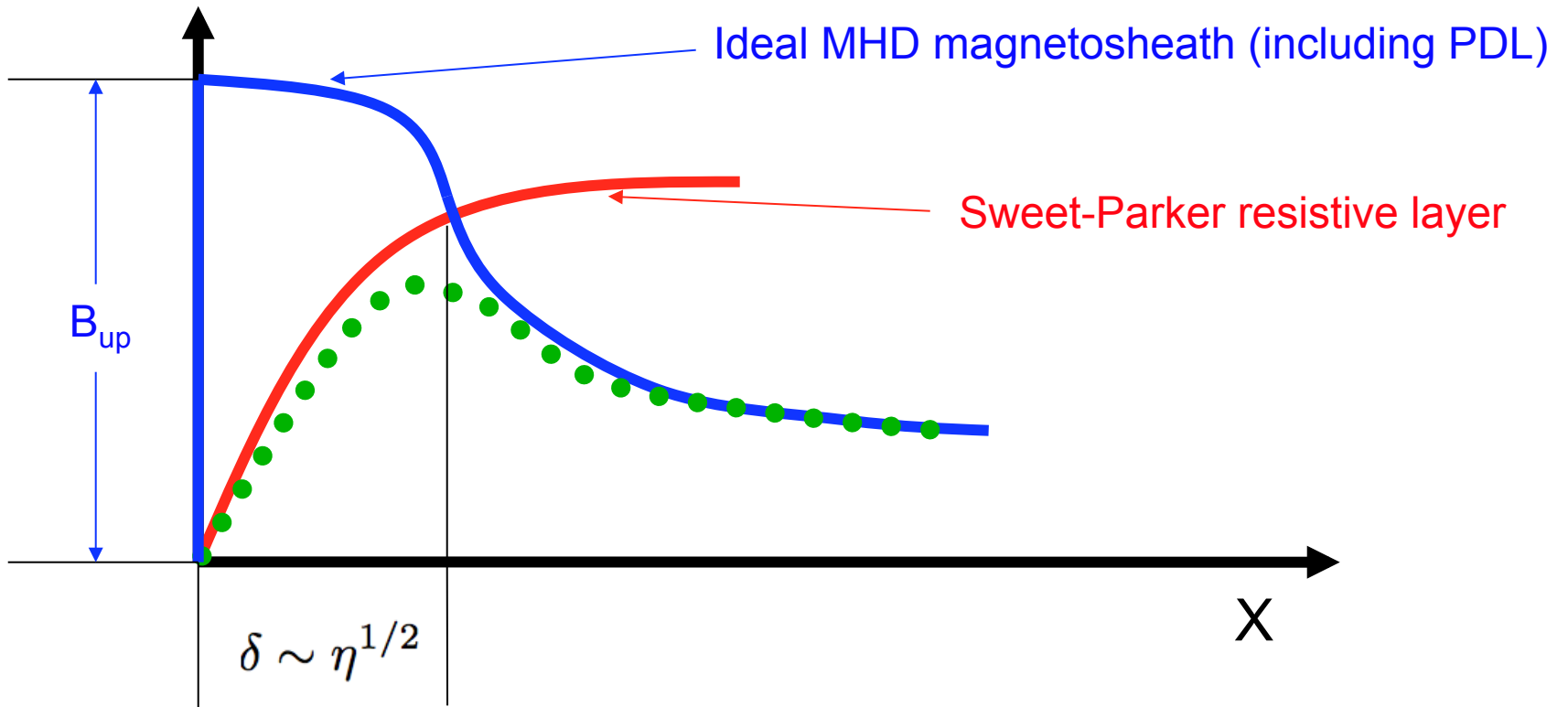


$$\nabla \cdot (\rho \mathbf{V}) = 0$$

$$\nabla \cdot \left[\rho \mathbf{V} \mathbf{V} + \left(p + \frac{B^2}{8\pi} \right) \mathbf{I} - \frac{\mathbf{B} \mathbf{B}}{4\pi} \right] = 0$$

$$\nabla \times (\mathbf{V} \times \mathbf{B}) + \frac{c^2 \eta}{4\pi} \nabla^2 \mathbf{B} = 0$$

Asymptotic matching of the PDL to the Sweet-Parker layer



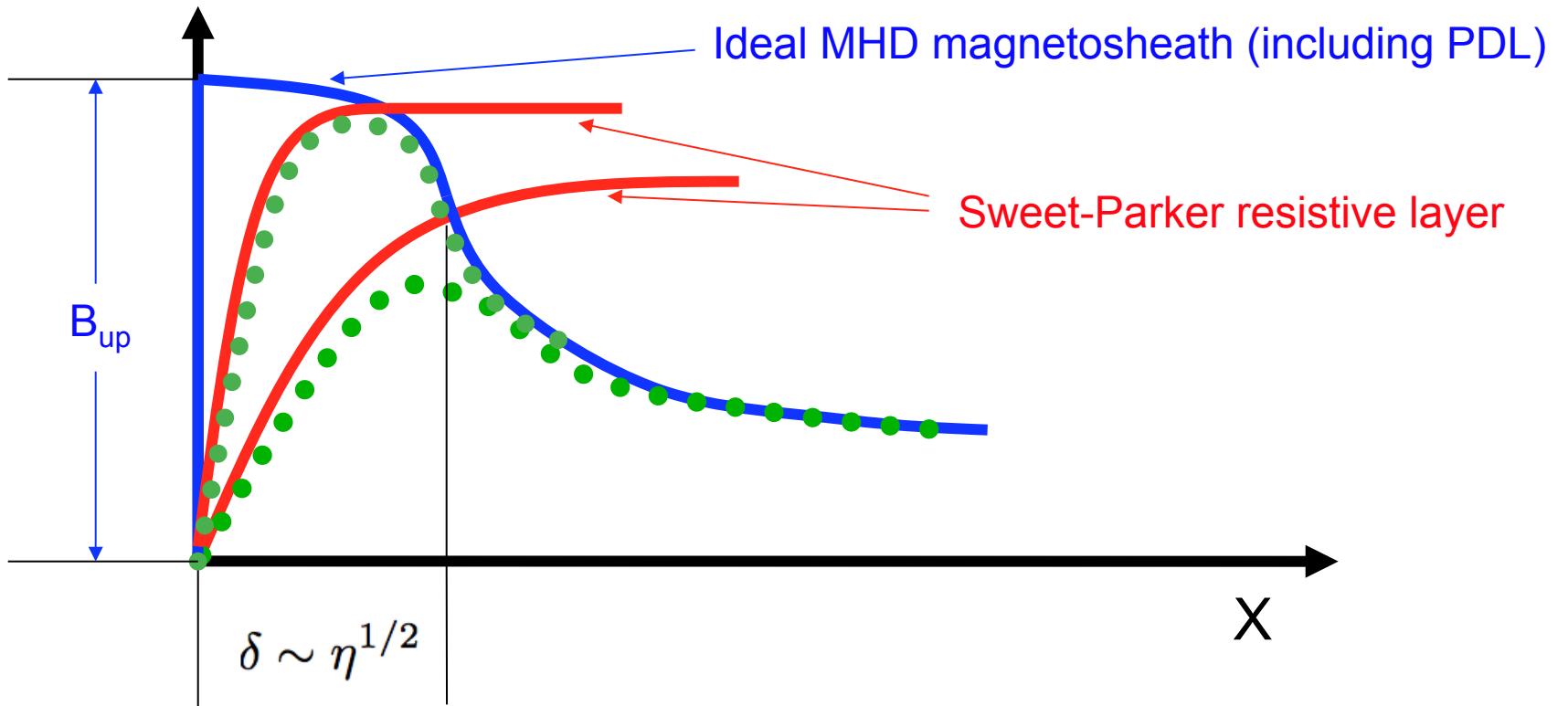
$$\epsilon \frac{d^2 B}{dx^2} + f(x) \frac{dB}{dx} + g(x) B = 0$$

$$B(0) = 0$$

$$B(L) = B_1$$

The ideal MHD sheath solution cannot simultaneously satisfy both boundary conditions!

What happens as resistivity decreases?



Limit as resistivity approaches zero

$$E = \eta J \approx \eta B_{up} / \delta \propto \eta^{1/2}$$

Summary so far....

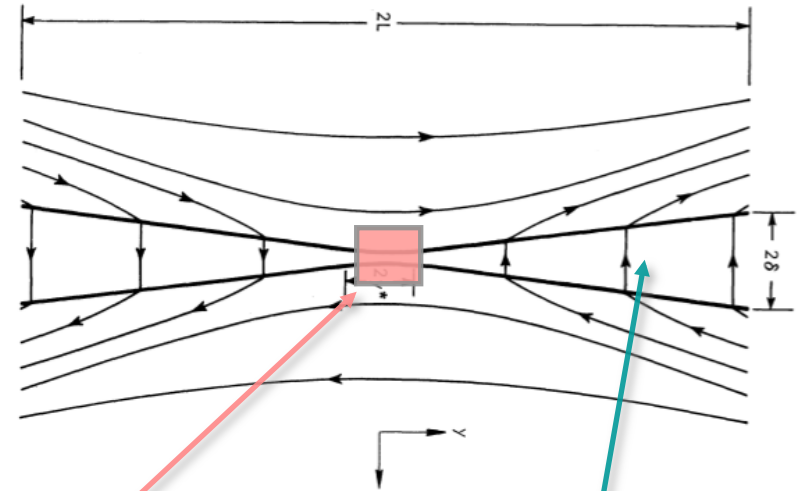
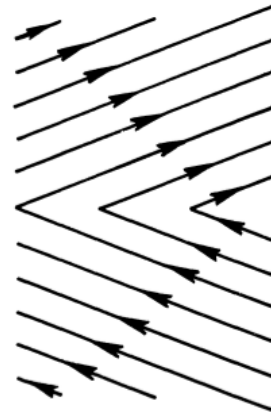
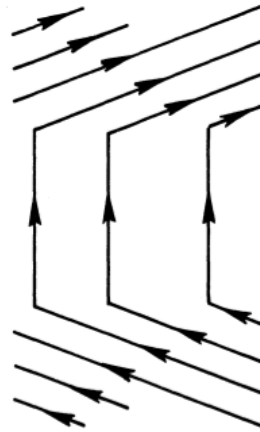
Ideal MHD magnetosphere

- o The Chapman-Ferraro current system completely separates Earth's magnetic field from the solar wind plasma.
- o The solar wind has no access to the magnetosphere
- o Far enough away from the magnetopause, the magnetosheath is well-described by gas dynamics (though the Spreiter *et al.*[1966] expression for the bow shock standoff distance must be modified as the upstream Mach number approaches 1).
- o A Plasma Depletion Layer develops near the subsolar magnetopause in response to magnetic flux pileup in the sheath (gas dynamics breaks down near the magnetopause in response to magnetic flux pileup in the magnetosheath).

The reconnecting magnetosphere

- o Separator reconnection at the dayside magnetopause allows solar wind access to the magnetosphere, drives global magnetospheric convection and is the ultimate driver of geomagnetic activity (e.g., magnetic storms).
- o In the resistive MHD model, the plasma depletion limits the amount of flux pileup that can occur in the collisionless limit; we therefore expect the reconnection rate to approach zero as resistivity approaches zero (**Sweet-Parker time scale problem**).

The importance of plasma waves



Harry Petschek

Diffusion

Waves

Waves play the dominant role (rather than diffusion) in converting magnetic energy to plasma energy.

Reconnection becomes insensitive to the plasma resistivity!

Dr. Sweet: I would like to make two points: One is that I am in favor of your theory, which I thoroughly approve. Dr. Parker and I have been living with this problem for several years and have got the feel of it. Your solution struck me at once as the solution for which we have been seeking.

Petschek, H., Magnetic field annihilation, in *Physics of Solar Flares*, ed. W. N. Ness, NASA SP-50, 425, 1964.

Did Petschek correctly match the wave solution to the diffusion region?

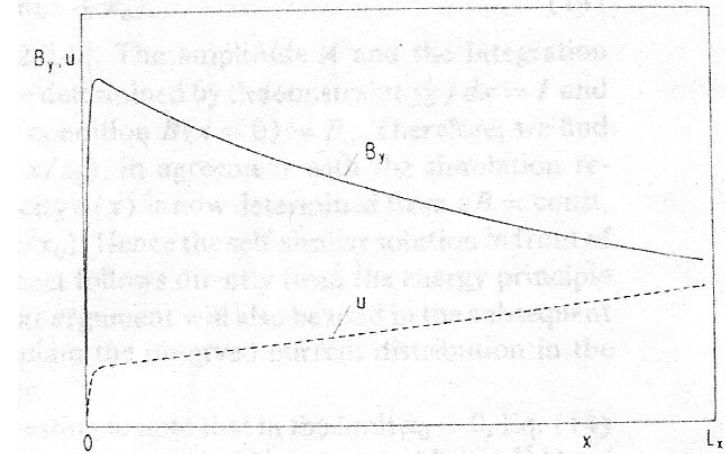
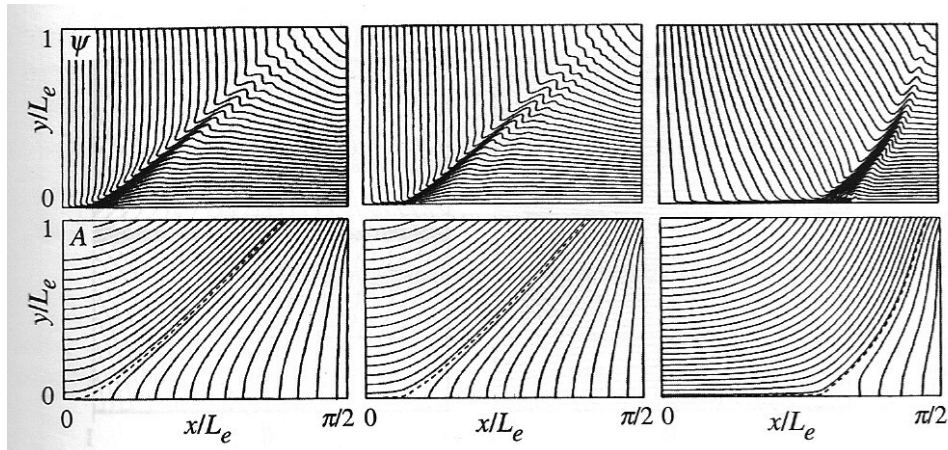


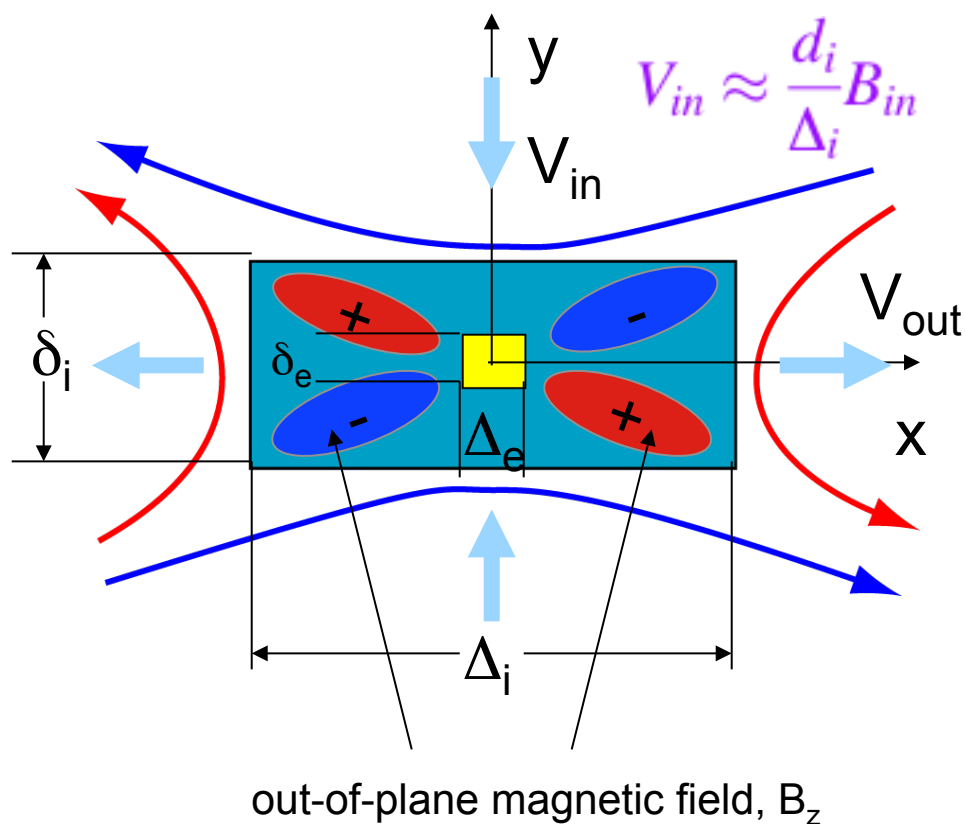
FIG. 4. $B_y(x), u(x)$ for $y = 0$ of a pile-up configuration (case 6 of Table I).

Biskamp, D., Magnetic reconnection via current sheets, *Phys. Fluids*, 29, 1520-1531, 1986.

Δ increases with decreasing resistivity; this directly contradicts the Petschek model, which requires $\Delta \sim \delta \sim \eta$.

the particular choice of boundary conditions. Because of the presence of a current sheet, the overall reconnection process is quite slow. This picture essentially agrees with Syrovatsky's [Sov. Phys. JETP 33, 933 (1971)] theory and disproves Petschek's [AAS/NASA Symposium on the Physics of Solar Flares, (NASA, Washington, DC, 1964) p. 425] mechanism of fast magnetic

Hall MHD to the rescue?



Whistler waves?

“The reconnection rate is found to be a universal constant, corresponding to an inflow velocity...of around $0.1 V_A$.”

M. Shay

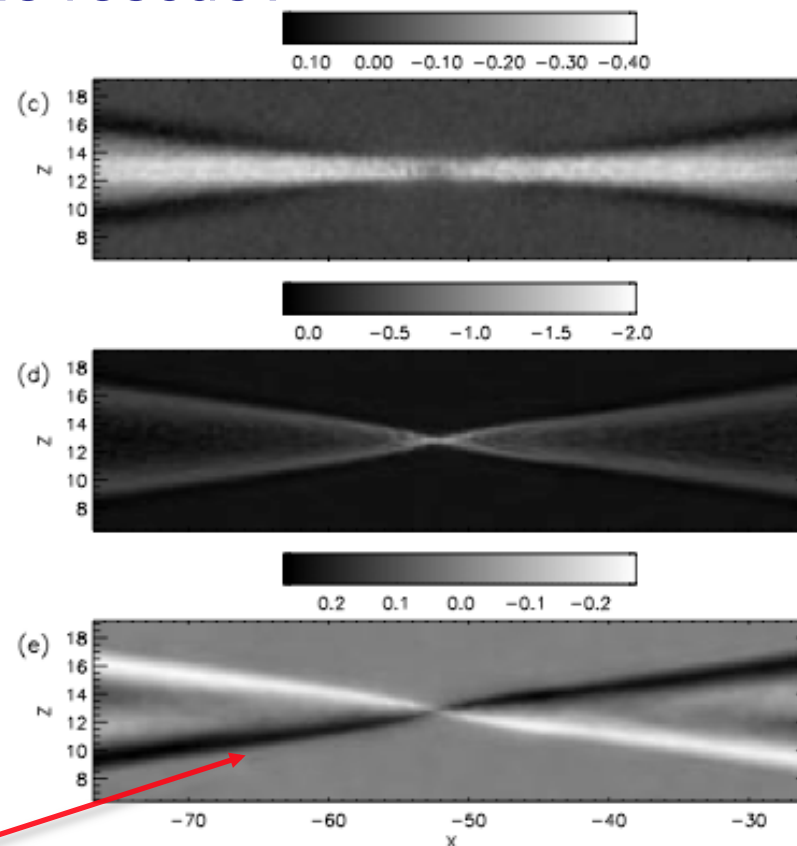
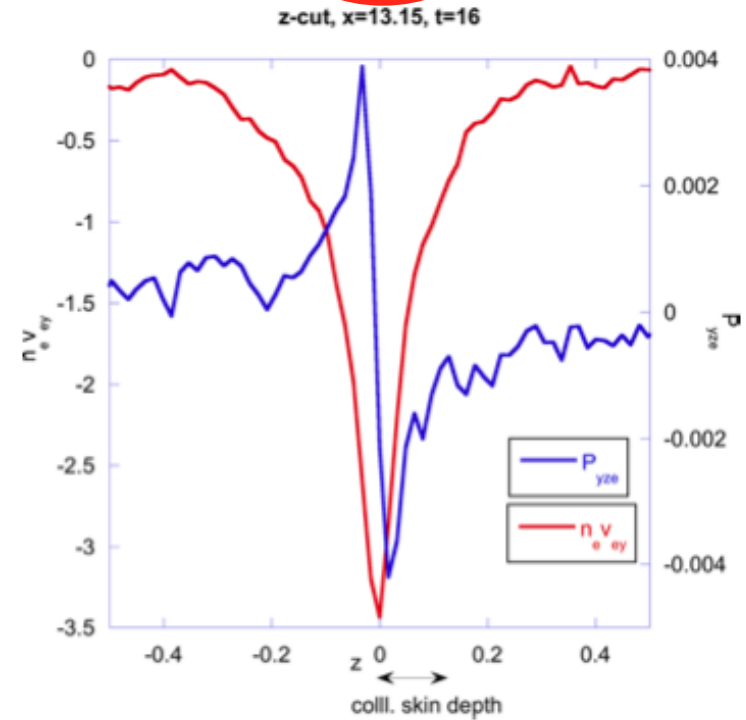
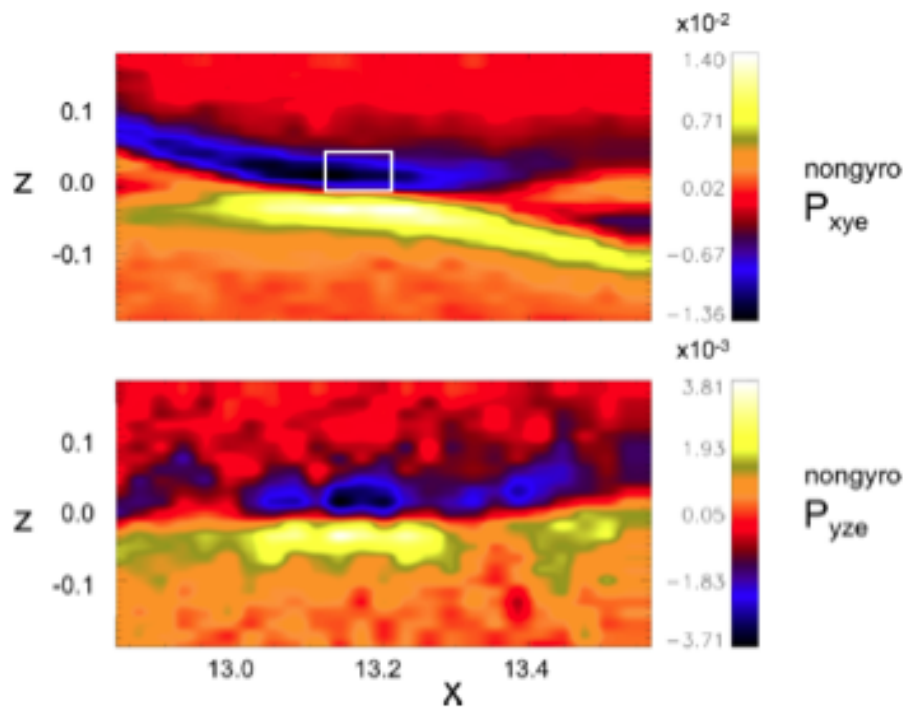


Figure 1. Structure of the x-line: (a) in-plane magnetic field, (b) in-plane ion velocity, (c) out-of-plane ion current, (d) out-of-plane electron current, (e) out-of-plane magnetic field.

Shay, M. A., J. F. Drake and B. N. Rogers, The scaling of collisionless magnetic reconnection for large systems, *Geophys. Res. Lett.*, 26, 2163-2166, 1999.

What breaks the frozen flux theorem?

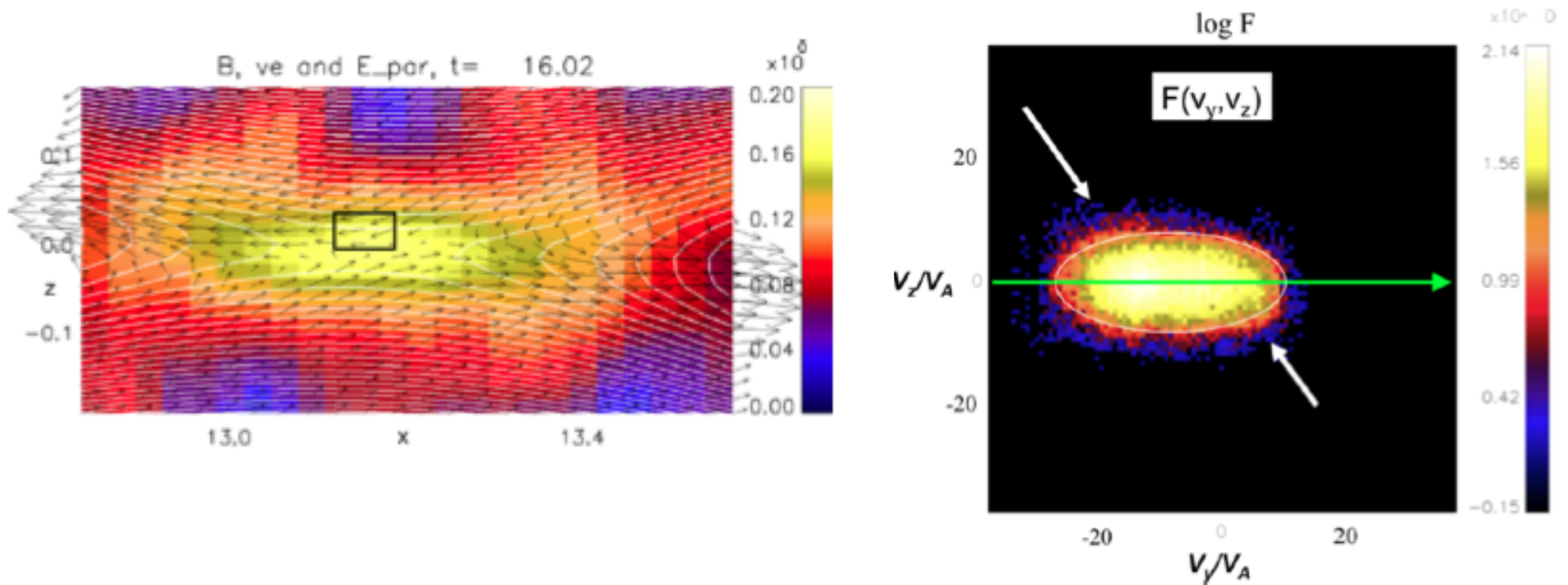
$$E = -\frac{V \times B}{c} + \frac{J \times B}{c} - \frac{\nabla \cdot P_e}{ne}$$



Hesse et al., The diffusion region of collisionless magnetic reconnection, Space Sci. Rev., 2011.

What breaks the frozen flux theorem?

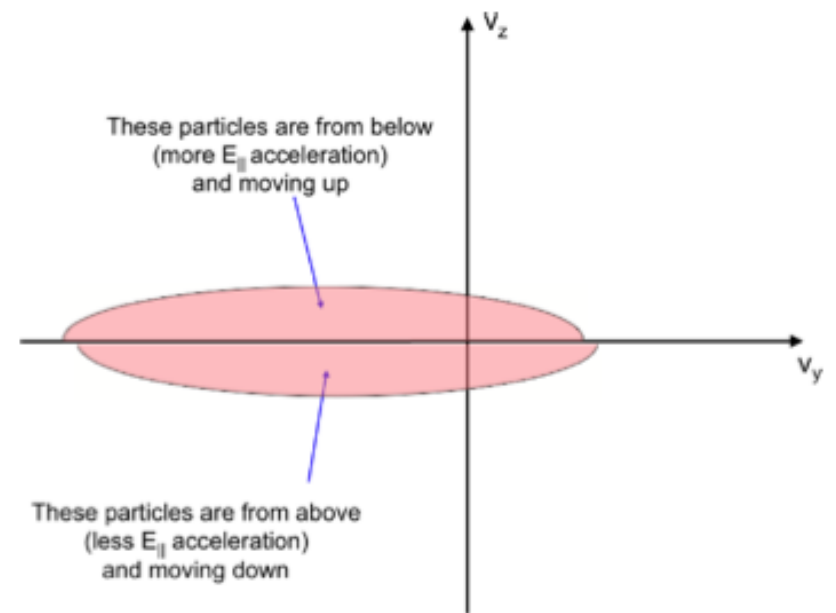
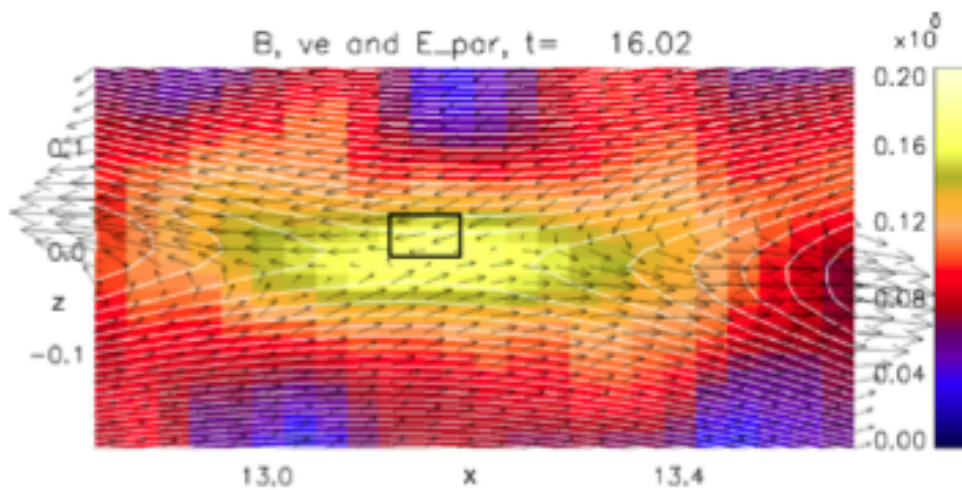
$$E = -\frac{V \times B}{c} + \frac{J \times B}{c} - \frac{\nabla \cdot P_e}{ne}$$



Hesse et al., The diffusion region of collisionless magnetic reconnection, Space Sci. Rev., 2011.

What breaks the frozen flux theorem?

$$\mathbf{E} = -\frac{\mathbf{V} \times \mathbf{B}}{c} + \frac{\mathbf{J} \times \mathbf{B}}{c} - \frac{\nabla \cdot \mathbf{P}_e}{ne}$$



Hesse et al., The diffusion region of collisionless magnetic reconnection, Space Sci. Rev., 2011.

Turbulent reconnection driven by 3D collisionless tearing?

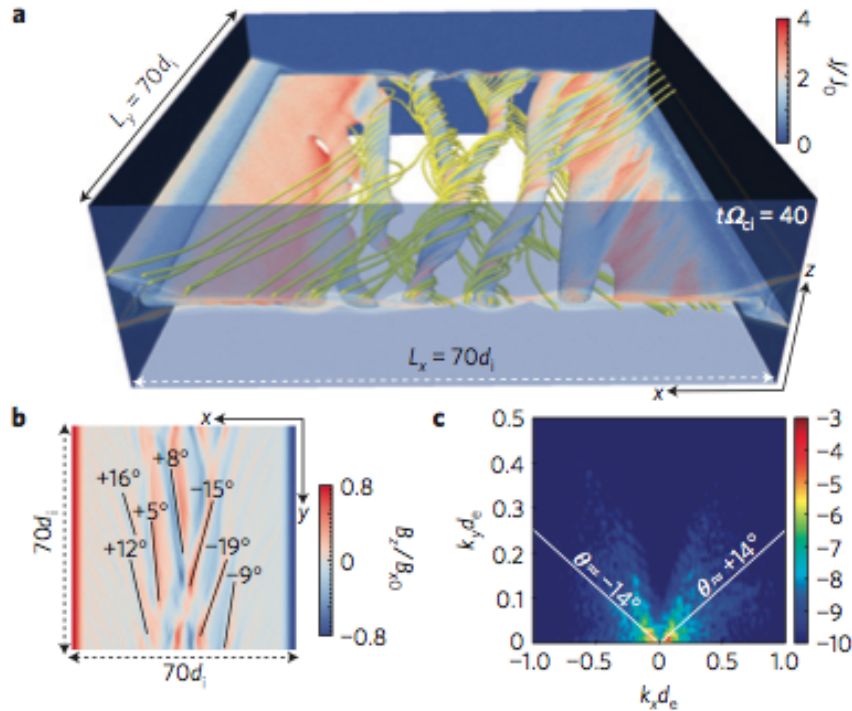


Figure 1 | Formation of primary flux ropes. **a**, At early time $t\Omega_{ci} = 40$, the tearing instability gives rise to flux ropes as illustrated by an isosurface of the particle density coloured by the magnitude of the current density (normalized by $J_0 \equiv cB_{x0}/(4\pi\lambda)$) along with sample magnetic-field lines (yellow). **b**, Typical angles $\theta \equiv \tan^{-1}(k_y/k_x)$ for these ropes are directly measured by examining B_z at the centre of the layer ($z = 0$). **c**, The power spectrum of $|\hat{B}_z|^2/B_{x0}^2$ is shown on a log scale. The solid white line corresponds to the dominant angle in the spectrum.

Daughton *et al.*, *Nature Phys.*, 2011.

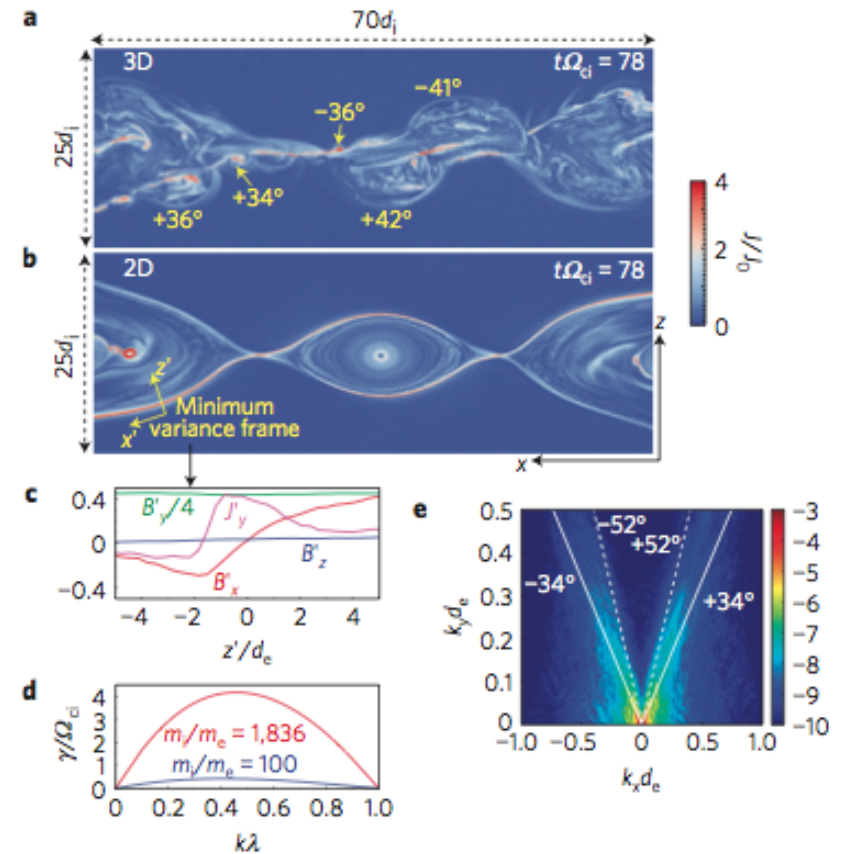
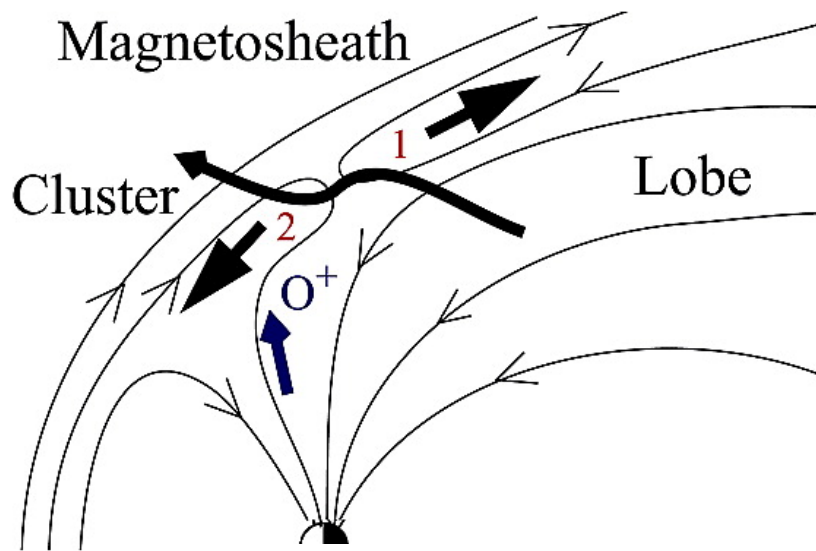


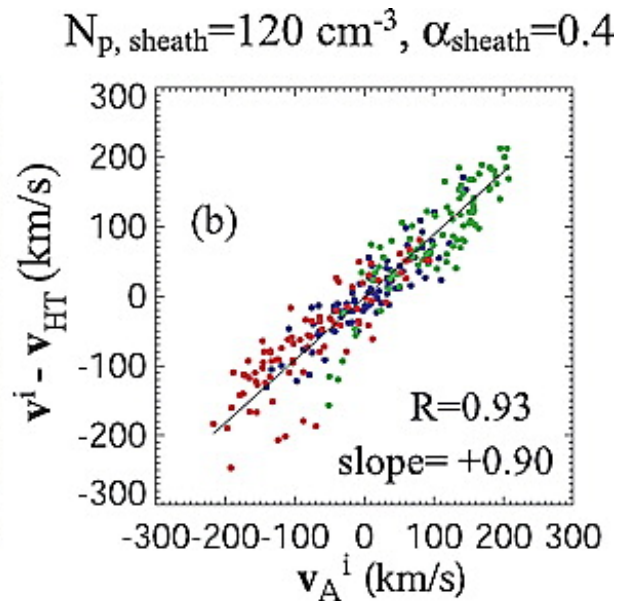
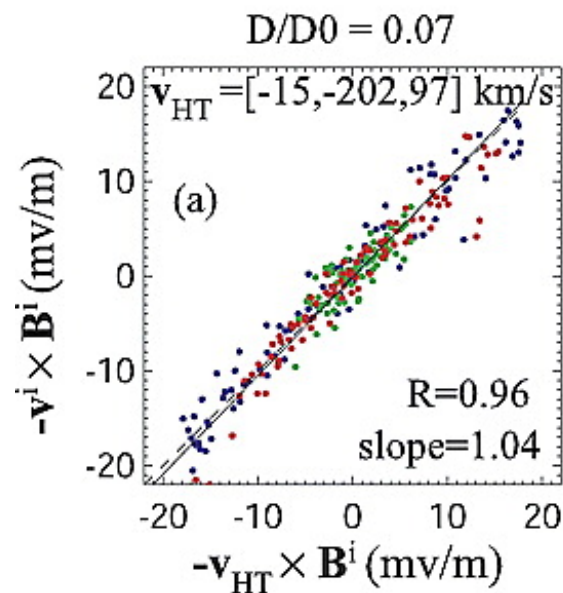
Figure 3 | Formation of secondary flux ropes. **a, b**, Slice of the current density at $y = 35d_i$ from the 3D simulation (**a**) compared with the corresponding 2D result (**b**). **c**, The structure of the separatrix layer at the location indicated. Profiles in **c** are shown in the minimum-variance frame (18° rotation about y followed by 52° rotation about z'). **d**, Fitting to a Harris profile gives a half-thickness $\lambda \approx 2d_e$ with guide field $B'_y \approx 4.4B'_{x0}$, resulting in the growth rate shown. **e**, The power spectrum $|\hat{B}_z|^2/B_{x0}^2$ for the 3D simulation on a log scale. The solid white line corresponds to the dominant angle, whereas the dashed line is the simple estimate from **c**.

Spacecraft observations are usually interpreted in the context of Dungey's 2D cartoons

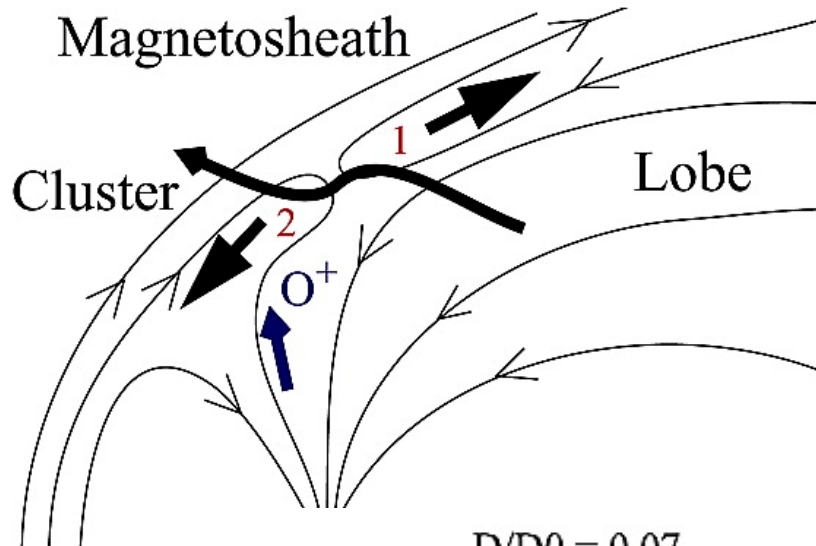


Evidence that the magnetopause locally looks like a rotational discontinuity

Phan et al., GRL, 30, 1509, 2003.



“Standard Toolkit” (flow reversals, de Hoffman-Teller analysis, Wal é n relation)

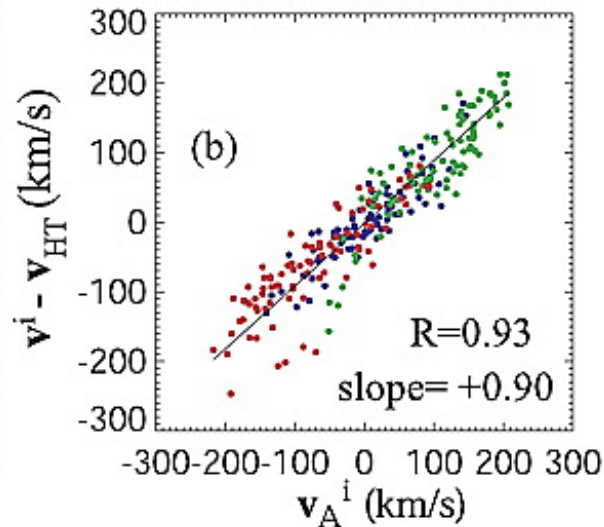
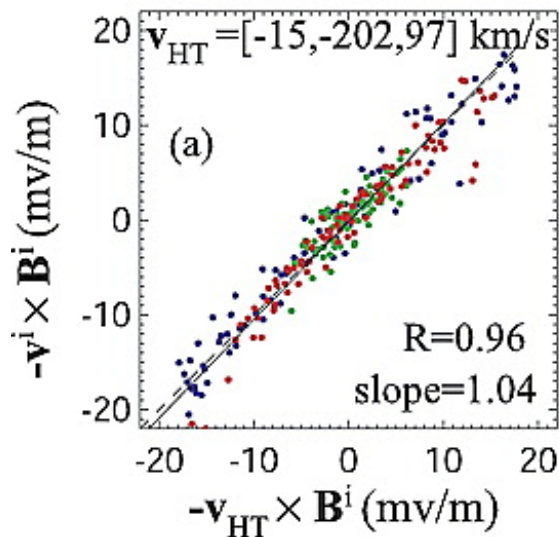


Evidence that the magnetopause locally looks like a rotational discontinuity

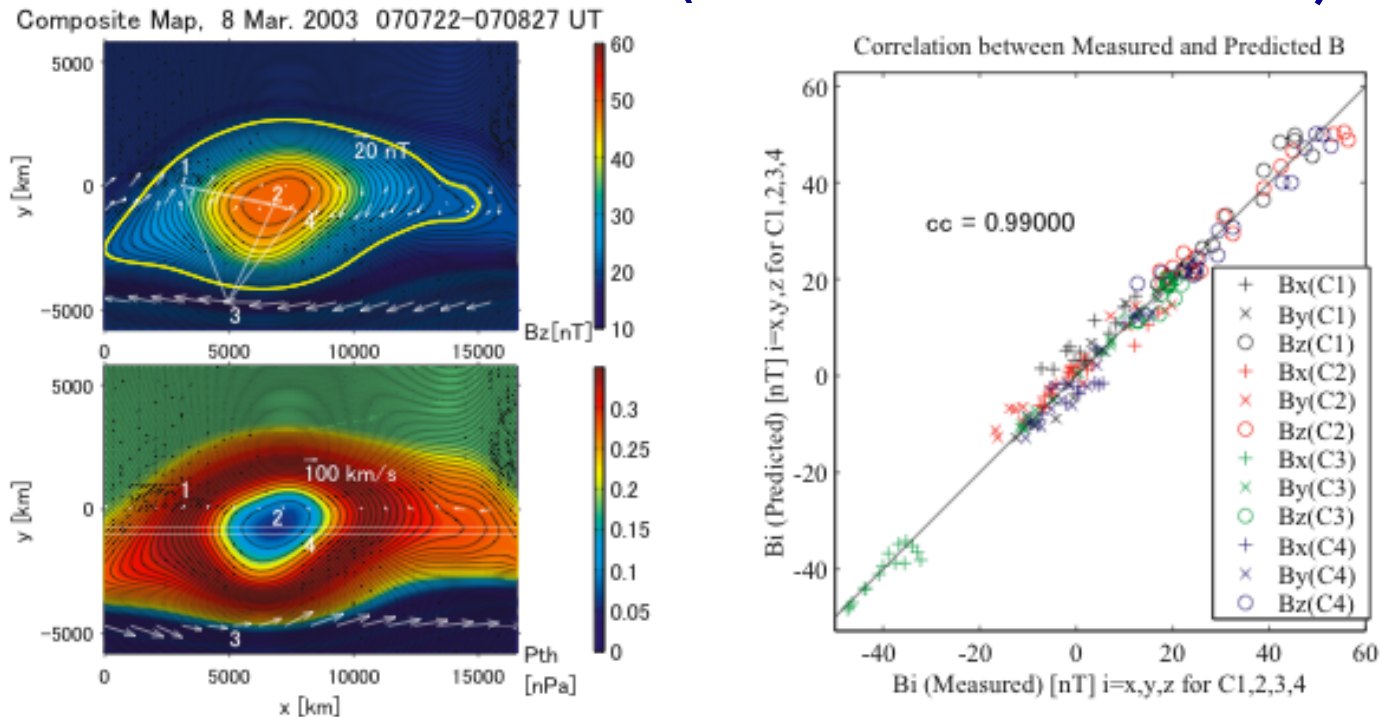
Phan et al., GRL, 30, 1509, 2003.

$D/D_0 = 0.07$

$N_{p, \text{sheath}} = 120 \text{ cm}^{-3}$, $\alpha_{\text{sheath}} = 0.4$



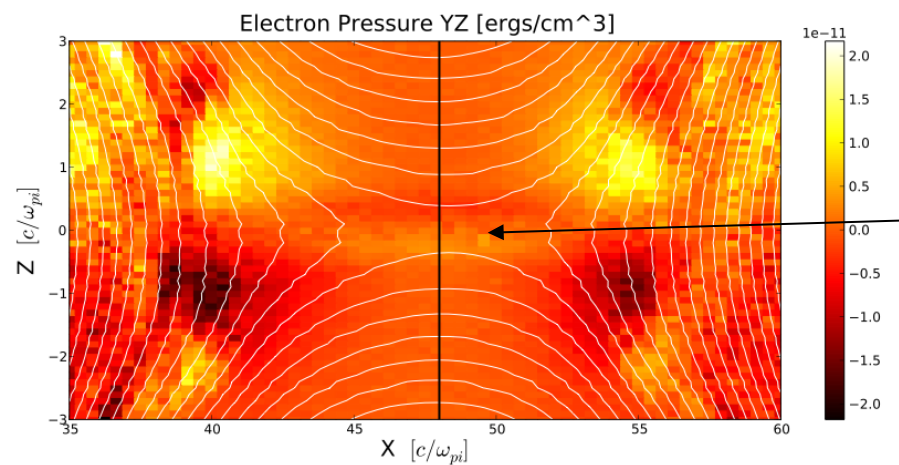
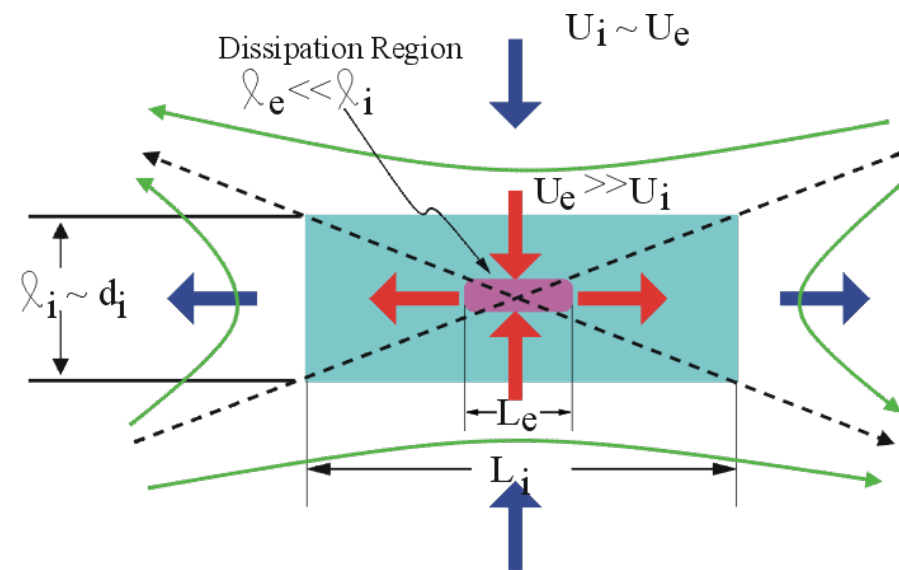
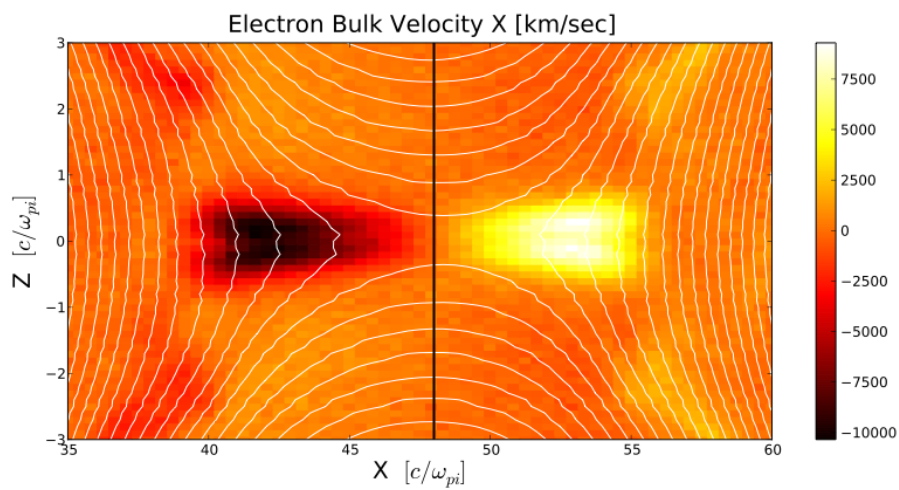
“Standard Toolkit” (2D Reconstruction)



Detects rigidly moving 2D structures by solving steady state fluid equations as an “initial value” problem, with initial conditions specified along a single spacecraft trajectory.

Sonnerup, B. U. Ö., H. Hasegawa, and G. Paschmann, Anatomy of a flux transfer event seen by Cluster, *Geophys. Res. Lett.*, 31, L11803, doi:10.1029/2004GL020134, 2004.
Sonnerup, B. U. Ö., Wai-Leong Teh, Reconstruction of two-dimensional coherent MHD Structures in a space plasma, *J. Geophys. Res.*, 113, A05202, doi:10.1029/2007JA012718.

Beyond the “Standard Toolkit”: Can we directly measure agyrotropic electron velocity distributions?



$$E \approx -\frac{1}{ne} \nabla \cdot \mathbf{P}_e$$

Magnetospheric Multiscale (MMS) Mission

SCIENCE OBJECTIVES

Discover the fundamental plasma physics process of reconnection in the Earth's magnetosphere

- Temporal scales of milliseconds to seconds
- Spatial scales of 10s to 100s of km

MISSION TEAM

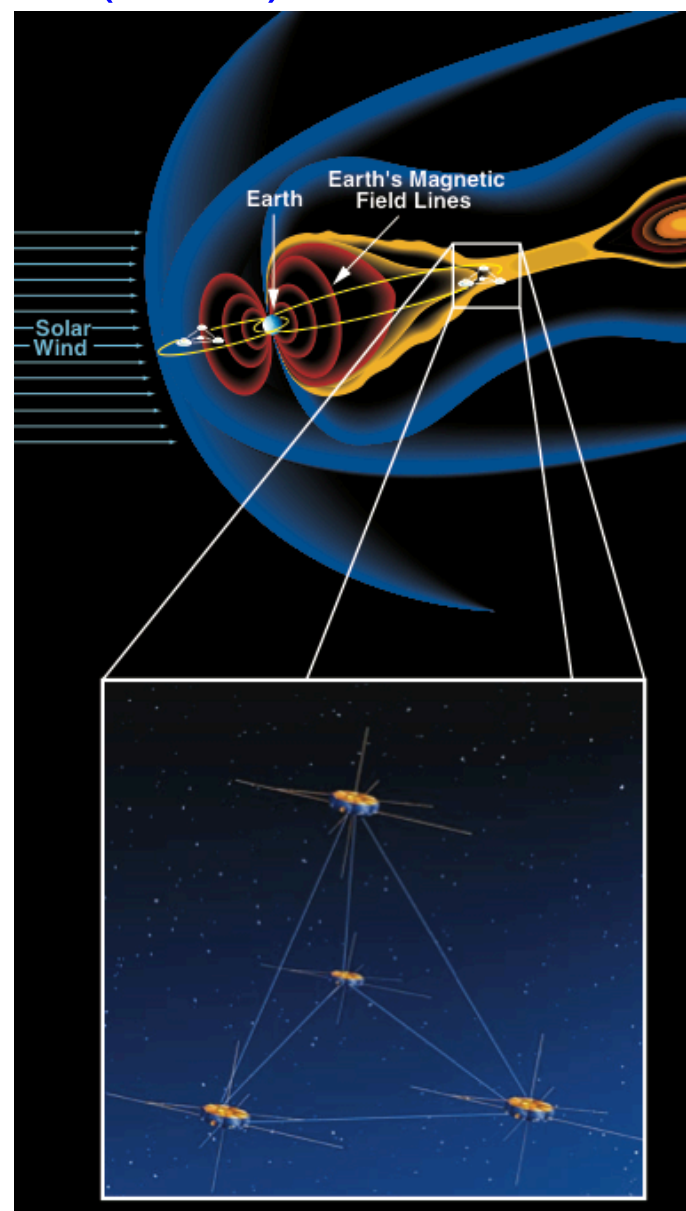
- NASA SMD
 - Southwest Research Institute
 - Science Leadership
 - Instrument Suite
 - Science Operations Center
 - Science Data Processing
- NASA GSFC
 - Project Management
 - Mission Systems Engineering
 - Spacecraft
 - Mission Operations Center
- NASA KSC
 - Launch Services

MISSION DESCRIPTION

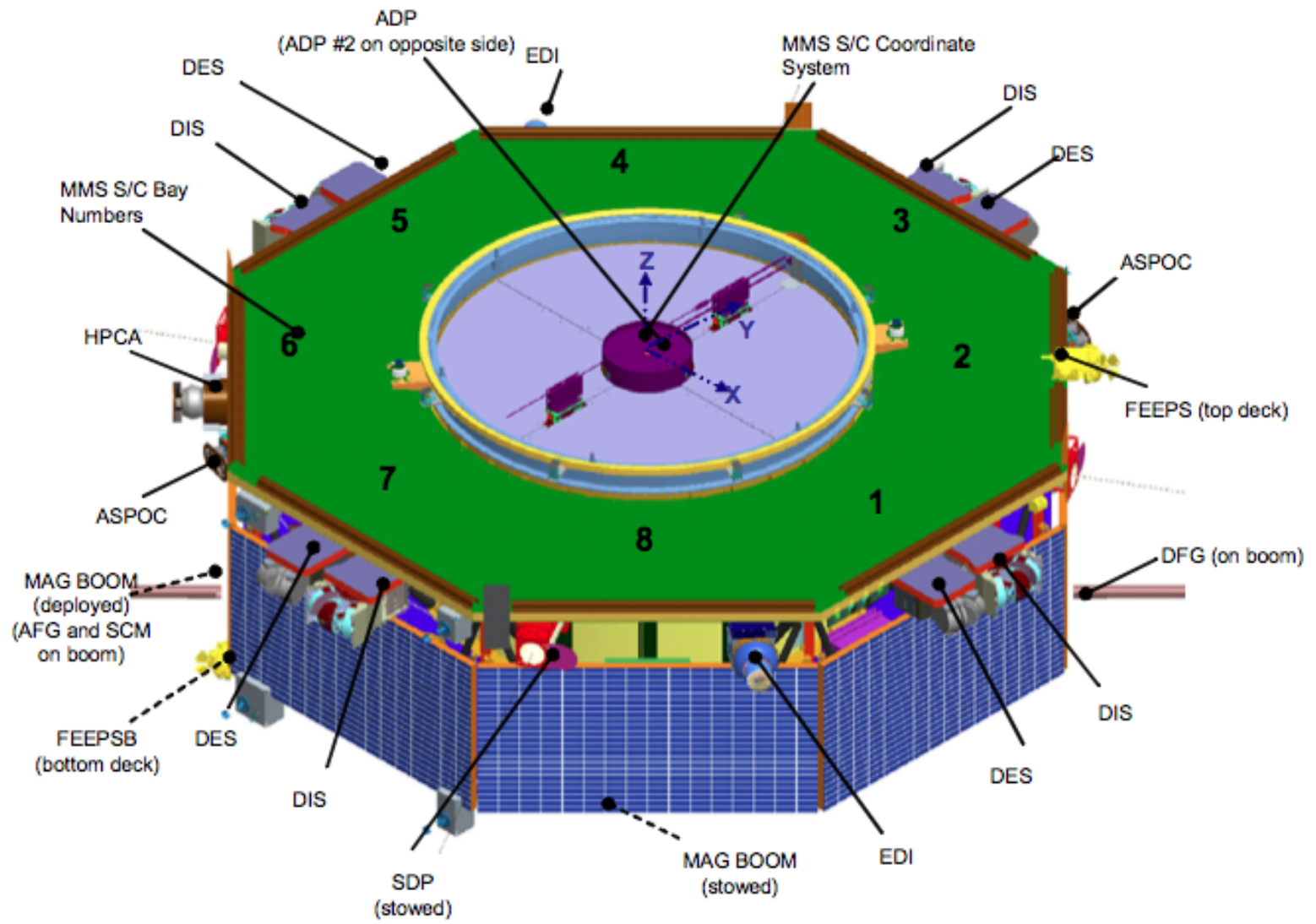
- 4 identical satellites
- Formation flying in a tetrahedron
- 2-year operational mission

ORBITS

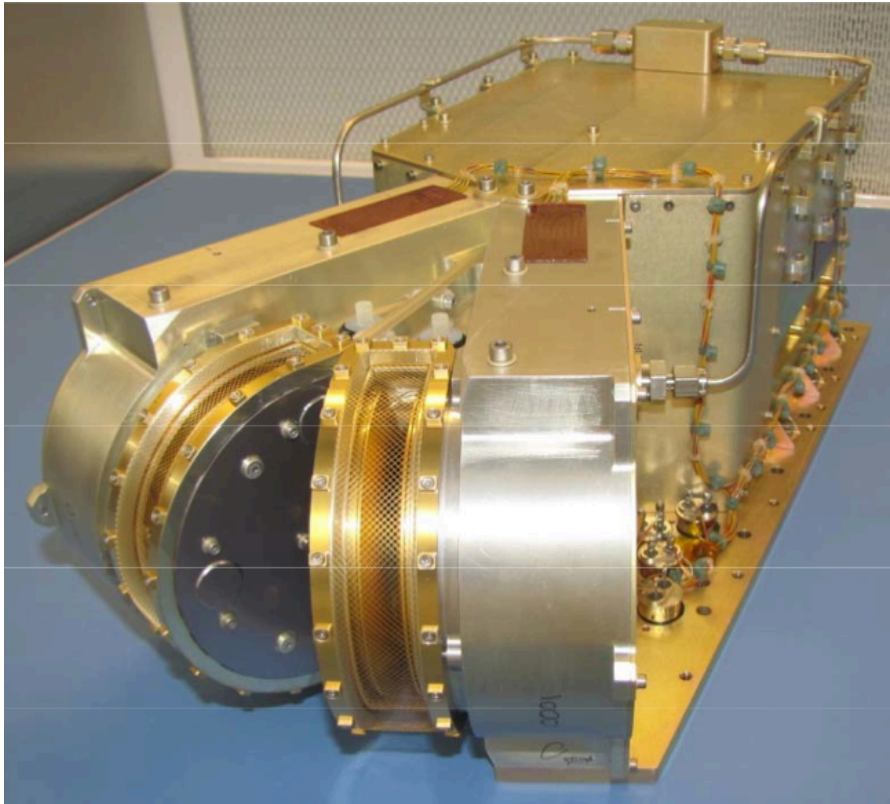
- Elliptical Earth orbits in 2 phases:
 - Phase 1 day side of magnetic field $1.2 R_E$ by $12 R_E$
 - Phase 2 night side of magnetic field $1.2 R_E$ by $25 R_E$
- Significant orbit adjust and formation maintenance



MMS Instrument Suite

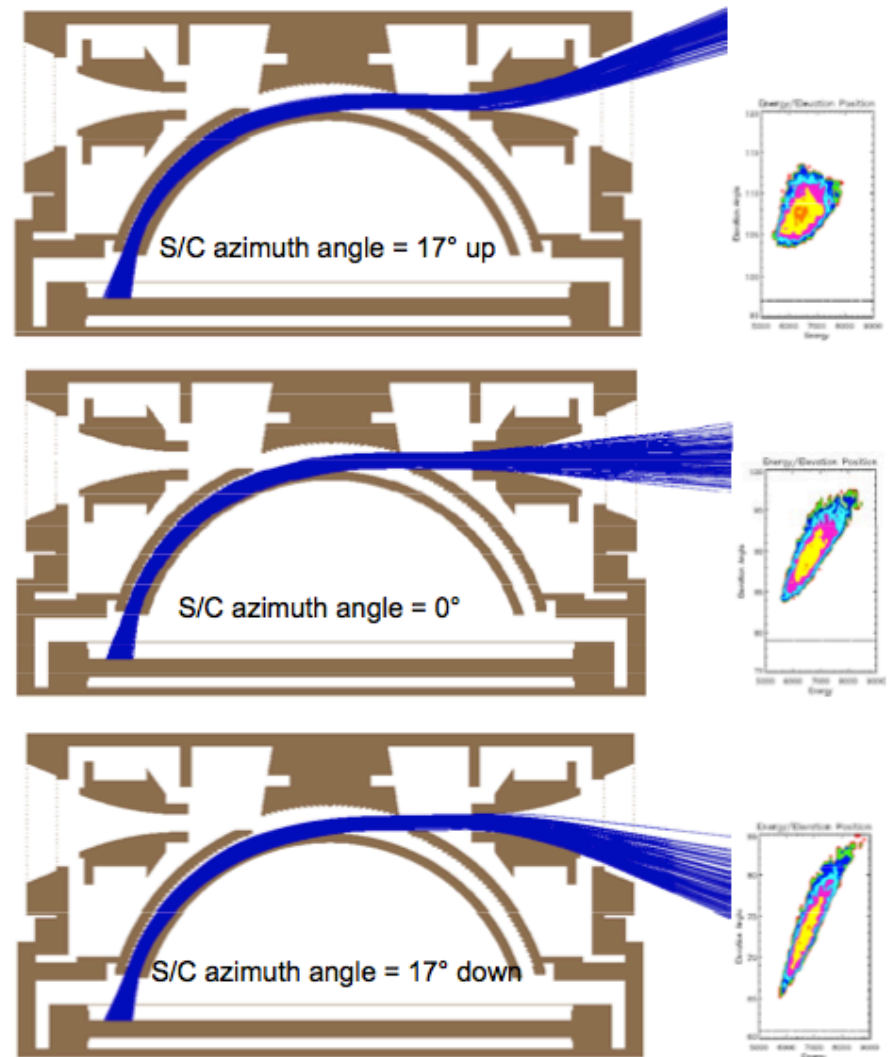


Fast Plasma Investigation (FPI)

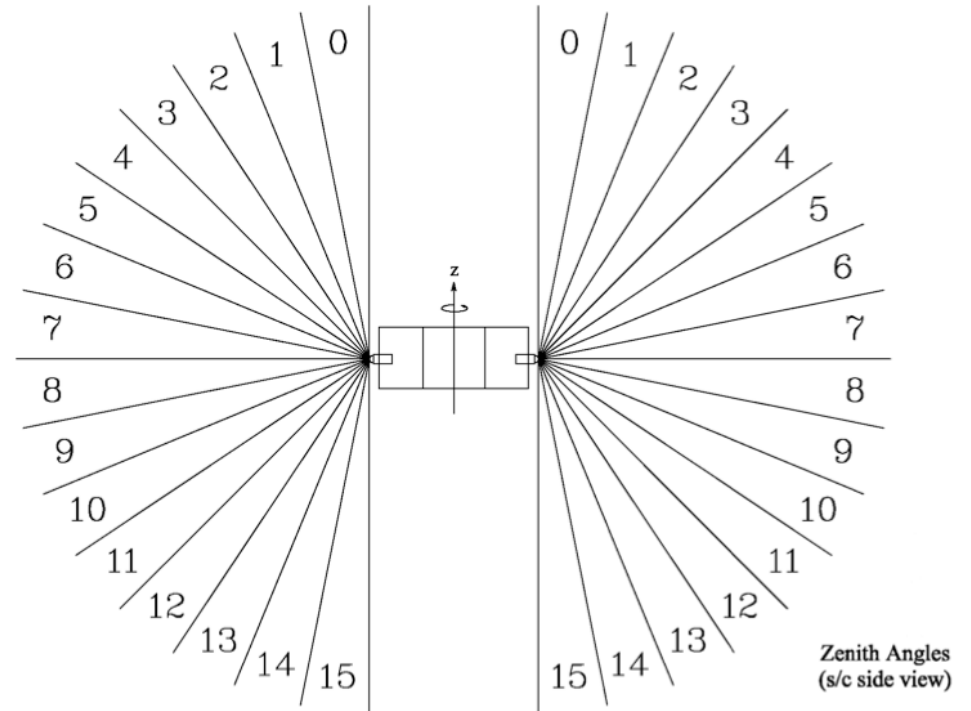
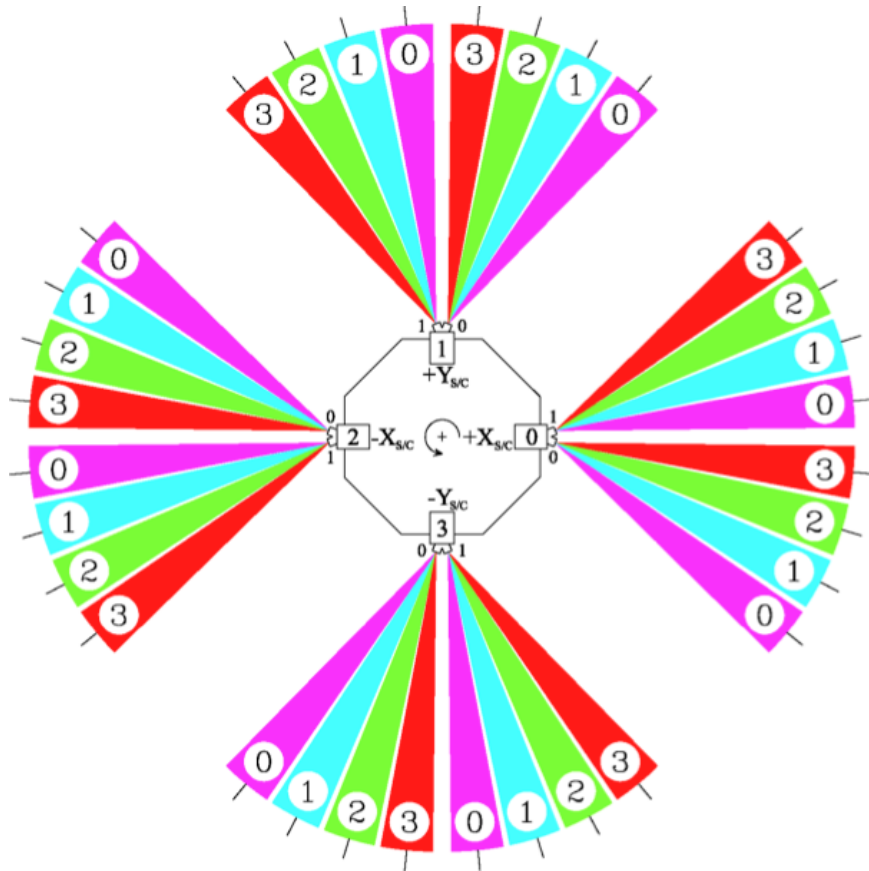


Flight units are currently being calibrated at GSFC (with 4 Instrument Data Processing Units, 36 flight boxes will be delivered!)

S/C Azimuthal/Energy Distribution

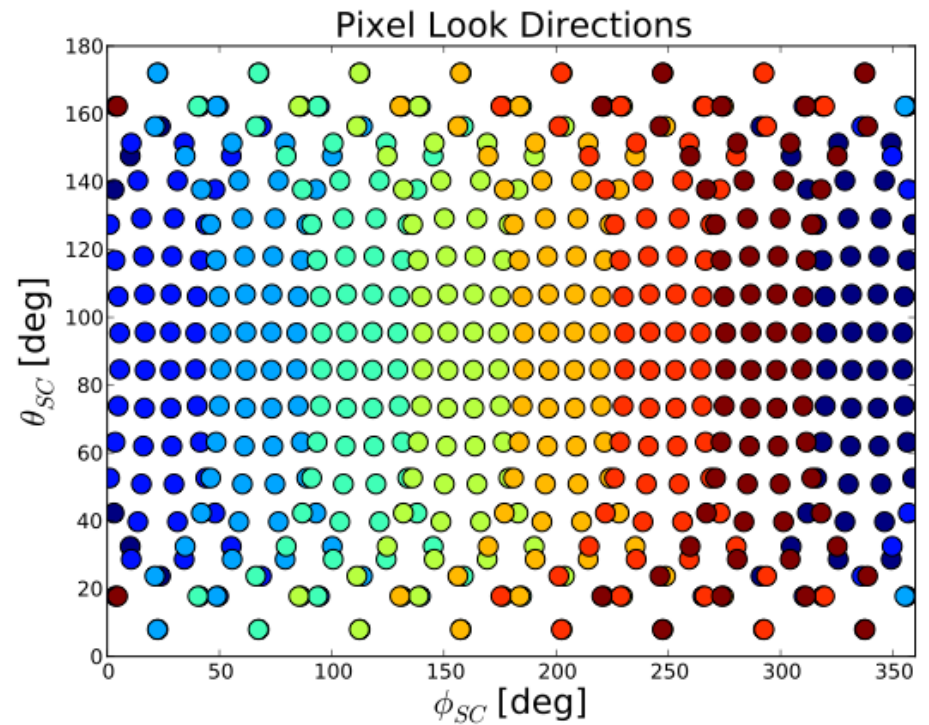
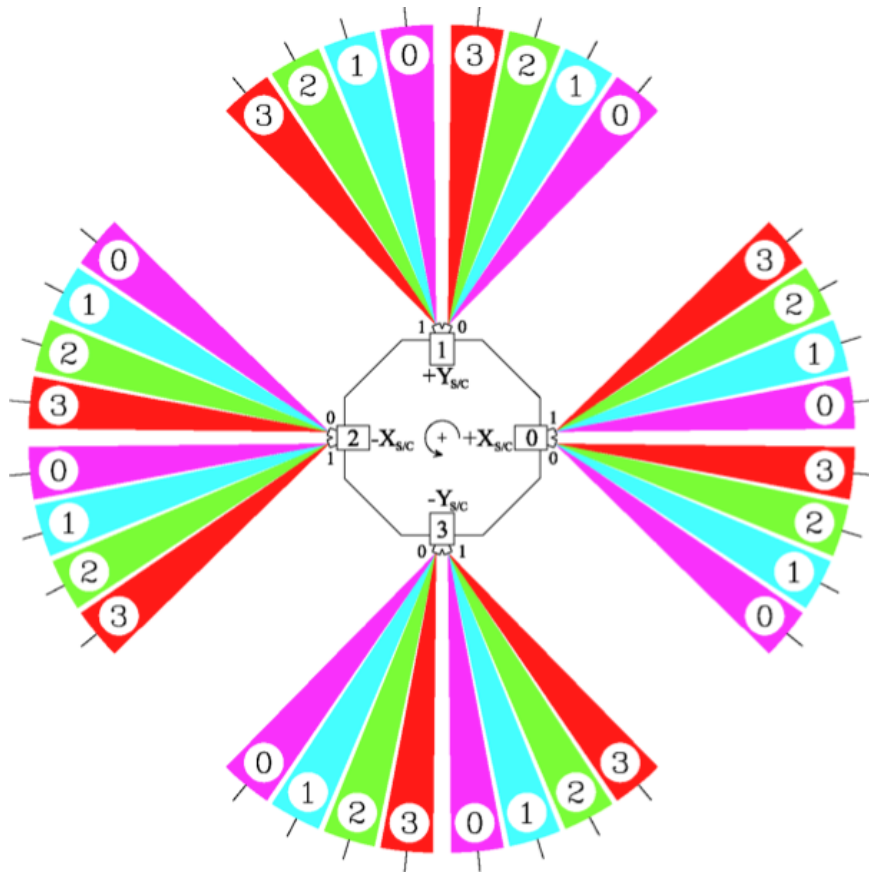


Fast Plasma Investigation (FPI)



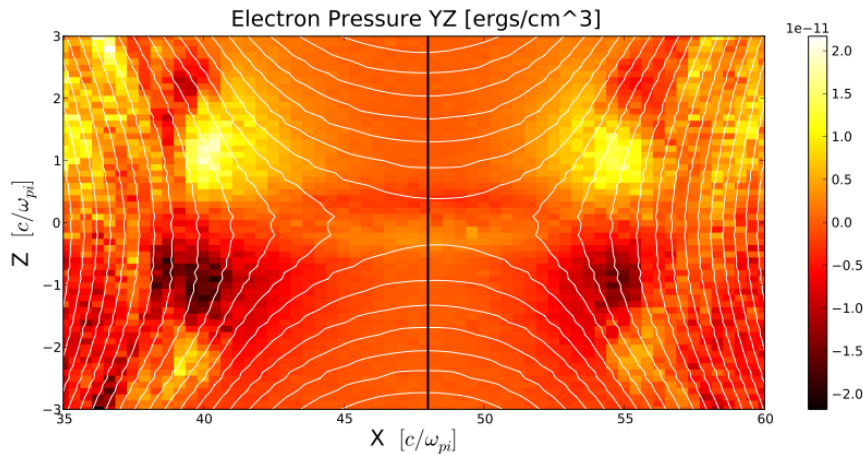
32-step energy sweep for each deflection state!

Fast Plasma Investigation (FPI)



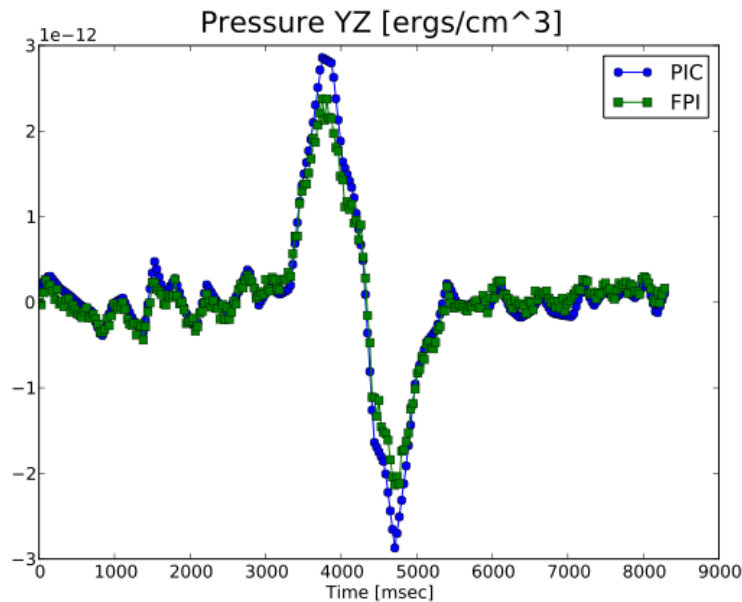
Full 32x16x32 phase space density every 30 (150) msec!

Resolving the off-diagonal elements of the electron pressure tensor with MMS



30 km/sec relative motion
between X line and S/C

$m_i/m_e = 25$ (electron layer is
thicker than it should be)



Previous missions (e.g., Cluster and THEMIS) make electron velocity distribution measurements roughly 100 times slower than MMS/FPI will.

MMS will, for the first time, resolve the electron diffusion region on the electron Larmor radius scale!

Some unsolved puzzles....

1. How does the geometry and topology of dayside magnetic reconnection vary with the orientation of the Interplanetary Magnetic Field?
2. How does “fast” magnetopause reconnection work in the collisionless magnetosphere (Sweet-Parker time scale problem)?
3. How does the structure of the (turbulent) magnetosheath influence the dayside magnetopause reconnection rate?
4. What is the role of secondary magnetic islands (Flux Transfer Events?) in dayside magnetopause reconnection (and solar wind-magnetosphere coupling in general)?
5. Solar wind-magnetosphere coupling: Can we derive a relatively simple yet predictively powerful mathematical equation relating the state of the solar wind to geomagnetic activity?